Proceedings and workbook of the

Electroporation-based Technologies and Treatments

International SCIENTIFIC WORKSHOP and POSTGRADUATE COURSE

Ljubljana, Slovenia
November 14-20, 2021

ISBN 978-961-243-423-6

Proceedings is available in PDF format at ***2021.ebtt.org/proceedings***

Electroporation-based Technologies and Treatments 2021

November 14-20, 2021
Ljubljana, Slovenia

Proceedings and workbook of the

Electroporation-based Technologies and Treatments

International SCIENTIFIC WORKSHOP and POSTGRADUATE COURSE

Edited by:
Peter Kramar
Damijan Miklavčič

Organised by:
University of Ljubljana
Faculty of Electrical Engineering

Institute of Oncology, Ljubljana

Supported by:
Donau Lab
Farapulse
IGEA
Iskra Medical
Jafral
Kobis
Leroy
Mediline
Medtronic
Omega
Pulse Biosciences

Bioelectrochemical Society (BES)

International Society for Electroporation-Based Technologies and Treatments (ISEBTT)

www.ebtt.org

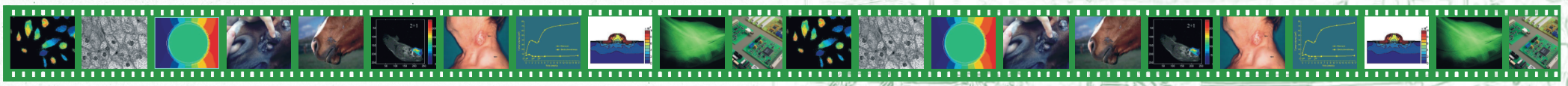

Univerza *v Ljubljani*

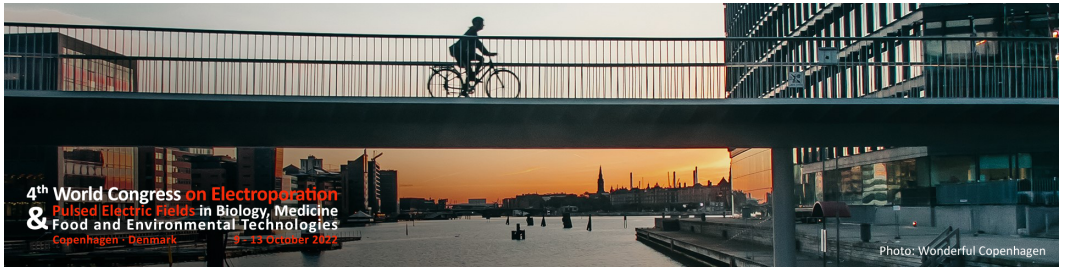

See you next time in **Copenhagen**!

4th World Congress on Electroporation
& Pulsed Electric Fields in Biology, Medicine
Food and Environmental Technologies
Copenhagen · Denmark **9 - 13 October 2022**

We will **all be there** again!

November 14-20, 2021
Ljubljana, Slovenia

Proceedings and workbook of the

Electroporation-Based Technologies and Treatments

International SCIENTIFIC WORKSHOP and POSTGRADUATE COURSE

Edited by:
Peter Kramar
Damijan Miklavčič

Organised by:
University of Ljubljana
Faculty of Electrical Engineering

Institute of Oncology, Ljubljana

Organising committee:
Chair:
Peter Kramar
Members:
Matej Kranjc, Helena Cindrič,
Aleksandra Cvetkoska, Duša Hodžič

Supported by:
Donau Lab
Farapulse
IGEA
Iskra Medical
Jafral
Kobis
Leroy
Mediline
Medtronic
Omega
Pulse Biosciences

Bioelectrochemical Society
(BES)

International Society for
Electroporation-Based
Technologies and Treatments
(ISEBTT)

www.ebtt.org

CIP - Kataložni zapis o publikaciji
Narodna in univerzitetna knjižnica, Ljubljana

602.621(082)
577.352.4(082)

ELECTROPORATION-based Technologies and Treatments (delavnica) (2021 ; Ljubljana)
Proceedings and workbook of the electroporation-based technologies and treatments : international scientific workshop and postgraduate course : [Ljubljana, Slovenia, November 14-20, 2021] / organised by University of Ljubljana, Faculty of Electrical Engineering [and] Institute of Oncology, Ljubljana ; edited by Peter Kramar, Damijan Miklavčič. - 1. izd. - Ljubljana : Založba FE, 2021

ISBN 978-961-243-423-6
COBISS.SI-ID 82349315

Založnik: Založba FE, Ljubljana
Izdajatelj: UL Fakuleta za elektrotehniko, Ljubljana
Urednik: prof. dr. Sašo Tomažič

Natisnil: Birografika Bori d.o.o.
Naklada: 100 izvodov
1. izdaja

Welcome note

Dear Colleagues, dear Students,

The idea of organizing the Workshop and Postgraduate Course on Electroporation-Based Technologies and Treatments (EBTT) at the University of Ljubljana had been developing for several years. After preliminary discussions, the Workshop and Course was organised for the first time in 2003. In 2021 the Course is organised for the 15th time! In these fifteen years, the Course has been attended by 895 participants coming from 42 different countries. And this year again – despite pandemics - we can say with great pleasure: "with participation of many of the world leading experts in the field" – unfortunately, as an online only event. The goals and aims of the Workshop and Course however remain unchanged: to provide the participants with sufficient theoretical background and practical knowledge to allow them to use electroporation effectively in their working environments.

It is a great pleasure to welcome you to the EBTT and in particular to the practical lab work taking place at the University of Ljubljana, Faculty of Electrical Engineering organised as an integral part of the Interdisciplinary doctoral programme Biomedicine. From the very beginning we were aiming to prepare lab work for participants, which would complement the lectures. As preparing lab work takes more time than preparing and organizing lectures, we introduced lab work at the second workshop in 2005. Lab work covers different aspects of research: biological experiments taking place in the cell culture labs, microbiological lab, lab for tissue and planar lipid bilayer; numerical and molecular dynamics modelling, e-learning using computer classrooms, pulse generator development and electrical measurements using electronic laboratory workshop and magnetic resonance electrical impedance tomography.

Following the experience gained last year when due to pandemic we organised the course entirely on-line, this year we decided to organise the course as a hybrid, to allow participation also to those who are still facing difficulties in traveling. The team here in Ljubljana will thus provide on-site hands-on labworks as well as live webinars of the lab works so that you will be able to benefit most even if not actually being in the lab.

The biological experiments were pre-recorded in the labs of the network of research and will be organised in infrastructural centre MRIC, University of Ljubljana, at the Faculty of Electrical Engineering in the Laboratory of Biocybernetics. Lab works would not be possible without extensive involvement and commitment of numerous members of the Laboratory of Biocybernetics and Igor Serša from Jožef Stefan Institute for what I would like to thank them all cordially.

It also needs to be emphasized that all written contributions collected in the proceedings have been reviewed and then thoroughly edited by Peter Kramar. We thank all authors and reviewers. Also, I would like to express our sincere thanks to the faculty members and invited lecturers for their lectures delivered during the course. Finally I would like to thank our sponsors who are making our EBTT possible:

Dunau Lab (Slovenia), Farapulse (USA), IGEA (Italy), Iskra Medical (Slovenia), Jafral (Slovenia), Kobis (Slovenia), Leroy (France), Mediline (Slovenia), Medtronic (USA), Omega (Slovenia), Pulse Bioscience (USA), Bioelectrochemical Society and ISEBTT International Society for Electroporation-Based Technologies and Treatments.

We sincerely hope that you will benefit from being with us.

Sincerely Yours,

Damijan Miklavčič

INVITED LECTURERS

The Biophysics of Cell Membrane Electroporation

Lea Rems; *University of Ljubljana, Faculty of Electrical Engineering, Tržaska 25, SI-1000 Ljubljana, SLOVENIA*

INTRODUCTION

The plasma membrane of a mammalian cell is a complex organization of lipids and proteins that separates the cell interior from the outside environment and transduces messages between the environment and the internal cellular apparatus. The membrane lipid bilayer is composed of hundreds of different types of lipids, asymmetrically distributed between the two bilayer leaflets and organized in domains, which are enriched (or depleted) with specific lipids like cholesterol. The lipid bilayer hosts numerous types of membrane proteins which tightly regulate transmembrane traffic and participate in cell signalling. The membrane also provides attachments for the underlying actin cortex, which dictates the membrane's mechanical properties, and acts as a dynamic modulator of the cell shape. When we electroporate cells, all membrane components (lipids, membrane proteins, and the actin cortex) are affected [1]. Since membrane organization and integrity are essential for the life and proper function of a cell, it is important to understand how, why and under which conditions these individual membrane components become affected. This lecture will focus on the known biophysical effects of electroporative pulses on the plasma membrane organization, using insights from computational and experimental studies on model membrane systems.

METHODS

Model membrane systems are indispensable because they enable a systematic bottom-up approach to study the biophysics of electroporation. The results presented in the lecture will be based on the following methods. Molecular dynamics (MD) is a computer simulation for analysing the physical movements of atoms and molecules. The output of MD is a trajectory, which is determined by solving the classical equations of motion for a system of interacting particles. MD offers spatiotemporal resolution superior to any experimental method. However, due to its computational demand, we can mainly use MD to study small systems with dimensions on the order of 10-100 nm and temporal scales on the order of 1-10 μs, depending on whether we use all-atom or coarse-grained representation of the molecular system. To study electroporation on the scale of single cells and cell clusters, we need to design a set of ordinary and partial differential equations that describe the physical behavior of the system. The equations can be solved with different numerical methods, such as finite elements, transport lattices, or similar. When studying electroporation experimentally, giant unilamellar vesicles (GUVs) have become very popular, since they resemble the cell size and can be easily visualized with optical microscopy. GUVs can be prepared with various types of lipids and lipid mixtures. Emerging techniques enable preparation of GUVs with embedded membrane proteins or actin cortex.

RESULTS AND DISCUSSION

The most accepted models, that describe electroporation on the whole-cell level, consider that pores can form only in the lipid domains of the plasma membrane and that all pores exhibit more or less the same kinetic behaviour. However, accumulating evidence from experiments and simulations on model systems speaks against these assumptions [2,3]. Poration kinetics of pores in pure lipid bilayers has been shown to depend on the type of lipids and their phase state; since the lipids in the plasma membrane organize in domains, there must exist locations which are more and less likely to porate. Indeed, coarse-grained MD simulations of membranes mimicking the realistic plasma membrane composition show that pores preferentially form in domain characterized by specific features such as high content of polyunsaturated lipids. Moreover, our research suggests that pores can nucleate also within some membrane proteins causing protein denaturation and lipid rearrangement. Such lipid/protein complex pores can be more stable than pure lipid pores and are more likely to explain the persistent increase in plasma membrane permeability following exposure to electric pulses. Studies on GUVs with encapsulated actin network have further shown that pore formation, expansion and resealing is affected by the actin network. Finally, electroporation has also been found to be associated with oxidative damage of polyunsaturated lipids. As lipids are oxidized, their tails become less hydrophobic and consequently more permeable to ions and molecules. Further research is, however, needed to connect these new findings into a coherent picture which will allow to understand what can or cannot happen in the plasma membrane depending on the parameters of the applied pulses and other experimental conditions.

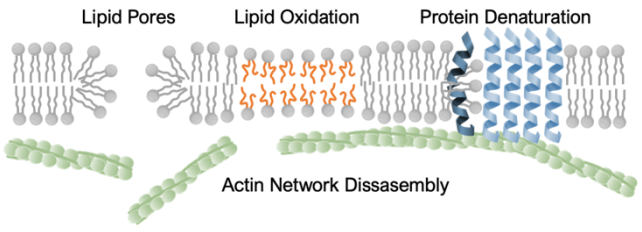

Figure 1: Molecular mechanisms of electroporation.

REFERENCES

[1] T. Kotnik, L. Rems, M. Tarek, D. Miklavčič, *Annu. Rev. Biophys.*, vol. 48, pp. 63-91, 2019.

[2] L. Rems, M. Kasimova, I. Testa, L. Delemotte, *Biophys. J.*, vol. 119, pp. 90-105, 2020.

[3] D. Perrier, A. Vahid, V. Kathavi, L. Stam, L. Rems, Y. Mulla, A. Muralidharan, G.H. Koenderink, M.T. Kreutzer, P.E. Boukany, Sci. Rep., vol. 9, pp. 8151, 2019.

Single-Cell Bioprocess Optimization by Pulsed Electric Field Processing

Iris Haberkorn, Alexander Mathys
Laboratory of Sustainable Food Processing, Institute of Food, Nutrition, and Health, Department of Health Sciences and Technology, Schmelzbergstrasse 9, 8092 Zurich, SWITZERLAND.

INTRODUCTION

Imminent challenges connected with a world population growth to 9.7 billion people by 2050 and anthropogenic causes fostering climate change are propelling the exploration of novel approaches that offer more sustainable value-chains for energy and food supply. To tackle these challenges by means of a nondestructive and long-term focused strategy, the bio-based domain, including food and feed systems, material, compound, and fuel production, is required to find sustainable solutions by employing novel resources and technological innovations. Renewable bio-based materials relying on single-cell biorefineries, such as those affiliated with yeasts, bacteria, microalgae, and mammalian cells could offer promising new applications. However, efficiency enhancement remains a main target in the bio-based domain for rendering the value-chains of single-cell biorefineries, such as those associated with microalgae, into economically viable scenarios. For example, the economic viability of microalgae feedstock production remains hampered by low upstream productivities, leading to an increase in total biomass production costs.

METHODS

The effect of nsPEF on different single-celled organisms groups including *Arthrospira platensis*, *Chlorella vulgaris,* and *Saccharomyces cerevisiae* was investigated applying energy inputs between 28 and 2030 J kg^{-1} by varying electric field strength, pulse repetition frequency, and pulse widths to scrutinize their effect on the biomass yield. Analyses were supported by a novel flow cytometric approach for cell count determination. To reveal possible stress response pathways, proteomics analysis was combined with integrative analytical investigations of single cells up to 10^7 Hz.
µsPEF-based reversible electropermeabilization was investigated using *C. vulgaris* to increase mass transfer across the cell membrane without impeding the cell's physiological state. Critical processing (pulse width: 10–100 µs, electric field strength: 10–20 kV cm^{-1}, pulse amplitude: 1–4000 V) and bioprocess (*e.g.*, growth stage, re-feeding) parameters were evaluated.

RESULTS

Applying nsPEF treatments at a specific energy input of 3 x 256 ± 67.5 J kg^{-1} significantly leveraged *A. platensis* biomass yield by 13.1 ± 1.6% (t-test, $p = 0.009$). Simultaneously, the content of the high-value added component phycocyanin (+19.2 ± 5.8%) was increased. nsPEF treatments also significantly increased biomass obtained from eukaryotic phototrophic *C. vulgaris* by up to 17.5 ± 10.5% (Mann-Whitney test, $p = 3.2 \times 10^{-5}$). Pigment and carbohydrate content were not affected, while a decrease in protein content was observed. The results indicate that nsPEF treatments enhance cell proliferation based on plasma membrane related effects and intracellular abiotic sub-lethal stress responses.
µsPEF processing allowed cyclic protein extraction while maintaining cell viability. Increasing protein extraction rates were observed with increasing electric field strength, up to 96.6 ± 4.8% of the free protein in the microalgae. However, increased extraction rates negatively influenced microalgae growth after PEF treatment. A free protein extraction rate up to 29.1 ± 1.1% without a significant influence on microalgal growth after 168 h was achieved (p=0.788).

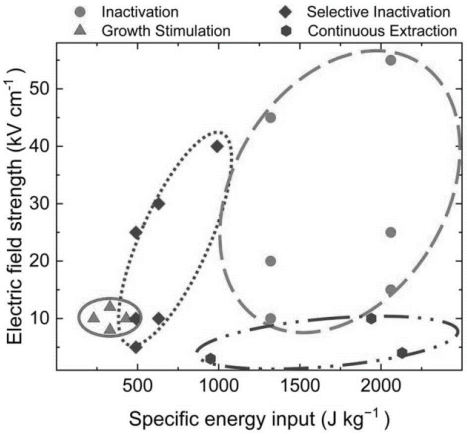

Figure 1: Treatment windows for growth stimulation, selective inactivation, inactivation, cyclic component extraction based on a case study with *Chlorella vulgaris*.

CONCLUSIONS

Pulsed electric field (PEF) processing is an energy efficient approach for single-cell process innovation. Upstream, nsPEF processing is gaining momentum as a physical means for single-cell bioconversion efficiency enhancement. The technology enhances microalgae bioconversion efficiencies (up to 17.5% enhanced biomass yield of phototrophic *C. vulgaris*) without additional needs for substrate or can be employed as a selective inactivation technology. Downstream, applying µsPEF enables gentle component recovery that maintains the structural and techno-functional properties of the extracted components at low energy demand.

REFERENCES

[1] Haberkorn, I., Siegenthaler, L., Buchmann, L., Neutsch, L., Mathys, A. (2021). Enhancing single-cell bioconversion efficiency by harnessing nanosecond pulsed electric field processing. *Biotechnol. Adv.*, (in press)
[2] Buchmann, L. and Mathys, A. (2019). Perspective on Pulsed Electric Field Treatment in the Bio-based Industry. *Front. Bioeng. Biotechnol.*, 7:265.

Tissue Cryopreservation: Methods, Novel Trends and Research Highlights

Oleksandr Gryshkov[1,2], Vitalii Mutsenko[1,2], Sara Leal-Marin[1,2], Ekaterina Riabchenko[3], Sven-Alexander Barker[1,2], Diaa Khayyat[1,2], Maksim Tymkovych[4], Alexander Yu. Petrenko[5], Clemens Ruppert[6], Oleh Avrunin[4], Damijan Miklavčič[7], Birgit Glasmacher[1,2]; *[1] Institute for Multiphase Processes, Leibniz University Hannover, An der Universität 1, Building 8143, 30823 Garbsen, GERMANY, [2] Lower Saxony Centre for Biomedical Engineering, Implant Research and Development, Stadtfelddamm 34, 30625 Hannover, GERMANY, [3] National Research University of Electronic Technology MIET, Moscow, RUSSIA, [4] Kharkiv National University of Radio Electronics, Nauky Ave. 14, 61166 Kharkiv, UKRAINE, [5] Institute for Problems of Cryobiology and Cryomedicine of the National Academy of Sciences of Ukraine, 61015 Kharkiv, UKRAINE, [6] Universities of Gießen & Marburg Lung Center (UGMLC), Justus-Liebig Universität Gießen, 35392 Gießen, GERMANY, [7] Faculty of Electrical Engineering, University of Ljubljana, Tržaska 25, SI-1000 Ljubljana, SLOVENIA*

INTRODUCTION

Cryopreservation is a viable approach to provide clinics and research facilities with ready-to-use stocks of clinically relevant cells, native tissues and tissue-engineered constructs (TECs). Stem cells such as multipotent (MSCs), and induced pluripotent stem cells, as well as native tissues can be utilised for a broad range of cell-based therapies and regenerative medicine for disease treatment, tissue and organ regeneration. In turn, artificial tissues (TECs) represent a combination of a biocompatible scaffold construct mimicking the extracellular matrix, and the above-mentioned organ-specific cells [1]. Such three-dimensional TECs can be produced by cultivation in a bioreactor at dynamic conditions using a range of mechanical, chemical and biological stimuli until the required functionalities are achieved. In terms of native tissues and TECs, their cryopreservation meets a number of challenges listed below.

1. Combination of more than two cell types that have to be cryopreserved under certain cell-type specific cryopreservation parameters.
2. Limitations in the diffusion of cryoprotective agents within a tissue, which hampers achieving their homogeneous distribution needed for efficient tissue cryopreservation
3. Unequal heat transfer within tissues leading to large temperature gradients.

This work aims to highlight the recent advances in cryopreservation of native tissues and TECs to achieve their efficient long-term storage for clinical application and research purposes.

METHODS

In this work, three different tissue types were cryopreserved and analysed: native lung tissue (precise cut lung slices, PCLSs), TECs including cell-seeded polycaprolactone-polylactid (PCL-PLA) and polycaprolactone-gelatine (PCL-GEL) scaffolds as well as cell-encapsulated hydrogel core-shell alginate capsules.

PCLSs were prepared by cutting mouse lungs using a vibratome with a laterally vibrating blade. The final thickness of each slice was 250 µm. Electrospinning was used to obtain PCL-PLA and PCL-GEL nanostructured fibrous scaffolds with a thickness of 100 µm as described previously [2]. The scaffolds were UV-sterilised and punched into circles with a diameter of 16 mm. The human osteosarcoma cells (SAOS-2) were seeded on the scaffolds with a density of 5×10^4 cell/cm^2. The MSCs were encapsulated in core-shell hydrogels produced from 2% alginate solution with a density of 5×10^6 cells/ml using a coaxial nozzle and electrospraying setup [3].

Slow freezing with a cooling rate of 1 K/min was used to cryopreserve all three tissue types in a controlled-rate freezer. CPAs including 10% dimethyl sulfoxide (DMSO), ethylene glycol (EG) and their combination with 0.3 M sucrose were used for tissue cryopreservation. After thawing and 24h of recultivation, the tissues were analysed using a number of structural and morphological methods as well as cell viability and metabolic activity assays. Moreover, cell-cell and cell-scaffold interactions were evaluated using confocal laser scanning and scanning electron microscopy. The results were compared to those before cryopreservation.

RESULTS AND FIGURES

The results indicate that application of 0.3 M sucrose and additional pretreament step significantly improves cell viability and metabolic activity of all tissue types after thawing. Utilisation of EG yielded comparable cell functionalities and could serve as an alternative to toxic DMSO. Moreover, application of cryobags as freezing containers resulted in improved tissue functionalities post-thaw, as compared to cryopreservation of TECs in plates.

REFERENCES

[1] P.F. Costa, A.F. Dias, R.L. Reis et al., "Cryopreservation of Cell/Scaffold Tissue-Engineered Constructs," *Tissue Eng Part C Methods*, vol. 18, pp. 852–858, 2012.

[2] O. Gryshkov, M. Muller, S. Leal-Marin et al., "Advances in the application of electrohydrodynamic fabrication for tissue engineering, " *J Phys Conf Series*, vol. 1236, pp. 12024, 2019.

[3] O. Gryshkov, V. Mutsenko, D. Tarusin et al., "Coaxial Alginate Hydrogels: From Self-Assembled 3D Cellular Constructs to Long-Term Storage," *Int J Mol Sci.*, vol. 22, pp. 3096.

Pulsed electric field effects in excitable neural cells - in vitro to in vivo studies using flexible organic electronics.

Rita Matta, Marie Lefevre, Romanos Poulkouras, Gerwin Dijk, Attila Kaszas, Martin Baca, David Moreau, Rodney P. O'Connor; *Department of Bioelectronics, Microelectronics Center of Provence, Mines Saint-Etienne, 880, route de Mimet, 13541 Gardanne cedex, FRANCE.*

INTRODUCTION

Neurons are the excitable cells found in our brain, spinal cord and peripheral nervous system. They generate and communicate with electric pulses and are the machinery for our thoughts, memories, dreams and actions. Neurons generate an action potential that can also be electrically excited by externally applied pulsed electric fields. But why is this so? And what is it that makes a neuron excitable? Can they be electroporated? This lecture will review some of the basics of cell excitability, whilst introducing our research on the influence of pulsed electric fields in the brain.

We are investigating new electrode materials that allow us to interface better with neurons *in vitro* and *in vivo*. We fabricate thin-film electrodes from the organic conductive polymer, poly(3,4-ethylenedioxythiophene) polystyrene sulfonate (PEDOT:PSS) as it interfaces well with cells and tissues. The resulting flexible electrodes can be used *in vitro* in single cell experiments or in surface electrocorticography (ECoG) recordings of the brain. If stiffened with bioresorbable polymers, such electrodes can also be implanted deep into the brain [1]

PEDOT:PSS has emerged as a popular material for biomedical devices due to its electrochemical properties and large charge injection capacity due to its mixed ionic–electronic conduction [1]. Our recent research has investigated PEDOT:PSS as a material for neurostimulation and higher voltage applications such as electroporation [2,3]. Here, we present our flexible, conformable, transparent electrodes for *in vivo* neuronal Ca^{2+} imaging.

METHODS

Organic electronic polymer electrodes were microfabricated in our cleanroom with photolithography, metal evaporation and spin casting, as previously described in [1-3]. Briefly, 7 µm of parylene C were deposited by a SCS Lab-coater 2 on a clean glass slide. Metal electrodes and connection leads were patterned using a lift-off process with a bi-layer of LOR5A resist and S1813 photoresist. Each electrode had 6 interdigitated fingers with a gap of 250 µm. Photoresist was exposed with a SUSS MBJ4 contact aligner. An adhesion layer of 10 nm chromium and 150 nm of gold was evaporated with a BOC Edwards thermal evaporator and the photoresist was lifted off. The outline of the probe was etched by a laser cutter. Finally, the device was washed with deionized water to delaminate it from the slide.

Adult Thy1-GCaMP6f mice (25-72 weeks old) expressing neuronally-targeted genetically encoded Ca^{2+} indicators were housed according to French regulations in the animal facility of Insitute de Neurosciences de la Timone. On the day of surgery, animals were sedated with 3% sevoflurane and then fixed in a stereotactic frame. After a subcutaneous lidocaine injection, the skull was exposed and a cranial window (4 mm diameter) was drilled above the visual cortex. A head plate was mounted onto the skull by light-curing dental resin, and the animal was placed into the microscope setup using the head plate. During the recording procedure, anesthesia was maintained with a 1.5% isoflurane and oxygen mixture.

Pulsed electric fields were delivered using a pulse generator built in our laboratory, triggered by the two-photon imaging system. Eight monophasic pulses of 100 µs were delivered with a repetition frequency of 1 Hz. The current and the voltage was measured on an RTM-3004 Rhode & Schwarz oscilloscope with RT-ZC15B current probe.

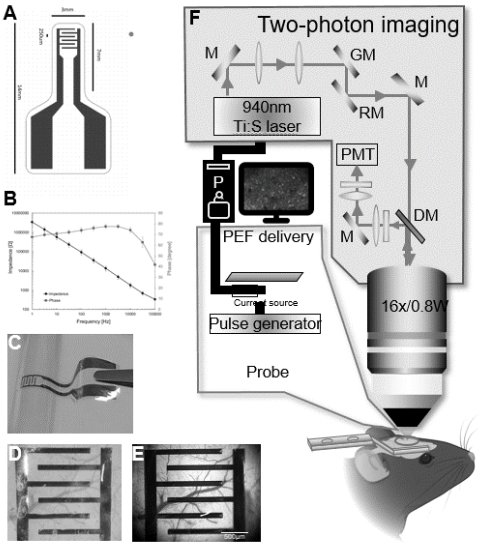

Figure 1: Flexible electrode delivery system for studying pulsed electric field effects *in vivo* in the mouse brain. **A**. Flexible organic interdigitated electrode design and dimensions, **B**. *In vivo* impedance spectroscopy of an implanted electrode system, **C**. Demonstration of device flexibility, **D**. Bright field image of a flexible electrode *in vivo* under a cranial window, **E**. Infrared image and cortical blood vessels stained with fluorescent dextrans, **F**. Two photon imaging setup for studying pulsed electric field effects in the brain with simultaneous *in vivo* neuronal Ca^{2+} imaging.

REFERENCES

[1] J. Pas, A.L. Rutz, P.P. Quilichini, A. Slézia, A. Ghestem, A. Kaszas, M.J. Donahue, V.F. Curto, R.P. O'Connor, C. Bernard, A. Williamson, G.G. Malliaras A bilayered PVA/PLGA-bioresorbable shuttle to improve the implantation of flexible neural probes. J Neural Eng. 2018 Dec;15(6):065001, 2018.

[2] G. Dijk, H.J. Ruigrok, R.P. O'Connor, Influence of PEDOT:PSS Coating Thickness on the Performance of Stimulation Electrodes. Adv. Mater. Interfaces, 7, 2000675, 2020.

[3] G. Dijk, H.J. Ruigrok, R.P. O'Connor, PEDOT: PSS-Coated Stimulation Electrodes Attenuate Irreversible Electrochemical Events and Reduce Cell Electropermeabilization Adv. Mater. Interfaces, 9, 2100214, 2021.

Cardiac ablation and defibrillation with pulsed electric fields

Christian Zemlin, *Department of Surgery, Washington University in St. Louis, St. Louis, MO 63110, USA*

INTRODUCTION

Cardiac arrhythmias have long been a major health concern. Two important treatment approaches are ablation and defibrillation. Ablation is the deliberate creation of lesions of dead tissue, in locations chosen so that the remaining live tissue no longer sustains re-entrant arrhythmia. The most important arrhythmia that is typically treated with ablation is atrial fibrillation. Defibrillation, i.e. the removal of fibrillation, is typically performed with a short intense electric shock that activates most of the tissue and thereby halts any waves that may be traveling across the heart at the time of the shock. Once the tissue repolarizes, the natural pacemaker of the heart can initiate the next regular heartbeat. Pulsed electric fields have shown great potential both for the ablation [1] and the defibrillation of cardiac tissue [2, 3].

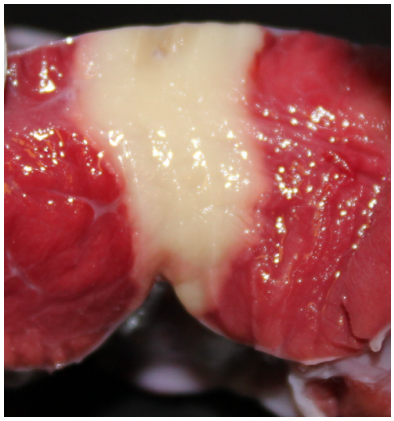

Figure 1: Cross section of ventricular lesion generated with a nanosecond pulsed electric field. Lesion is stained with triphenyl tetrazolium chloride, so ablated tissue appears white and surviving tissue is stained red. Wall thickness is 12 mm.

ABLATION WITH PULSED ELECTRIC FIELDS

In domestic pigs (n=10), hearts were exposed via sternotomy and either ablated *in vivo* (n=5) or excised, placed in a Langendorff perfusion system, and ablated (n=5). The nsPEFs consisted of 6-36 shocks of 300 ns each, delivered at 3-6 Hz with a clamp electrode; the voltage applied varied from 10-13 kV. The transmurality of each lesion was determined at three points along the lesion using a triphenyl tetrazolium chloride (TTC) stain. All atrial (94/94) and all ventricular lesions (3/3) were transmural. This includes 13/13 purse string lesions and had highly consistent width across the wall. There were no shock-induced arrhythmias or other complications during the procedure. NsPEF ablation has far better penetration than either radiofrequency or cryoablation, as demonstrated in Fig. 1, which shows an ablation through a pig left ventricle. NsPEF ablation is also faster than both radiofrequency ablation and cryoablation and it is free from thermal side effects.

DEFIBRILLATION WITH PULSED FIELDS

New Zealand white rabbit hearts (n=12) were Langendorff-perfused and two planar electrodes were placed on either side of the heart. We induced fibrillation (35 episodes) and found that single shock nanosecond-defibrillation could be achieved, with a defibrillation threshold of 2.3–2.4 kV (over 3 cm), and consistent success at 3 kV (11/11 successful attempts). Shocks uniformly depolarized the tissue, and the threshold energy needed for nanosecond defibrillation was almost an order of magnitude lower than the energy needed for defibrillation with a monophasic 10 ms shock delivered with the same electrode configuration. For the parameters studied here, nanosecond defibrillation caused no baseline shift of the transmembrane potential (that could be indicative of electroporative damage), no changes in action potential duration, and only a brief change of diastolic interval, for one beat after the shock was delivered. Histological staining with tetrazolium chloride and propidium iodide showed that effective defibrillation was not associated with tissue death or with detectable electroporation anywhere in the heart (six hearts).

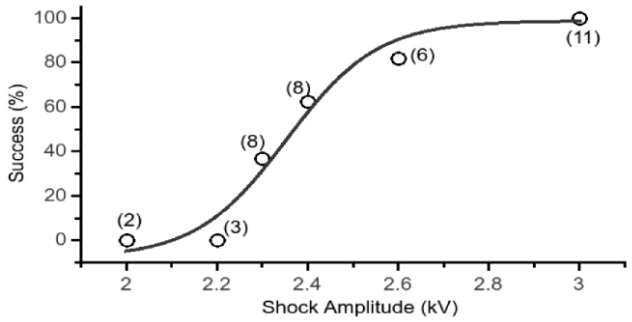

Figure 2: Defibrillation success rate as a function of stimulus amplitude. Numbers in parentheses indicate how many observations contributed to each of the data points. Solid line shows a sigmoidal function fitted to the data.

REFERENCES

[1] F. Xie et al., "Ablation of Myocardial Tissue With Nanosecond Pulsed Electric Fields," PLoS One, vol. 10, p. e0144833, (2015).

[2] F. Varghese, J. U. Neuber, F. Xie, J. M. Philpott, A. G. Pakhomov, and C. W. Zemlin, "Low-energy defibrillation with nanosecond electric shocks," Cardiovasc Res, vol. 113, pp. 1789-1797 (2017).

[3] J. U. Neuber, F. Varghese, A. G. Pakhomov, and C. W. Zemlin, "Using Nanosecond Shocks for Cardiac Defibrillation," Bioelectricity, vol. 1, pp. 240-246 (2019).

Prophylactic and Therapeutic Applications of Gene Electrotransfer

Richard Heller[1], Megan Scott[2], Chelsea Edelblute[2] and Guilan Shi[1]; *[1] Department of Medical Engineering, University of South Florida, Tampa, Florida, 33612, USA [2] Frank Reidy Research Center for Bioelectrics, Old Dominion University, Norfolk, Virginia,23508, USA*

INTRODUCTION

Gene-based medicine has made tremendous progress during the past decade including several gaining regulatory approvals. However; there are still lingering questions related to efficacy and toxicity. Delivery still remains an important hurdle to overcome. Physical delivery methods have shown increased utility. Electrotransfer has demonstrated the most progress. Gene electrotransfer (GET; electroporation) uses electric pulses to transiently permeabilize cell membranes allowing entry of extracellular nucleic acids.

Our group has explored the use of GET and have developed several delivery protocols for a variety of tissues. The focus has been to find the correct parameters that deliver the transgene in a manner that yields a reproducible expression pattern with minimal to no adverse effects. In addition, it is critical to demonstrate that delivery results in the appropriate therapeutic or prophylactic response.

PROPHYLACTIC APPLCATIONS

DNA vaccines are an attractive alternative to standard vaccines, due to potential for decreased toxicity, quick modifications to address pathogen mutation and relatively quick manufacture. The key issue with plasmid DNA-based vaccine approaches has been effective delivery. However, GET has been demonstrated to be an effective tool to enhance delivery and increase immune response [1-2].

We have recently established that the addition of moderate heat (43ºC) in combination with GET can significantly enhance delivery. We evaluated this concept for delivering a DNA vaccine against Hepatitis B Virus. Guinea pigs were injected intradermally with a plasmid encoding Hepatitis B viral surface antigen (HBSAg) followed by GET with or without moderate heating. After a prime/boost vaccination, αHBSAg serum titers indicated a 230-fold increase in antibodies when delivered with moderate heat compared to injection only and 20-fold over the delivery with GET without heat (Figure 1).

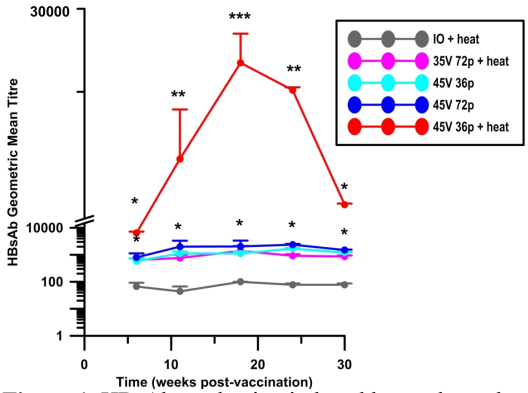

Figure 1. HBsAb production induced by moderate heat-assisted GET after a prime-boost DNA vaccination protocol against HBV. Prime and boost were separated by two weeks.

THERAPEUTIC APPLCATIONS

We previously demonstrated that treatment with plasmid IL-12 delivered with GET alone resulted in prolonged disease-free survival and induced long term immune memory protecting against challenge in a mouse melanoma model [3-4]. To further test the potential of this approach, we utilized a metastatic model consisting of subcutaneous (subq) B16.F10 tumor and B16.F10 cells expressing luciferase injected via the intraperitoneal route. Treatment with pIL-12 GET while successful in reducing or eliminating the subcutaneous tumor was only successful in about 50% of the mice in reducing or eliminating the peritoneal spread. When combining a subq injection of anti-PD-1 and pIL-12 GET to the subq tumor results were enhanced.

Observations of mice on day 60 after treatment using an In Vivo Imaging System revealed luminescence reduced to background levels in 90% of mice. The subq tumors of these mice also regressed resulting in long-term disease-free survival. Mice treated with anti-PD-1 alone or with pIL-12 without GET did not result in a response at either site.

CONCLUSIONS

GET is a powerful tool that can be utilized to efficiently deliver plasmid DNA for a variety of applications. Dependent on the therapeutic or prophylactic target a specific tissue target and transgene can be utilized. Developing a specific delivery protocol is essential to achieving the desired clinical outcome. In addition to delivering of DNA vaccines to the skin this approach could also be utilized to deliver a plasmid encoding Human Factor IX as a protein replacement therapy for treating Hemophilia B. In addition to immunotherapy for melanoma other tumor types can also be treated with this approach including breast and pancreatic cancer. Translation of GET has been moving forward and has now utilized in over 100 clinical trials.

REFERENCES

[1] NY Sardesai, DB Weiner, "Electroporation delivery of DNA vaccines; prospects for success" Curr Opin Immuno, 23(3) pp421-429, 2011.

[2] A Donate, D Coppola, Y Crua, R Heller, "Evaluation of a novel non-penetrating electrode for use in DNA vaccination" Plos One, 6(4) pp e19181, 2011.

[3] ML Lucas, R Heller, "IL-12 gene therapy using an electrically mediated nonviral approach reduces metastatic growth of melanoma" DNA Cell Biol, 22(12 pp 755-763, 2003.

[4] G Shi, C Edelblute, S Arpag, C Lundberg, R Heller, "IL-12 gene electrotransfer triggers a change in immune response within mouse tumors" Cancers, 10(12) pp 498, 2018.

Calcium electroporation as a possible novel anticancer treatment

Erika Kis *Plastic Surgery, Department of Dermatology, Medical University of Szeged, Koranyi fasor 6, 6721 Szeged, HUNGARY*

INTRODUCTION

Electroporation in combination with calcium (calcium electroporation, CaEP) has been tested as a novel anticancer treatment in vitro, in vivo and in clinical trials showing promising effect [1,2] and providing similar features to the widely used electrochemotherapy (ECT).

During ECT, a chemotherapeutic drug, bleomycin or cisplatin is electroporated into the tumour cells resulting in an increased cytotoxic effect. In CaEP calcium is administered intratumorally, followed by electrical pulses similar to ECT, causing reversible electroporation.

CELLULAR EFFECT OF CaEP

In CaEP the high intracellular concentration of calcium induces cytotoxicity; a cell is trying to re-establish the calcium homeostasis by exporting calcium from the cell with calcium ATPase and sodium potassium ATPase, which leads to increased ATP consumption. On the other hand if calcium enters the mitochondria, which is responsible for ATP production of the cell, probably will limit or destroy the mitochondrial respiration, therefore ATP production will be decreased or lost. [1,3] The resulting energy (ATP) depletion with other cellular effects (increased activity of lipases and proteases and increased concentration of reactive oxygen species) are observed to be associated with necrotic cell death.

DIFFERENCE IN SENSITIVITY BETWEEN NORMAL AND MALIGNANT CELLS

Most preclinical studies show that cancer cells are more sensitive to CaEP in comparison to normal healthy tissues. This difference in sensitivity may be explained, in part, by differences in membrane repair after electroporation, differences in the expression of calcium transporters, and changes in cellular structures. A difference in sensitivity between normal and malignant cells allow sparing normal surrounding tissue when treating tumours with calcium electroporation, which has also been observed in a veterinary study and in clinical trials.[4,3]

SYSTEMIC IMMUNE RESPONSE

Although calcium electroporation is a local treatment, it has been demonstrated in vivo that CaEP initiates a systemic immune response similarly to ECT. On immunocompetent mice, CaEP treatment of colon cancer tumors induced a complete response. When the treated mice were re-challenged with the same cancer cells, no new tumours were formed while tumours developed when pre-treated mice were challenged with different cancer cell types [5]. Systemic immune effects could be explained with increased systemic release of pro-inflammatory cytokines during CaEP. A systemic immune response was also observed in a dog treated with CaEP [6] and, in human in the first clinical trial.[7]

CLINICAL TRIALS

The results of the first clinical studies suggest that CaEP is efficient locally on different tumour types, including cutaneous metastases from breast cancer and malignant melanoma and recurrent head and neck cancer [2,8]. Although CaEP is a local treatment limited by the access to the tumour for intratumoral calcium administration and electrode placement, the first clinical trial showed that this novel anticancer treatment is also able to induce a systemic immune effect to target untreated metastases.[7] Therefore CaEP is a promising local and systemic anti-cancer treatment. Currently ongoing trials are investigating CaEP in patients with colorectal cancer in a palliative and neoadjuvant setting.

CONCLUSIONS

CaEP is a novel, efficient, safe and inexpensive cancer treatment, that does not involve any administration of cytotoxic chemotherapy. Thus it would be possible to use on patients for whom chemotherapy is contradicted.Though it is a local anticancer treatment, systemic immune effects have been observed in different studies. Further investigation is needed to fully elucidate the mechanism of action of the difference in sensitivity between normal and cancer cells and also the potential of this novel treatment.

REFERENCES

[1] Frandsen, S.K. et al Direct therapeutic applications of calcium electroporation to effectively induce tumor necrosis. *Cancer Res*. 2012, 72, 1336–1341.

[2] Falk, H. et al Calcium electroporation for treatment of cutaneous metastases; a randomized double-blinded phase II study, comparing the e_ect of calcium electroporation with electrochemotherapy. *Acta Oncol*. 2018, 57, 311–319.

[3] Frandsen, S.K. et al A Comprehensive Review of Calcium Electroporation-A Novel Cancer Treatment Modality *Cancers* 2020, 12, 290;

[4] Landstrom, F et al Electrochemotherapy.Evidence for Cell-type Selectivity In Vitro. *Anticancer Res*. 2015, 35, 5813–20

[5] Falk, H et al Electroporation Induces Tumor Eradication, Long-lasting Immunity and Cytokine Responses in the CT26 Colon Cancer Mouse Model. *Oncoimmunology* 2017,6.

[6] Kulbacka, J.P.J et al. Electrochemotherapy combined with standard and CO2 laser surgeries in canine oral melanoma. *Slov. Vet. Res*. 2017, 54, 181–186.

[7] Falk, H et al. Electrochemotherapy and calcium electroporation inducing a systemic immune response with local and distant remission of tumors in a patient with malignant melanoma. *Acta Oncol*. 2017, 56, 1126–1131.

[8] Plaschke, C.C et al Calcium electroporation for recurrent head and neck cancer: A clinical phase I study. Laryngoscope Investig. *Otolaryngol*.2019, 4, 49–56.

SHORT PRESENTATIONS

Pulsed electric field and plasma assisted treatment of microalgae *Chlorella vulgaris*

Kamilė Jonynaitė[1], Arūnas Stirkė[1], Liutauras Marcinauskas[2], Mindaugas Aikas[2], Andrius Tamošiūnas[2], Airingas Šuopys[2], Rolandas Uscila[2], Gintarė Dalmantaitė[3]; *[1] Laboratory of Bioelectrics, State Research Institute Center for Physical Sciences and Technology, Sauletekio ave. 3, LT-10257, Vilnius, LITHUANIA, [2] Lithuanian Energy Institute, Plasma Processing Laboratory, Breslaujos str. 3, LT-44403 Kaunas, LITHUANIA, [3] Vilnius University, Sauletekio Ave 7, LT- 10257 Vilnius, LITHUANIA.*

INTRODUCTION

Microalgae are increasingly viewed as renewable biological resources for a wide range of chemical compounds that can be used as or transformed into biomaterials to foster the bioeconomy of the future. Most of valuable algae compounds are accumulated inside the cell and protected by strong, rigid cell wall. Therefore, various treatment methods are used to disrupt the cell wall and extract the valuable compounds. In contrast to conventional disruption methods pulsed electric field (PEF) and non-thermal plasma treatments are considered as an alternative to overcome high energy demand [1, 2]. The aim of this work was to investigate the effect of PEF and plasma treatments combination on microalgae *Chlorella vulgaris*. Here we report our first results.

METHODS

Due to already extensively investigated microalgae treatment using PEF, the effect of plasma treatment was examined first. The gliding arc discharge technology was applied on *Chlorella vulgaris* cultivated in BG-11 medium and aquaculture wastewater. The plasma treatment was performed using these parameters: compressed air flow rate ~22.8 l/min, distance between the "knife-edge" type electrodes and surface of the algae suspension was 30 mm, treatment duration 300 s, output power 35–265 W and frequency 270 kHz. Changes of the electrical conductivity of untreated and treated algae suspension was monitored as an indicator of cell damage and leakage of intracellular compounds. Chlorophyll *a* content was determined (on 1st and 5th day after treatment) as an indication of algae viability.

Furthermore, immediately after plasma treatments, different PEF pulses (E= 26–30 kV/cm, τ = 10 µs, n = 30, f = 1 Hz) were applied to the samples. The effectiveness of combinational treatment was determined using Bradford protein assay.

RESULTS

Results obtained show that conductivity and chlorophyll a concentration in microalgae suspension depends on the treatment discharge power. When strongest plasma treatment (200–255 W) were applied increase of solution conductivity up to 50% and decrease of pigment concentration up to 40% were observed (Figure 1). However, when algae, cultivated in BG-11, was treated with lower power plasma, change of viability was not observed. Meantime, algae cultivated in wastewater exhibited growth promotion when weakest plasma power was applied.

Primary results from combinational treatment showed, that protein concentration increased up to 15% when algae was exposed to 255 W plasma and 30 kV/cm PEF treatment.

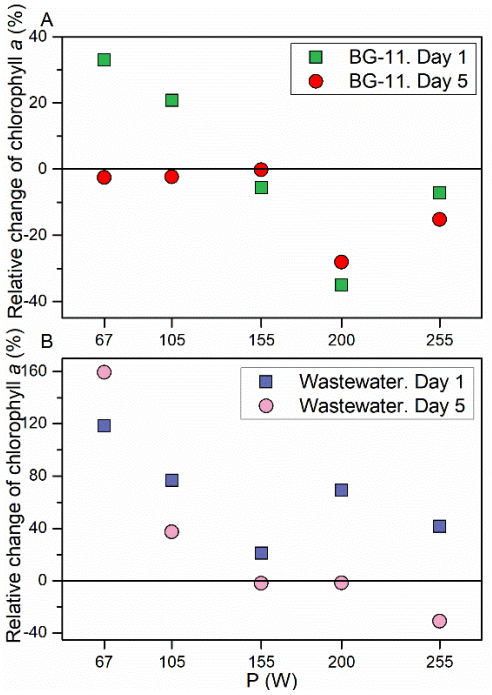

Figure 1. Relative change of extracted chlorophyll a in C. vulgaris after plasma treatment. Microalgae cultivated in BG-11 (A) and wastewater (B).

CONCLUTIONS

The combination of PEF and plasma for microalgae treatment have not been examined yet. However, our preliminary results indicates that application of intensive plasma treatment causes significant increase of conductivity and decrease of algae viability. Moreover, combination of PEF and plasma treatmentenhances protein extraction. However, further examination is needed to determine whether there is a significant increase of algae cell disruption and valuable compounds extraction.

ACKNOWLEDGMET

This work is part of ExtraIMTA project which is supported by **RTO Lithuania** association.

REFERENCES

[1] H.-J. Kim, et al, "Cold Plasma Treatment for Efficient Control over Algal Bloom Products in Surface Water," *Water*, vol. 11, no. 7, Art. no. 7, Jul. 2019.

[2] C. Eing, et al, "Pulsed Electric Field Treatment of Microalgae—Benefits for Microalgae Biomass Processing," *IEEE Transactions on Plasma Science*, vol. 41, no. 10, pp. 2901–2907, Oct. 2013.

Biological response of *Chlorella vulgaris* to pulsed electric field treatment for improvement of protein extraction

Damaris Krust[1,2], Christian Gusbeth[1], Alexander S. K. Müller[2], Georg Müller[1], Wolfgang Frey[1], Peter Nick[2]; *[1] Institute for Pulsed Power and Microwave Technology, Karlsruhe Institute of Technology, Hermann-von-Helmholtz-Platz 1, 76344 Eggenstein-Leopoldshafen, GERMANY [2] Botanical Institute, Karlsruhe Institute of Technology, Fritz-Haber-Weg 4, 76131 Karlsruhe, GERMANY*

INTRODUCTION

Pulsed electric field (PEF) treatment provides an energy-efficient and gentle alternative compared to mechanical extraction methods. However, biological processes involved are poorly understood. A recent study [1] conducted with the unicellular green microalga *Chlorella vulgaris* was able to detect proteins of nuclear, chloroplastic, and mitochondrial origin in the water-soluble extract after PEF treatment, indicating a breakdown of these cell organelles. Additionally, the DNA of the cellular residue was analysed and found to show clear DNA laddering from as soon as 2 h after PEF treatment. These are indications for a cell death that is not necrotic but regulated and these observations suggest that it might be a biotechnological strategy to administer PEF treatment at lower energy as a signal to induce cell death, rather than to use energy-intensive PEF treatments to breach membranes electrically. For this purpose, the cellular mechanisms behind cell death after PEF treatment must be understood.

METHODS

A method was established to monitor cell viability after PEF treatment in *C. vulgaris* by using cell sorting based on fluorescein diacetate (FDA). Next, the experimental parameters of PEF treatment were calibrated to a point, where a set ratio of cells undergoes cell death after treatment and the other part stays viable. With these tools in hand, the cell-death response to PEF treatment can be analysed on a quantitative base.

RESULTS AND FIGURES

PEF treatment can be applied at different specific energies. Very low energies like 0.8 J·ml^{-1} only cause a small portion of cells to die after treatment. PEF treatment as extraction method requires high biomass concentrations to make the technology cost effective. This experiment aimed at analysing the influence factor of cell density on mortality after PEF treatment by diluting high cell density suspensions directly after PEF treatment to low cell density suspensions (Figure 1). When monitoring mortality at low cell density after PEF treatment, these low energies result in a constant mortality of around 30 %. However, at higher cell density an increasing mortality over a period of 24 h can be observed. Since the cells had been separated only after pulsing, the difference cannot come from physical parameters during the PEF treatment itself but must arise from biological processes occurring after the pulse.

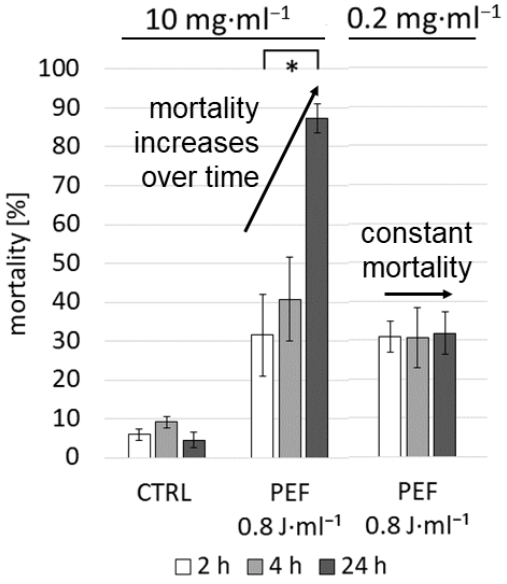

Figure 1: Influence of cell density on the mortality induced by PEF treatment. *C. vulgaris* were concentrated to high cell density of 10 mg·ml^{-1} and immediately after PEF treatment, the sample was divided. One set remained at high density, while the other set was diluted by adding sterile medium. CTRL: control without PEF treatment. Bracket indicates significant difference at $P \leq 0.05$ (*), using two-sample t-test.

CONCLUSION

A water-soluble factor released by PEF treated cells induces untreated cells to die. This cannot be merely a physical phenomenon but must involve a biological process. The high specificity is consistent with a model, where PEF treatment deploys active signalling culminating in the observed induction of programmed cell death while specifically releasing a cell-death inducing factor. Low-energy PEF treatment with subsequent incubation period could be a novel biotechnological strategy.

REFERENCES

[1] D. Scherer, D. Krust, W. Frey, G. Mueller, P. Nick, and C. Gusbeth, "Pulsed electric field (PEF)-assisted protein recovery from Chlorella vulgaris is mediated by an enzymatic process after cell death," *Algal Research*, vol. 41, p. 101536, 2019, doi: 10.1016/j.algal.2019.101536.

Current Density Imaging for Assessing Electrical Anisotropy in Muscle Tissue

Marko Stručić[1], Rok Šmerc[1], Samo Mahnič-Kalamiza[1], Igor Serša[2], Damijan Miklavčič[1], Matej Kranjc[1], *[1]University of Ljubljana, Faculty of Electrical Engineering, Tržaška 25, SI-1000 Ljubljana, SLOVENIA, [2]Jozef Stefan Institute, Jamova cesta 39, 1000, Ljubljana, SLOVENIA*

INTRODUCTION

Muscle tissue when compared to other tissue types has unique electrophysiological properties due to its fibre structure. Thus, when external electric field is applied to the muscle sample it exhibits different relative permittivity and conductivity depending on the angle of the electric field with respect to the direction fibres. This is called electrical anisotropy [1]. Measuring and assessing electrical changes in real time is of crucial importance for novel treatment approaches electroporation. Therefore, an efficient tool for electric field monitoring in observed tissue during the delivery of electroporation pulses is needed. The electric field can be reconstructed by magnetic resonance electric impedance tomography (MREIT) from current density distribution data [2]. So far, no research has assessed the usage of current density imaging (CDI) in the context of monitoring electroporation in muscle tissue. The objective of this work was to assess the feasibility of CDI to detect and assess electrical anisotropy in pork muscle tissue *ex vivo*.

MATERIALS AND METHODS

Sample tissue was collected from a domestic pig *(Sus domesticus)*, approximately one hour after slaughter. Pork tissue was collected from neck and thigh regions. Prior to the experiment samples were stored at 4°C for 48 hours.

Samples were cut in 20 mm high cylinder shapes with the diameter of 26 mm. Needle electrodes measured 1 mm in diameter and were placed either in parallel or perpendicular to the muscle fibres 10.4 mm apart.

The container was placed inside the horizontal bore superconducting magnet together with the radio-frequency (RF) probe. Electrodes were connected to an electric pulse generator, which was triggered by an MRI control unit and synchronized with the CDI pulse sequence [3]. For imaging protocol 2 consecutive 800 µs pulses were introduced with the magnitude of 100 V which provided sufficient signal-to-noise ratio. Data was collected from 6 samples that were placed so that the shared axis of both electrodes was in parallel with the muscle fibres and 6 that were placed in perpendicular position. Data was later evaluated with ImageJ (National Institutes of Health, Bethesda, MD, USA) and MatLab 2021b (Mathworks, Natick, MA).

RESULTS

Data collected from CDI imaging consistently showed displacement of current density vectors in all 6 samples where muscle fibres were perpendicular to electrode axis when compared to samples where electrode axis and muscle fibres were parallel. Additionally, magnitude diagrams show significantly higher current density amplitudes in line between electrodes for samples where fibres were parallel to the electrode axis when weighed against the samples where orientation was perpendicular. This core differences are best observable from the magnitude and vector diagrams as shown in Fig. 1.

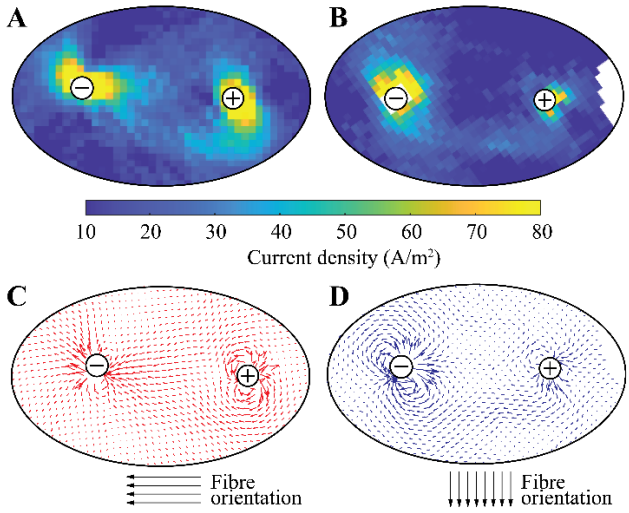

Figure 1: Diagrams A and B correspond to the magnitude of current density whereas diagrams C and D show vector representation of it. A and C show representative sample where electrode axis was placed in parallel with muscle fibres unlike B and D, which show representative sample, where electrode axis was placed perpendicularly to muscle fibres. Diagrams were cropped to exclude the surrounding noise.

CONCLUSION

In conclusion, CDI technique is suitable for detecting tissue anisotropy in biological muscle samples. It also shows great potential to be used alongside MREIT for evaluating electroporation process in real time, however additional studies are needed.

ACKNOWLEDGEMENTS

This work was supported by the Slovenian Research Agency (research core funding No. P2-0249, funding for Junior Researcher to MS and project No. J2-1733 to MK).

REFERENCES

[1] Akay, M., 2006. Wiley encyclopedia of biomedical engineering. Hoboken, N.J: John Wiley, pp.3578-3589.

[2] M. Kranjc, F. Bajd, I. Serša, and D. Miklavčič, "Magnetic resonance electrical impedance tomography for measuring electrical conductivity during electroporation," Physiological Measurement, vol. 35, no. 6, pp. 985–996, 2014.

[3] M. Kranjc, F. Bajd, I. Sersa, and D. Miklavcic, "Magnetic resonance electrical impedance tomography for monitoring electric field distribution during tissue electroporation," IEEE Transactions on Medical Imaging, vol. 30, no. 10, pp. 1771–1778, 2011.

Custom-made Four-electrode Probe for Measurement of Electrical Conductivity of Human Blood at Frequencies below 100 kHz

Niko Ištuk[1], Alessandra La Gioia[1], Hamza Benchakroun[1], Martin O'Halloran[1]; *[1] Translational Medical Device Lab, National University of Ireland Galway, University Road, H91 TK33 Galway, IRELAND*

INTRODUCTION

The knowledge of the conductivity of human blood is fundamental for medical electromagnetic applications. However, at frequencies below 1 MHz and in particular below 100 kHz data availability is limited due to the measurement challenges, including electrode polarization (EP), limited availability of human blood and difficulties in maintaining the temperature of blood. The most commonly used methods of eliminating EP is the four-electrode technique [1].

This study presents the measurements of low-frequency (i.e. below 100 kHz) conductivity of whole human blood at body temperature using the four-electrode technique using a custom made four-electrode probe.

MATERIALS AND METHODS

Measurements of electrical impedance of human blood were performed with a four-electrode probe method using a custom-made four-electrode probe. Electrical impedance was measured on ten (N=10) human blood samples. Electrical impedance data was measured using the PGSTAT204 potentiostat/galvanostat (Metrohm Autolab B.V., Utrecht, The Netherlands) in a galvanostatic mode. The measured electrical impedance was used to calculate electrical conductivity of the samples.

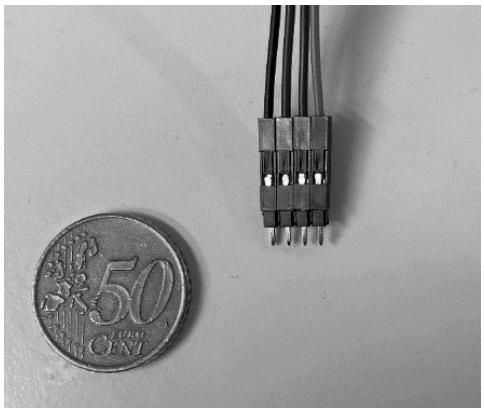

Figure 1: The four-electrode probe. The compact size of the probe allows for measurement of small samples (i.e. 6 mL).

The custom-made four-electrode probe was assembled with the parts from a standard electronics development kit and is shown in Figure 1. Four pins of a gold plated pin header (Harvin, Portsmouth, United Kingdom) were used as four electrodes in a linear array. Four male-to-female breadboard jumper cables (MikroElektronika, Belgrade, Serbia) were used to connect the pins to the PGSTAT204. The pins were connected to the PGSTAT204 in a four-electrode configuration.

RESULTS

The comparison of the results from this study and the data from the literature are shown in Figure 2 [2].

The data from this study matches very closely the data from Hirsch et al. [3] (triangle up marker) and Texter et al. [4] at 30°C (triangle left marker) as well as the data from Rosenthal and Tobias [5] (triangle right marker).

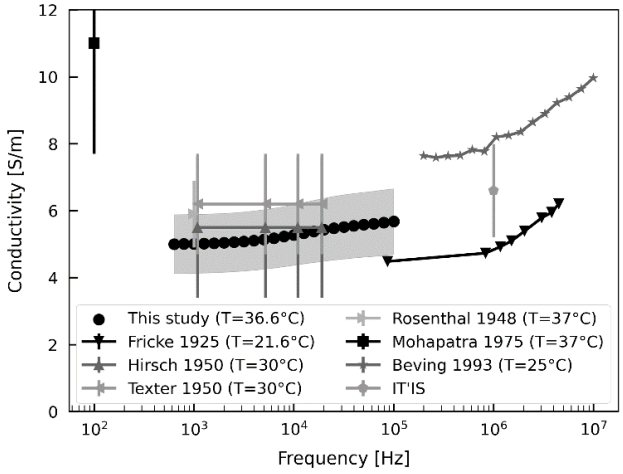

Figure 2: Mean conductivity in S/m of: human blood samples (black circles is data points, shaded is mean ± SD); and blood conductivity value from literature for human blood conductivity (mean ± SD) [2].

CONCLUSION

This study introduces a simple and low-cost four-electrode probe as a practical tool for measurements of electrical conductivity of human blood at lower frequencies.

The values of the measured conductivity are in good agreement with the data from the literature, thus validating our methodology.

REFERENCES

[1] H. P. Schwan, "Electrode polarization impedance and measurements in biological materials," Ann. N. Y. Acad. Sci., vol. 148, no. 1, pp. 191–209, Feb. 1968

[2] N. Ištuk, B. McDermott, and M. O'Halloran, "Relationship Between the Conductivity of Human Blood and Blood Counts," p. 9.

[3] F. G. Hirsch et al., "The electrical conductivity of blood : I. Relationship to erythrocyte concentration," Blood, Nov. 1950

[4] E. C. Texter et al., "The electrical conductivity of blood: II. Relation to Red Cell Count," Blood, Nov. 1950

[5] R. L. Rosenthal and C. W. Tobias, "Measurement of the electric resistance of human blood; use in coagulation studies and cell volume determinations," J. Lab. Clin. Med., Sep. 1948.

A flexible, implantable, bioelectronic electroporation device for targeted ablation of seizure foci in the brain in temporal lobe epilepsy

Rita Matta[1], Attila Kaszas[1], Martin Baca[1], David Moreau[1], Rodney O'Connor[1]; [1]*Ecole des Mines de Saint-Etienne, Campus George Charpak, 880 Route de Mimet, 13120 Gardanne, FRANCE*

INTRODUCTION

The primary method of treatment for patients suffering from drug-resistant focal-onset epilepsy is resective surgery, which adversely impacts neurocognitive function [1]. Radio frequency (RF) ablation and laser ablation are the methods with the most promise, achieving seizure-free rates similar to resection but with less negative impact on neurocognitive function. However, there remains a number of concerns and open technical questions about these two methods of thermal ablation, primarily: 1) Heating, 2) Haemorrhage and bleeding, and 3) Poor directionality. Irreversible electroporation (IRE) is a proven method of focal ablation, which circumvents all three of the primary concerns regarding focal RF and laser ablation [2]. Here, we propose a flexible implant with organic electrodes for focal ablation of epilepsy foci using electroporation. By using flexible organic electrodes, we endeavour to minimize the damage caused by the penetration of the electrodes into the brain tissue and all the adverse reactions associated therein.

METHODS

First, we designed a flexible probe for electroporation. Several geometrical configurations of microelectrodes were designed with different electrode spacing, Figure 2A shows one example. For the fabrication, we made poly(3,4-ethylenedioxythiophene)-poly(styrenesulfonate) (PEDOT:PSS) coated electrodes using an adapted photolithographic technique suitable for organic layers. In short, a parylene sacrificial layer was deposited onto a glass substrate and patterned using photolithography, to form a contact mask on which the conductive polymer was deposited. Mechanical lift-off of the parylene leaves behind a patterned conducting polymer film. Metal (Au) contact pads were pre-patterned on the substrate using lithography to facilitate reproducible electrical contact with the probes of a probe station.

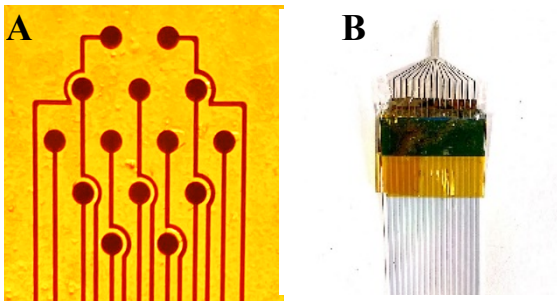

Figure 1: **A)** 14 Electrodes covered with PEDOT:PSS. **B)** Probe connected to ZIF cable.

Devices were then connected to a ZIF cable (zero insertion force), as well as a micro packaging technique to form a high barrier packaging solution, resistant to light, liquid and heat.

Next, devices were electrically characterized in order to assess the behaviour of probes at the high voltages and short pulse widths used in electroporation. The behaviour of electrodes was tested when stimulated with pulse widths ranging from 1-100 µs, in the range useful for irreversible electroporation. The impedance and electrochemical behaviour of electrodes was also be characterized by fast cyclic voltammetry (CV). For implantation, a surgical procedure was performed, as described previously [3]. Briefly, adult Thy1-GCaMP6f mice (25-72 weeks old) were anesthetised (0.9 % isoflurane), and the device implanted in the 4 mm craniotomy above the visual cortex, covered with a coverslip and cemented in.

RESULTS AND FIGURES

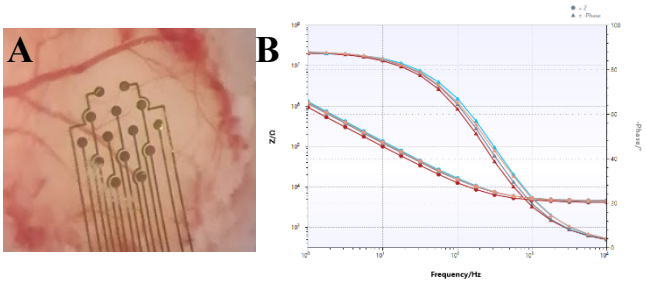

Figure 2: **A)** Implanted probe above the mouse visual cortex. **B)** Electrochemical impedance spectrum (EIS) of 4 selected electrode pads.

REFERENCES

[1] P. Kwan and M. Brodie, "Early identification of refractory epilepsy," *The New England Journal of Medicine,* vol. 3, no. 342, pp. 314-319, 2000.

[2] M. Howenstein and K. Sato, "Complications of Radiofrequency Ablation of Hepatic, Pulmonary, and Renal Neoplasms," *Semin intervent Radiol,* vol. 3, no. 27, pp. 285-295, 2010.

[3] M. J. Donahue, A. Kaszas, G. F. Turi, B. Rozsa, A. Slézia, I. Vanzetta, G. Katona, Malliaras, George G., G. G. Malliaras and A. Williamson, "Multimodal characterization of neural networks using highly transparent electrode arrays," eNeuro, pp. 0187-18.2018, 2018.

Overcoming Diverse Length-Scales During Gene Electro-Transfer

Shaurya Sachdev[1], Tjasa Potočnik[1], Aswin Muralidharan[2], Dipendra K. Choudhary[2], Sara Feijoo Moreira[2], Yasmine Keehnen[2], Dayinta L. Perrier[2], Lea Rems[1], Michiel T. Kreutzer[2], Pouyan E. Boukany[2], Damijan Miklavčič[1]; *[1]Faculty of Electrical Engineering, University of Ljubljana, Trzaska 25, SI-1000 Ljubljana, SLOVENIA, [2]Department of Chemical Engineering, Delft University of Technology, van der Maasweg 9, Delft 2629 HZ, The NETHERLANDS*

During *in vivo* gene electro-transfer (GET), the DNA molecules carrying the therapeutic gene must overcome multiple barriers – interstitial, cell membrane and the cytoplasmic – before they can reach the nucleus of target cells. These barriers define multiple length-scales that DNA molecules must traverse for a successful GET. In the interstitium, DNA molecules must overcome length-scales ranging from *O*(1-1000) µm, whereas the cell membrane defines a length-scale of only O(1-10) nm for the DNA molecules to overcome.

In this work, work we look at the role of electrophoresis provided by the pulsed electric fields (PEF) in overcoming the length-scales associated with the cell membrane and the interstitial barriers.

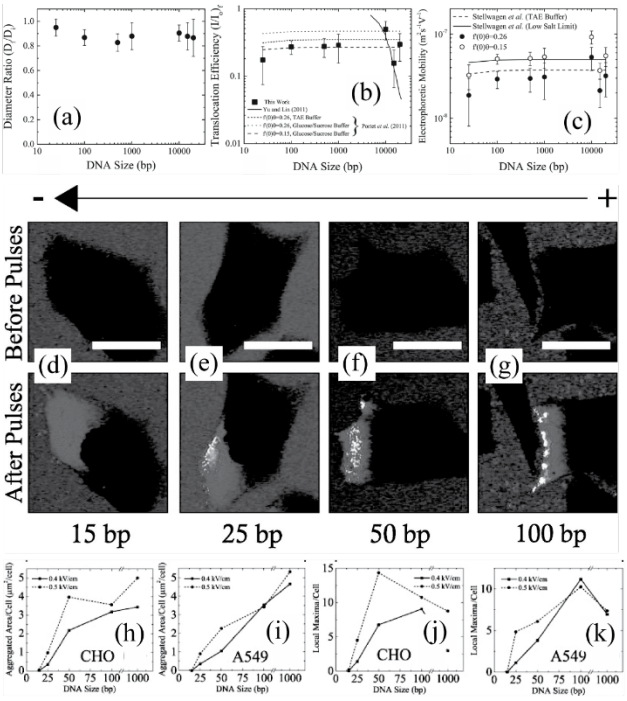

Figure 1: DNA molecules traversing the cell membrane barrier with a length-scale of *O*(1-10) nm. (a-c) DNA translocation across lipid-bilayer of vesicles [1]. (d-k) DNA translocation across the cell membrane of CHO and A549 cells [2].

We find that both electrophoresis (by PEF) and electrostatics (DNA aggregation) dictate the transport of DNA across the cell membrane [1-2] (Figure 1). The electrophoretic mode of transport is independent of DNA size [1-2], whereas the electrostatic (aggregated) mode of transport depends on DNA size [2]. The size at which DNA molecules begin to aggregate at the cell membrane is 15 bp, which is consistent with Onsager's theory of isotropic to nematic phase transition of rod-like (DNA) molecules [2].

For the interstitial barrier, DNA molecules can be found in high and low concentration zones *in vivo* [3-5]. Our calculations show that DNA molecules are present at an average distance of *O*(1-10) µm and *O*(0.1-0.5) µm from the closest cell membrane in the low and high DNA concentration zones, respectively [5] (Figure 2 – a, b). The electrophoresis provided by high voltage (HV) PEF (Figure 2) is insufficient to bring DNA molecules close to cells in low concentration zones which exist *in vivo* due to inhomogeneous DNA distribution, thus requiring additional low voltage (LV) PEF. However, electrophoresis provided by HV PEF is sufficient to bring DNA molecules in contact with the cell membrane in high concentration zones (Figure 2). These calculations are consistent with experimental observations on HV and LV PEF for different DNA concentrations [3-4].

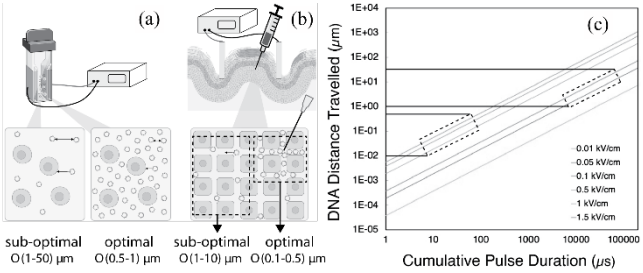

Figure 2: Average cell-DNA distance *in vitro* and *in vivo*. Electrophoresis provided by PEF.

REFERENCES

[1] Sachdev, S. *et al*., DNA translocation to giant unilamellar vesicles during electroporation is independent of DNA size. *Soft matter* 2019, 15(45), pp.9187-9194.

[2] Sachdev, S. *et al*., DNA-membrane complex formation during electroporation is DNA size-dependent. *Biochimica et Biophysica Acta (BBA)-Biomembranes* 2020, 1862(2), p.183089.

[3] Pavlin, M., *et al*., The role of electrophoresis in gene electrotransfer. *The Journal of membrane biology* 2010, 236(1), pp.75-79.

[4] Kandušer, M., *et al*., Mechanisms involved in gene electrotransfer using high-and low-voltage pulses—an in vitro study. *Bioelectrochemistry* 2009, 74(2), pp.265-271.

[5] Sachdev, S., Potocnik. T., Rems, L., Miklavcic, D., Submitted (*in review*, 2021).

Gene Electrotransfer for Vaccination Against COVID-19

Živa Modic[1,2], Špela Kos[1], Tanja Jesenko[1,2], Katarina Žnidar[1], Eva Reberšek[3], Helena Jakopič[3], Urška Kamenšek[1,3], Boštjan Markelc[1, 4], Gregor Serša[1, 4] and Maja Čemažar[1,5]; *[1] Institute of Oncology Ljubljana, Department of Experimental Oncology, Zaloška cesta 2, SI-1000 Ljubljana, SLOVENIA [2]Faculty of Medicine, University of Ljubljana, Vrazov trg 2, SI-1104 Ljubljana, SLOVENIA [3]Biotechnical Faculty, University of Ljubljana, Jamnikarjeva ulica 101, SI-1000 Ljubljana, SLOVENIA [4]Faculty of Health Sciences, University of Ljubljana, Zdravstvena pot 5, SI-1000 Ljubljana, SLOVENIA [5]Faculty of Health Sciences, University of Primorska, Polje 42, SI-6310 Izola, SLOVENIA*

INTRODUCTION

DNA vaccination is one of the immunotherapeutic approaches being developed for vaccination against COVID-19 and other diseases [1]. Due to poor responses often observed in clinical trials, different methods are being investigated for increasing its efficacy. Among them, gene electrotransfer (GET) is used to enhance the delivery of DNA vaccines [2]. The aim of this study was to investigate the feasibility of this approach *in vitro* in the context of vaccination against SARS-CoV-2 antigens.

METHODS

We used two murine cell lines: myoblast cell line C2C12 and fibroblast cell line L929 as model cell lines (ATCC) for muscle and skin vaccination, respectively. GET of a combination of commercially available plasmid DNA encoding spike (S) or nucleocapsid (N) protein of COVID-19 (InvivoGen) was performed using IGEA Cliniporator connected to plate electrodes with 2 mm gap, using 8 pulses with a voltage-to-distance ratio of 1300 V/cm, duration of 100 µs, and pulse repetition frequency of 5 kHz. The expression of N and S proteins was assessed on mRNA level via qRT-PCR as well as on protein level using ELISA assays (Abcam, Krishgen Biosystems).

RESULTS

N and S proteins were expressed on mRNA level after GET with individual plasmids encoding for N or S proteins or using their combination (Figure 1). Furthermore, N protein was detected on the protein level both in the cell lysate as well as in the cell medium of both cell lines after GET (Figure 2). S protein was not detectable using the available commercial ELISA kits.

CONCLUSIONS

In the present study, we have successfully transfected murine myoblast and fibroblast cell lines C2C12 and L929 using GET with plasmids encoding for N or S protein of COVID-19 or their combination. We have shown that GET of a combination of N and S expression plasmids results in the expression of N and S mRNA. Production of N was further confirmed on protein level, while other assays are required for S protein detection. This approach can now be tested in *in vivo* setting.

ACKNOWLEDGEMENTS

This work received funding from Slovenian Research Agency (ARRS): research programme P3-0003.

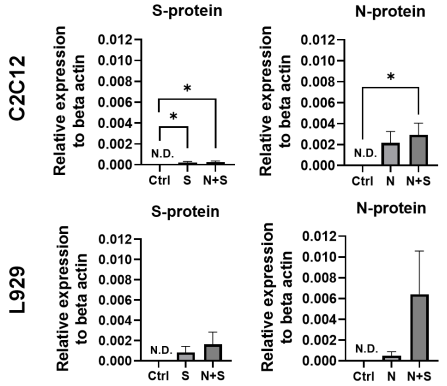

Figure 1: Expression of N and S on mRNA level after GET with N or S encoding plasmids as determined with qRT-PCR (*: p value ≤ 0.05; unpaired t test).

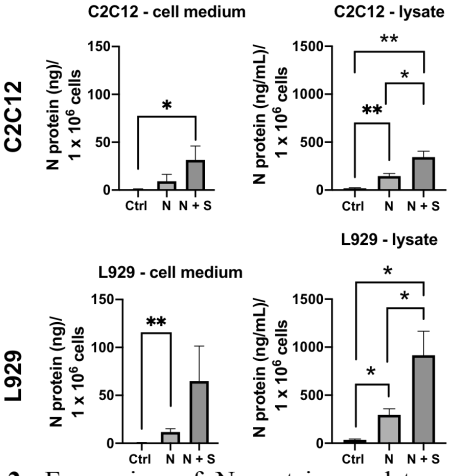

Figure 2: Expression of N protein as determined with ELISA (*: p value ≤ 0.05, **: p value ≤ 0.005; unpaired t test).

REFERENCES

[1] K. L. Flanagan, C. R. MacIntyre, P. B. McIntyre, and M. R. Nelson, "SARS-CoV-2 Vaccines: Where Are We Now?," *J. Allergy Clin. Immunol. Pract.*, 2021, doi: 10.1016/J.JAIP.2021.07.016.

[2] L. Lambricht, A. Lopes, S. Kos, G. Sersa, V. Préat, and G. Vandermeulen, "Clinical potential of electroporation for gene therapy and DNA vaccine delivery," *Expert Opin. Drug Deliv.*, vol. 13, no. 2, pp. 295–310, Feb. 2016, doi: 10.1517/17425247.2016.1121990.

The influence of ion channel blockers on prolonged membrane depolarization following conventional electroporation

Anja Blažič[1], Manon Guinard[1,2], Lea Rems[1]; [1]*University of Ljubljana, Faculty of Electrical Engineering, Trzaska 25, SI-1000 Ljubljana, SLOVENIA;* [2] *Université de Strasbourg, Télécom Physique Strasbourg, FRANCE*

INTRODUCTION

The integrity of the cell membrane presents a barrier that sometimes needs to be transiently disrupted to deliver molecules into the cell. High-intensity pulsed electric fields with pulse durations ranging from nanoseconds to milliseconds are used to achieve such increase in cell membrane permeability. The applied electric field triggers a phenomenon called electroporation [1].

In the cell membrane there exists a wide variety of ion channels that can influence membrane permeability. Indeed, a previous study has shown that ion channel blockers can influence the prolonged membrane depolarization, following electroporation induced by 10 ns, 34 kV/cm pulse [2]. In our study we have tested four ion channel blockers using a fluorescent indicator of transmembrane potential for their ability to inhibit membrane depolarization response caused by a longer, more conventional 100 µs, 1.4 kV/cm pulse.

METHODS

U-87 MG human glioblastoma cells were plated in Nunc Lab-Tek II chambered coverglass three to four days before the experiments. On the day of the experiments, the cells were stained for 30 min at 37°C with the Component A of the FLIPR Membrane Potential Assay Red (Molecular Devices, #R7291), which was diluted in Live Cell Imaging Solution (Invitrogen, #A14291DJ). Afterwards, the cells were incubated for 5 min with the chosen ion channel blocker and placed on the microscope stage. The cells were exposed to a single 100 µs, 1.4 kV/cm pulse, delivered by βtech B10 pulse generator through a pair of Pt-Ir wire electrodes. Time lapse images of the cells were acquired before and after pulse application. The cells were imaged on inverted microscope Leica DMi8 with LED8 illumination source controlled by the LasX software (all Leica Microsystems). The membrane potential dye was excited with green LED (555/28 nm) and its florescence was passed through DFT51010 filter and detected with the Leica DFC9000 Gt camera.

RESULTS

Upon electroporation, the membrane potential depolarizes and remains depolarized for several minutes, as can be seen by the prolonged increase in the fluorescence of the membrane potential indicator (control curve in Fig. 1). We tested whether ion channels blockers are able to influence this post-pulse membrane depolarization. We used four ion channel blockers, which have been previously shown to influence depolarization in U-87 MG cells following exposure to 10-ns-long pulses [1]: the potassium channel blocker TEA, the calcium channel blockers nifedipine and mibefradil, and the TRPM8 channel blocker AMTB. Indeed, in the presence of ion channel blockers AMTB and TEA, the membrane depolarized significantly less. The ion channel blockers nifedipine and mibefradil, however, had marginal influence on depolarization.

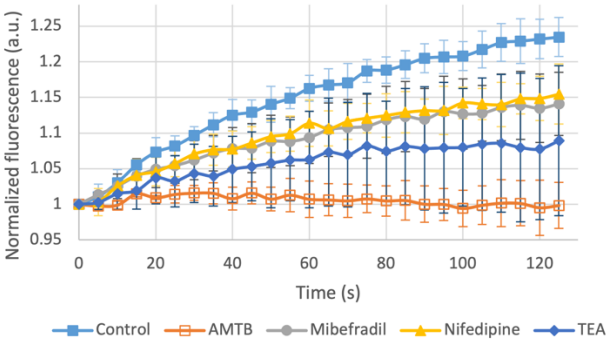

Figure 1: The influence of four ion channels blockers (AMTB, mibefradil, nifedipine, TEA) on membrane depolarization. Cells were exposed to a single 100 µs, 1.4 kV/cm pulse, which was delivered at time 0 s.

CONCLUSIONS

Our preliminary results suggest that ion channel blockers, such as AMTB and TEA, can reduce the extent of membrane depolarization following electroporation with conventional 100-µs-long pulses, similarly as has been previously observed after exposure nanosecond pulses [1]. Our future experiments will focus on testing whether these ion channel blockers can also influence cell survival after electroporation and can be used for fine-tuning the outcomes in electroporation-based treatments.

ACKNOWLEDGEMENTS

This work was supported by funding from the European Union's Horizon 2020 research and innovation programme under the Marie Skłodowska-Curie grant agreement No. 893077, and by funding from Slovenian Research Agency (ARRS) under project no. J2-2503.

REFERENCES

[1] M.L. Yarmush, A. Golberg, G. Serša, T. Kotnik, and D. Miklavčič, "Electroporation-Based Technologies for Medicine: Principles, Applications and Challenges", Annu. Rev. Biomed. Eng. 2014, 16:295-320.

[2] R.C. Burke, S.M. Bardet, L. Carr, S. Romanenko, D. Arnaud-Cormos, P. Leveque, and R.P. O'Connor, " Nanosecond Pulsed Electric Fields Depolarize Transmembrane Potential via Voltage-Gated K+, Ca2+ and TRPM8 Channels in U87 Glioblastoma Cells," *BBA – Biomembranes*, vol. 1859, pp. 2040-50, 2017.

Modelling of non-invasive drug delivery through skin electroporation

Georgios Kougkolos[1,2], Juliette Simon[1,3], Lionel Laudebat[2,4], Sorin Dinculescu[2], Muriel Golzio[3], Zarel Valdez-Nava[2], Emmanuel Flahaut[1]; *[1]CIRIMAT, Université de Toulouse, CNRS UMR 5085, INPT, UPS, 31062 Toulouse, France, [2]LAPLACE, Université de Toulouse, CNRS UMR 5213, INPT, UPS, 31062 Toulouse, FRANCE, [3]IPBS, Université de Toulouse, CNRS UMR 5089, UPS, 31077 Toulouse, FRANCE, [4]INU Champollion, Université de Toulouse, 81012 Albi, FRANCE*

INTRODUCTION

The skin presents an accessible and convenient route for non-invasive drug delivery. Transdermal delivery platforms, such as nicotine patches, can effectively administer drugs through the epidermis in a controlled manner. Advantages include increased bioavailability, sustained steady-state blood concentration levels, self-administration and reduced frequency of dosing, which in turn improve patient compliance and quality of life. However passive diffusion of drugs through the skin is only achieved for low MW (<400-500 Da), relatively lipophilic molecules (log*P* around 2 to 3) [1]. Electroporation can temporarily increase the permeability of the skin allowing bigger or more hydrophilic molecules to overcome the skin barrier. We have developed a drug delivery platform, consisting of a nanocomposite, electrically-conductive hydrogel, acting as a drug reservoir and an electrode for the application of electrical pulses [2].

METHODS

Double-wall Carbon Nanotubes (DWCNTs, 2.5 mg/ml) are incorporated into an agarose hydrogel matrix, to increase the electrical conductivity and rigidity of the system.

The electrical conductivity and impedance of the nanocomposite hydrogels under varying water content and DWCNT concentration is measured. DC conductivity is measured using an Ampere meter with an integrated electrical source (Keithley 2410 SMU), while AC impedance is measured with a broadband dielectric analyser (Novocontrol Alpha-A). Electroporation experiments are made on freshly isolated, hairless mouse skin.

A numerical model of mouse skin is developed, considering the conductivity and width of the skin layers [3]. Finite Element Method (FEM) simulations of the model in steady state, under electrical field application are computed.

RESULTS

The incorporation of CNTs increases the conductivity of agarose hydrogels from 10^{-6} to 10^{-4} S/m (Figure 1).

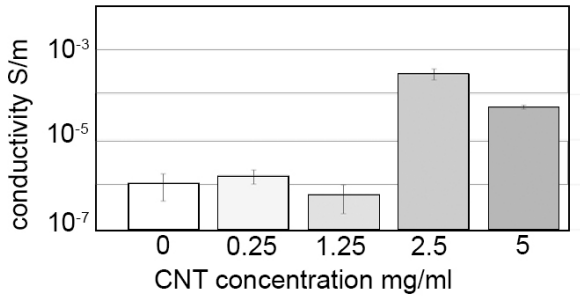

Figure 1: Nanocomposite hydrogel electrical conductivity (measured at 1 V DC) with increasing DWCNT content.

The simulations show that for a hydrogel conductivity ≥ 10^{-4} S/m, an electric field of 0.5 kV/cm penetrates into the stratum corneum. The current density passes through the skin and the substrate (a wet gauze) and exits through the second hydrogel/electrode (Figure 2).

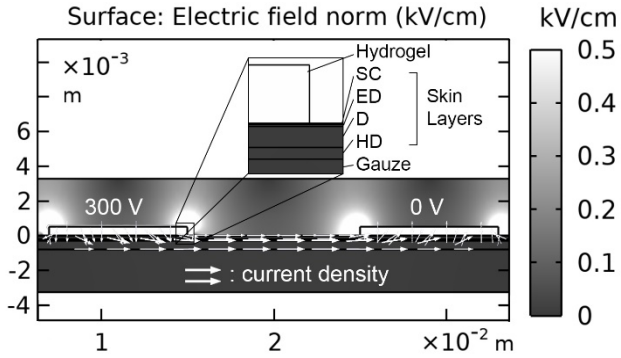

Figure 2: FEM steady state simulation of electric field and current density distribution in hydrogels and mouse skin during electroporation. The skin layers modelled are Stratum Corneum (SC), Epidermis (ED), Dermis (D) and Hypodermis (HD). Applied voltage is 300 V.

CONCLUSIONS

The conductivity measurements reveal an electrical percolation threshold between 1.25 and 2.5 mg/ml CNT, concentration after which the conductivity increases by two orders of magnitude.

The FEM simulations show that the system's electrical and geometrical properties play an important role in the distribution of the electric field through the skin, under electroporation conditions. These simulations will allow us to optimize the parameters before applying them to *ex vivo* experiments for validation.

REFERENCES

[1] S. Wiedersberg et R. H. Guy, Transdermal drug delivery: 30+ years of war and still fighting!, Journal of Controlled Release, vol. 190, p. 150-156, sept. 2014.

[2] J.-F. Guillet, E. Flahaut, et M. Golzio, A Hydrogel/Carbon-Nanotube Needle-Free Device for Electrostimulated Skin Drug Delivery, ChemPhysChem, vol. 18, no 19, p.2715-2723, 2017.

[3] N. Pavselj et D. Miklavcic, Numerical Models of Skin Electropermeabilization Taking Into Account Conductivity Changes and the Presence of Local Transport Regions, Plasma Science, IEEE Transactions on, vol. 36, p. 1650-1658, sept. 2008.

Bleomycin based electrochemotherapy for deep-seated soft tissue sarcomas- initial results in Szeged, Hungary

Aurel Ottlakan[1], Gyorgy Lazar[1], Judit Olah[2], Renata Koszo[2], Katalin Hideghety[2], Andras Nagy[3], Gabor Vass[4] Erika Gabriella Kis[4], [1]University of Szeged, Department of Surgery, 6720, Szeged, Semmelweis str. 8, HUNGARY, [2]University of Szeged, Department of Oncotherapy, 6720, Szeged, Koranyi alley 12, HUNGARY, [3]University of Szeged, Department of Radiology, 6725, Szeged, Semmelweis str. 6, HUNGARY, [4]University of Szeged, Department of Dermatology and Allergology, 6720, Szeged, Koranyi alley 6, HUNGARY

INTRODUCTION

Recently bleomycin based electrochemotherapy (ECT) has emerged not only as the treatment of superficial skin tumors, but also in case of advanced, metastatic and surgically inoperable deep-seated lesions [1].

PATIENTS AND METHODS

During a 2-year period (February 2019- February 2021) 6 cases of inoperable soft tissue sarcomas (STS) have been treated by bleomycin based electrochemotherapy at the University of Szeged Department of Surgery. All treatments were performed under general anesthesia, with the use of long needle VGD (variable geometry) electrodes. In each case treatment planning for VGD electrode placement was preoperatively carried out by Pulsar software. In anatomically challenging cases ECT electrode positioning was confirmed by intraoperative ultrasonography. Each procedure was started 8 minutes after intravenous bleomycin administration (15000 IU/m2) and ECT lasted for a maximum of 40 minutes [2]. Prior to- and after treatment (1 week, 1-2-4-6 months) prospective data collection was carried out. Patient health status and QoL was assessed at each follow-up visit. Tumor response was evaluated through imaging (CT/MRI) 2 months after ECT treatment as per RECIST 1.1 guidelines, adverse events were evaluated and graded according to Common Terminology Criteria for Adverse Events (CTCAE) version 4.0 [3].

RESULTS

Four male- and 2 female patients (6 cases in total, 1 patient treated twice) with deep seated, histologically confirmed fibromyxoid sarcoma (n=3), epitheloid sarcoma (n=3) and liposarcoma (n=1) were treated. Mean age was 63.66 years, mean BMI (body mass index) 29.21, mean ASA (American Score of Anaesthesiologists) 2.5, mean CCI (Charlson Co-morbidity Index) 6.66. Two tumors were located in the axilla, 3 in the lower extremities and 2 at the gluteal region, with mean tumor size of 11.05 cm (as largest tumor diameter). Mean operative time was 40 minutes, with mean hospital stay of 1.83 days. Follow-up CT/MRI at two months confirmed 2 CR (complete response), 3 PR (partial response) and 1 case of PD (progressing disease). No major postoperative adverse events were observed, and only mild level postoperative pain (mean VAS: 2) was observed.

CONCLUSION

Our results suggest, that bleomycin based ECT is safe and effective alternative treatment for inoperable deep-seated advanced- and metastatic tumors resulting in decreased burden to the patient in terms of operative time and hospital stay.

REFERENCES

[1] Simioni, S. Valpione, et al. “Ablation of soft tissue tumours by long needle variable electrode-geometry electrochemotherapy: final report from a single-arm, single-centre phase-2 study,” *Sci Rep,* vol 10, p. 2291, 2020.

[2] J. Gehl, G. Sersa G, et al. “Updated standard operating procedures for electrochemotherapy of cutaneous tumours and skin metastases,” *Acta Oncol,* vol. 57, pp. 874-882, 2018.

[3] P.G. Casali, N. Abecassis, et al. “ESMO Guidelines Committee and EURACAN. Soft tissue and visceral sarcomas: ESMO-EURACAN Clinical Practice Guidelines for diagnosis, treatment and follow-up,” *Ann Oncol,* vol. 29, pp. 268-269, 2018.

New non-invasive and real-time imaging modality to evaluate the effects of electrochemotherapy on melanoma

Bastien Jouanmiqueou[1], Marie-Pierre Rols[1], Xavier Orlik[2], Muriel Golzio[1] ; *[1]Institute of Pharmacology and Structural Biology (IPBS), 205 rte de Narbonne, 31077 Toulouse cedex 4, FRANCE (CNRS UMR 5089); [2]National Office for Aerospace research studies (ONERA), 2 Av Edouard Belin, 31000 Toulouse, FRANCE*

INTRODUCTION

According to the World Health Organization, the incidence of skin cancer has increased sharply in recent decades. Currently, the diagnosis of melanoma by dermatologists is carried out using a subjective method for appearance assessment (ABCDE rule), however, 20% of melanomas are not detected and can progress to metastases. Therefore, the development of new technologies to facilitate clinical examination is necessary. The early detection of skin cancer and the study of tumor neoangiogenesis using a novel polarimetric imaging method based on the DYnamic Polarized Speckle Analysis (DYPSA), based on the polarimetric properties of light [1] is proposed as a safe method, in real time. It optimizes the detection of signals scattered from deep layers under the skin and uses a different approach compared to currently available optical instruments. Namely, we observe movements generated by vascular activity at the micrometric scale. In this study, we used real time DYPSA imaging to visualize the effects of electropermeabilization (EP) on tumor vascularization [2], and to evaluate the effectiveness of the treatment of tumors by electrochemotherapy (ECT) [3].

MATERIALS AND METHODS

In vivo acquisitions by DYPSA were carried out on anesthetized adult female mice (C57Bl/6). Observations using a Microvasculoscope (ITAE, France, https://www.itae.fr/en), Such imaging was made before the intradermal injection of $0.5.10^6$ B16-F10 cells (20 µL), during the tumor growth to see the tumor vascular angiogenesis as well as after treatments. For ECT treatment, bleomycin (1 mg/kg) was IV injected and combined with electrical parameters (8 pulses lasting 100µs, 1100V/cm, 1Hz).

RESULTS

Few days after the cell injection, the DYPSA signals showed the establishment of a "tumoral vascular network" which correlated with the location of the tumor on the contrast images. Immediately after EP, we could also observe the well-known "vascular lock" as evidenced by an absence of DYPSA signal. Finally, during the days following ECT, the "tumoral vascular network" in the ECT treated area between the electrodes disappeared, as well as the tumor, which disappeared few days later (figure 1).

DISCUSSIONS

At early stages, this new imaging modality allowed us to observe the establishment of tumor microvascularization, even when the tumor was not visible to the naked eye. In addition, real-time visualization led to optimal positioning of the electrodes when treating tumors. It was also possible to verify the correct delivery of the EP, by observing the "Vascular Lock". Finally, this system allowed the evaluation of the effectiveness of an anti-tumor treatment.

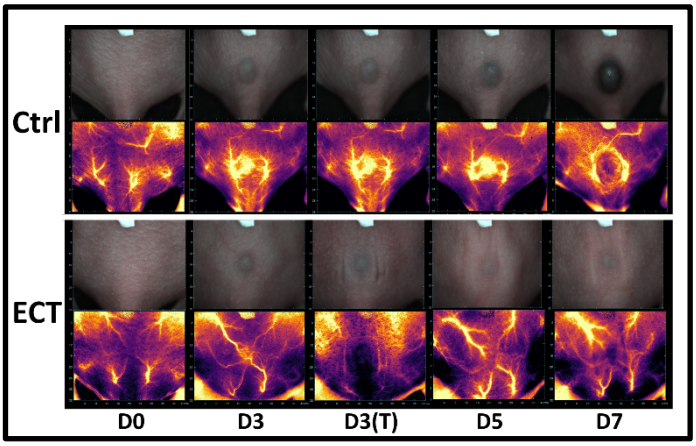

Figure 1: Photographs and DYPSA images taken on the same mice over different time points, evidencing tumor angiogenesis in the control (D3) as well as the vascular lock (D3T) in the treated mice, in which the tumor gradually resorbed (D5, D7).
ECT (Electrochemotherapy); (D): Day ; (T): 30 sec After Treatment

CONCLUSIONS

This innovative approach of non-invasive real-time imaging allows studying tumor vessels genesis as well as evaluating the efficacy of anti-tumor treatments such as electrochemotherapy.

REFERENCES

[1] C. Li and R. Wang, "Dynamic laser speckle angiography achieved by eigendecomposition filtering" *Journal Biophotonics*, vol. 10(6-7), pp. 805-810, 2017.

[2] B. Markelc, E. Bellard, G. Sersa, T. Jesenko, S. Pelofy, J. Teissié, R. Frangez, M.P Rols, M. Cemazar and M. Golzio, "Increased permeability of blood vessels after reversible electroporation is facilitated by alteration in endothelial cell-to-cell junctions" *Journal of Controlled Release*, vol. 276, pp. 30-41, 2018.

[3] T. Garcia-Sanchez, B. Mercadal, M. Polrot, A. Muscat, H. Sarnago, O. Lucia and LM. Mir "Successful tumor Electrochemotherapy using Sine Waves" *IEEE Transactions on Biomedical Engineering*, vol. 67(4), pp. 1040-1049, 2019.

Expression of leukocytes and PMCA isoform 1 and 4 in calcium electroporated cutaneous metastases from different cancer histologies

Sara Willum Bro[1], Mille Vissing[2], Julie Gehl[3], Anja Sørensen[1]. *[1] University, Department of Science and Environment, Universitetsvej 1, 4000 Roskilde, DENMARK. [2] Center for Experimental Drug and Gene Electrotransfer (C*EDGE), Department of Clinical Oncology and Palliative Care, Zealand University Hospital, Roskilde, DENMARK. [3] Department of Clinical Medicine, Faculty of Health and Medical Sciences, University of Copenhagen, Copenhagen, DENMARK.*

INTRODUCTION

Calcium electroporation (CaEP) is a novel anti-cancer treatment for cutaneous metastases which is simple and safe to use with relatively low treatment cost [1]. Electroporation causes the cell membrane to permeabilize leading to loss of ATP and influx of extracellular calcium, initiating the plasma-membrane calcium ATPase (PMCA) pumps to re-establish the calcium concentration. Permeability transition pores open causing deprivation of the electrochemical gradient conducting ATP production, which might lead to a total ATP depletion and necrosis of the tumour [2]. This effect is proven in different cancer histologies, with a difference in sensitivity [3]. Additionally, CaEP is shown to increase pro-inflammatory cytokines, eliminate tumours in CT26 colon mouse model and initiate further protective immunity, indicating a T-cell-response [4]. This thesis-planned study is going to investigate the presence of leukocytes infiltration in CaEP-treated cutaneous metastases and the expression and importance of PMCA pumps in cutaneous metastases and cancerous cell lines.

METHODS

Patients with different cancer diagnoses are enrolled in a clinical trial (NCT nr: **NCT04259658)** at Zealands University Hospital and receive CaEP treatment for cutaneous metastases. Biopsies from the treated cutaneous metastases are snap frozen immediately after excision. We wish to quantitatively measure the expression of different leukocyte markers in vivo using quantitative polymerase chain reaction (qPCR), see table 1. Furthermore, expression of PMCA isoform 1 and 4 will be measured by qPCR. The protein content of both leukocyte markers and PMCA 1 and 4 in the biopsies will be determined by Western blot.

Table 1: Overview of leukocyte qPCR targets.

Leukocytes	**Targets**
Th1	IFNγ, IL-12
Th2	IL-4, IL-10
Th17	IL-6, GCSF

EXPECTATIONS

Previous studies have measured increase in pro-inflammatory cytokines and found indication of T-cell response. It is therefore expected to see an increase in expression of leukocyte makers [4]. A decrease in the expression of isoform 1 and 4 of the PMCA pumps is expected. It is shown that healthy cells cope better than cancer cells when treated with CaEP. The isoform 4 has the highest ability to export calcium and can be decreased in cancer cells compared to healthy cells [3], [5].

ACKNOWLEDGEMENTS

A special thanks to `Det Sundhedsvidenskabelige Forskningsfond (RSSF)´ for the generous grant given to Sara Willum Bro.

REFERENCES

[1] H. Falk, L. W. Matthiessen, G. Wooler, and J. Gehl, 'Calcium electroporation for treatment of cutaneous metastases; a randomized double-blinded phase II study, comparing the effect of calcium electroporation with electrochemotherapy', *Acta Oncol.*, vol. 57, no. 3, pp. 311–319, Mar. 2018, doi: 10.1080/0284186X.2017.1355109.

[2] Frandsen, H. Gissel, P. Hojman, T. Tramm, J. Eriksen, and J. Gehl, 'Direct Therapeutic Applications of Calcium Electroporation to Effectively Induce Tumor Necrosis', *Cancer Res.*, vol. 72, no. 6, pp. 1336–1341, Mar. 2012, doi: 10.1158/0008-5472.CAN-11-3782.

[3] Frandsen *et al.*, 'Normal and Malignant Cells Exhibit Differential Responses to Calcium Electroporation', *Cancer Res.*, vol. 77, no. 16, pp. 4389–4401, Aug. 2017, doi: 10.1158/0008-5472.CAN-16-1611.

[4] H. Falk *et al.*, 'Calcium electroporation induces tumor eradication, long-lasting immunity and cytokine responses in the CT26 colon cancer mouse model', *OncoImmunology*, vol. 6, no. 5, p. e1301332, May 2017, doi: 10.1080/2162402X.2017.1301332.

[5] S. K. Frandsen, L. Gibot, M. Madi, J. Gehl, and M.-P. Rols, 'Calcium Electroporation: Evidence for Differential Effects in Normal and Malignant Cell Lines, Evaluated in a 3D Spheroid Model', *PLOS ONE*, vol. 10, no. 12, p. e0144028, Dec. 2015, doi: 10.1371/journal.pone.0144028.

LABORATORY SAFETY

Laboratory safety S1

Duša Hodžić
University of Ljubljana, Faculty of Electrical Engineering

BIOSAFETY

There are four biosafety levels (BSLs) for working with live organisms; each BSL consists of combinations of laboratory practices and techniques, safety equipment and laboratory facilities. Each combination is specifically appropriate for the operations performed, the suspected routes of transmission of the organisms and the laboratory function or activity.

Biosafety Level 1 represents a basic level of containment. It is suitable for work involving well-characterized agents not known to cause disease in healthy adult humans. The potential hazard to laboratory personnel and the environment is minimal.

Biosafety Level 2 is suitable for work involving agents that can cause human disease and have a moderate potential hazard to personnel and the environment. Precautions must be taken for handling and disposing of contaminated material, especially needles and sharp instruments. The laboratory must have limited access.

Biosafety Level 3 is used in laboratories where work is done with pathogens, indigenous or exotic agents which may cause serious or potentially lethal disease as a result of exposure by the inhalation route. Such microorganism can present a serious hazard to workers and a risk of spreading to the community, but there is usually effective prophylaxis or treatment available. BSL 3 requires special facilities with self-closing double doors and sealed windows, decontamination of clothing before laundering and controlled access.

Biosafety level 4 is required for work with pathogens which pose a high individual risk of aerosol-transmitted laboratory infections and life-threatening disease, for which there is no effective prophylaxis or treatment available. Such organisms present a serious hazard to workers and may present a high risk of spreading to the community. The BSL 4 facility is generally a separate building with specialized ventilation and waste management systems to prevent release of live pathogens to the environment.

GENERAL SAFETY RULES FOR WORKING IN THE LABORATORY

The following basic safety rules should be observed at all times in the laboratory:

1. Wash your hands with liquid soap and dry them with paper towels upon entering and prior to leaving the laboratory.
2. Wear laboratory coat and gloves. Tie back loose hair.
3. Do not carry your personal belongings in the laboratory; place them in specified locations – never on bench tops.
4. Do not smoke, eat, drink, apply cosmetics or insert contact lenses in a laboratory.
5. Keep doors and windows closed during the laboratory session to prevent contamination from air currents.
6. Contaminated spots on clothes or body can be sprayed with disinfectant and washed with water. Contaminated material should be put into special containers.
7. If you had any contact with hazardous chemicals while wearing your gloves, change the gloves before you touch other laboratory equipment, do not touch your face or your clothes with contaminated gloves.
8. Do not allow water or any water-based solution to come into contact with electrical cords or conductors. Make sure your hands are dry when you handle electrical equipment.

9. Report all accidents immediately to the instructor.

RULES FOR HANDLING CHEMICALS

Almost all chemicals can be harmful in some way and prolonged exposure may cause long-term effects as yet unknown. Preparation of hazardous chemicals must be conducted under the fume hood.

When handling chemicals the following rules must be strictly met:

1. **Always read labels before handling any chemical**. Learn hazard warning symbols which are displayed on the labels.
2. Take care to avoid spillage - if this occurs, neutralize any hazard and clean up immediately, including the outside of the container.
3. Some chemicals have a delayed or cumulative effect. Inform the instructor if any feeling of being unwell occurs when using chemicals.
4. Chemicals must not be disposed of by indiscriminate washing down the sink. Carefully read the appropriate material safety data sheet and follow the instructions.

CHEMICAL HAZARD SYMBOLS


Explosive


Mutagenic, carcinogenic, causing respiratory sensitization


Oxidizing


Corrosive


Extremely/Highly flammable


Dangerous for the environment


(Very) Toxic


Pressurized gasses


Harmful

PIPETTING TECHNIQUE

Pipetting is one of the most frequent tasks in the laboratory and it directly affects the success and repeatability of the experiments. It is critical to follow good pipetting practice techniques.

ASEPTIC TECHNIQUE

Aseptic technique is a combination of procedures designed to reduce the probability of infection. In spite of the introduction of antibiotics, contamination with microorganisms remains a problem in tissue culture. Bacteria, mycoplasma, yeasts and fungal spores may be introduced by operator, atmosphere, work surfaces, solutions and many other sources. In order to avoid contamination aseptic technique should be used while handling cell cultures.

Correct aseptic technique provides a barrier between microorganisms in the environment and the culture within its flask or dish. Hence, all materials that will come into direct contact with the culture must be sterile and manipulations designed in such manner that exclude direct link between the culture and its nonsterile surroundings.

The elements of aseptic technique are a sterile work area, good personal hygiene, sterile reagents and media, and sterile handling.

Rules for sterile work:

1. Start with completely clear work area and wipe the surface with 70% alcohol and a sterile gauze.
2. Spray and wipe your hands with 70% ethanol.
3. Clean the outside of the containers and other objects with 70% ethanol before placing them in the microbiological safety cabinet.
4. The work surface should be uncluttered and contain only items required for a particular procedure; it should not be used as a storage area.
5. Remove everything that is no longer required and clean with 70% alcohol before the next procedure.
6. Arrange items to have easy access to all of them without having to reach over one item to get to another.
7. Work within your range of vision, e.g., insert a pipette in the pipetting device with the tip of the pipette in your line of sight continuously and not hidden by your arm.
8. Clean up any spillage immediately with absorbent tissues and wipe with 70% alcohol.
9. Remove everything when you finish and wipe the work surface with 70% ethanol.
10. Use ultraviolet light to sterilize the air and exposed work surfaces in the microbiological safety cabinet between uses.

GMO

GMO is an abbreviation for genetically modified organism. GMO is an organism that is created when a recipient (host) organism, with the help of a vector, successfully incorporates the insert in its genetic material and can transfer it to its descendants.
Closed system is a laboratory or some other closed room for GMO work.

Recipient (host) organism = cell/organism which accepts genetic material from the original organism or the environment, replicates and expresses it and can transfer it to its descendants.
Parent organism = recipient organism before the genetic change
Original organism = organism from which the genetic material for transfer in the host is acquired
Vector = DNA tool used in genetic engineering to harbour genes of interest and transfer them to the host
Insert = genetic material that is integrated into a vector.

Example: In cell and molecular biology, the GFP **(**green fluorescent protein) gene **[insert]** is frequently used as a reporter of expression. GFP is a protein that exhibits bright green fluorescence when exposed to light in the blue to ultraviolet range. It was first isolated from the jellyfish *Aequorea victoria* **[original organism]**, although many marine organisms have similar green fluorescent proteins. It is carried on plasmids **[vector]** to the target cells **[parent organism].** The cells that manage to express the protein are called **host organisms** (GMO).

When working with GMO, traceability is essential. For that it is necessary to keep a good operating and autoclave log book. Operating log is used for writing down essential GMO information, work procedure, solid and liquid waste management and potential work related accidents. Autoclave log is a record of all waste that has been autoclaved.

GMO waste can be deactivated in two different ways – thermic or chemical treatment. Deactivation prevents the GMO`s to migrate out of the closed system. Sterilized liquids can be washed down the sink, dry sterilized solid waste can be thrown in municipal waste.

In case of a GMO accident the biosafety commissioner needs to be informed and his/her directions should be followed. If a spillage occurs there has to be enough absorbent material to absorb all the liquid. Work surfaces should be decontaminated with a disinfectant.

FURTHER READING:

Freshney R. I. Culture of animal cells: a manual of basic technique.3rd ed. Wiley-Liss, Inc. New York, 1994.

http://www.biotechnology-gmo.gov.si/eng/genetically-modified-organisms/

NOTES

Electroporation hardware safety S2

Eva Pirc
University of Ljubljana, Faculty of Electrical Engineering

ELECTRIC SHOCK

Possible consequences of the current flow through the human body are ventricular fibrillation, cardiac asystole, respiratory arrest and burns. Voltages greater than 50 V applied across dry unbroken human skin or pulse energies above 50 J can cause ventricular fibrillation, if they produce electric currents above 30 mA in body tissues through the chest area. Frequently, the individual cannot let go of the power source due to involuntary muscle contraction. Side effect are conditioned by path of electric current, its magnitude, tissue characteristics and exposure time. The most sensitive organs to electric properties in human body are the heart and the brain. Human body is much more sensitive to mains-frequency alternating current (50/60 Hz) then to either direct current or high-frequency currents. Pain perception and muscle contraction at a given current level depend strongly on body weight and voltage/current frequency. For example, 10 mA current at frequency of 50/60 Hz can result in strong muscle contraction, in a person that weights approximately 50 kg, but sensitivity decreases with the frequency increase. The amount of voltage needed to produce same effects depends on the contact resistance between the human and the power source. When dealing with high voltages we always have to keep in mind that air breakdown voltage is about 30 kV/cm, so also a non-direct contact can be dangerous.

GENERAL SAFETY PRECAUTIONS FOR WORKING WITH HIGH VOLTAGES

The following basic safety rules should be observed at all times in the laboratory:

1. Never work alone when dealing with high voltages. Consider having a co-worker with knowledge about equipment and risks.
2. Never leave electrical circuits/devices under high voltages when you are not present.
3. Before working with high voltage devices consider the potential risks. Do not have any contacts with conductive parts of device and keep distance from conductors under high voltage. Keep in mind that air breakdown can occur when dealing with voltages above 30 kV/cm.
4. Before high voltage circuit manipulation, switch OFF the power supply and discharge all high voltage capacitors (preferably through high voltage resistor).
5. Check if all high voltage capacitors are discharge using voltmeter.
6. Use only your right hand to manipulate high voltage electronic circuits, avoid simultaneous touching of two elements and make sure you are not grounded. Wear rubber bottom shoes or sneakers. Set up your work area away from possible grounds that you may accidentally contact.
7. When using electrolytic capacitors:
    a. DO NOT put excessive voltage across them,
    b. DO NOT put alternating current (AC) across them,
    c. DO NOT connect them in reverse polarity.
8. Make sure all high voltage connections, tools and instruments are adequately insulated and rated for the voltage and current used.
9. If someone comes in a contact with a high voltage, immediately shut off the power. Do not attempt to move injured person in contact with a high voltage.
10. In the event of an electrical fire do not use water but special fire extinguishers used for fires caused by electric current.
11. Do not wear any jewellery or other objects that could accidentally come in contact with the conductive parts of electrical circuit.
12. Protect your ears and eyes due to possible discharge sounds and element explosions.

NOTES

LABORATORY EXERCISES

The influence of Mg^{2+} ions on gene electrotransfer efficiency L1

Saša Haberl Meglič, Mojca Pavlin
University of Ljubljana, Faculty of Electrical Engineering

Duration of the experiment: day 1: 60 min; day 2: 60 min
Max. number of participants: 4
Location: Cell Culture Laboratory 3
Level: Basic

PREREQUISITES

Participants should be familiar with the Safety rules and Rules for sterile work in cell culture laboratory. No other specific knowledge is required for this laboratory practice.

THEORETICAL BACKGROUND

Gene electrotransfer is a non-viral method used to transfer genes into living cells by means of high-voltage electric pulses. An exposure of a cell to an adequate amplitude and duration of electric pulses leads to transient increase of cell membrane permeability for molecules which are otherwise deprived of membrane transport mechanisms. This allows various nonpermeant molecules, including DNA, to be transported across the membrane and enter the cell. Although mechanisms of the process are not yet fully elucidated, it was shown that several steps are crucial for gene electrotransfer: interaction of plasmid DNA (pDNA) with the cell membrane, translocation of pDNA across the membrane, migration of pDNA towards the nucleus, transfer of pDNA across the nuclear envelope and gene expression (Figure 1).

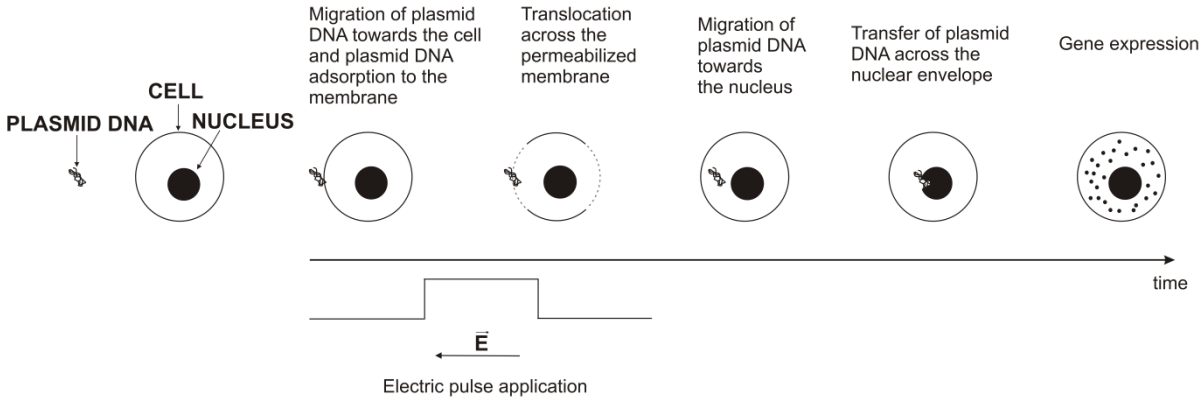

Figure 1. Steps involved in gene electrotransfer.

Many parameters have been described, which can influence the efficiency of gene electrotransfer. A few published reports have shown that the concentration of Mg^{2+} ions in electroporation medium has important impact on forming a complex between DNA and the cell membrane during application of electrical pulses. Namely, DNA is negatively charged polyelectrolyte and Mg^{2+} ions can bridge the DNA with negatively charged cell membrane. But it was shown that Mg^{2+} ions at higher concentrations may bind DNA to the cell membrane strong by enough to prevent translocation of DNA across the membrane and into the cell during electroporation consequently gene electrotransfer efficiency is decreased.

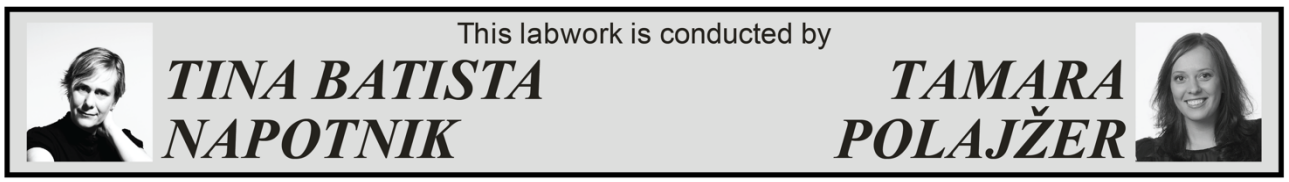

The aim of this laboratory practice is to demonstrate how different Mg^{2+} concentrations in electroporation medium affect the efficiency of gene electrotransfer and cell viability.

EXPERIMENT

We will transfect Chinese hamster ovary cells (CHO-K1) with plasmid DNA (pEGFP-N_1) that codes for GFP (green fluorescent protein) using two different electroporation media (see Protocol section). To generate electric pulses Jouan GHT 1287 electroporator (Jouan, St. Herblain, France) will be used. Pulses will be monitored on osciloscope (LeCroy 9310C).

We will determine gene electrotransfer efficiency and cell viability for both electroporation media.

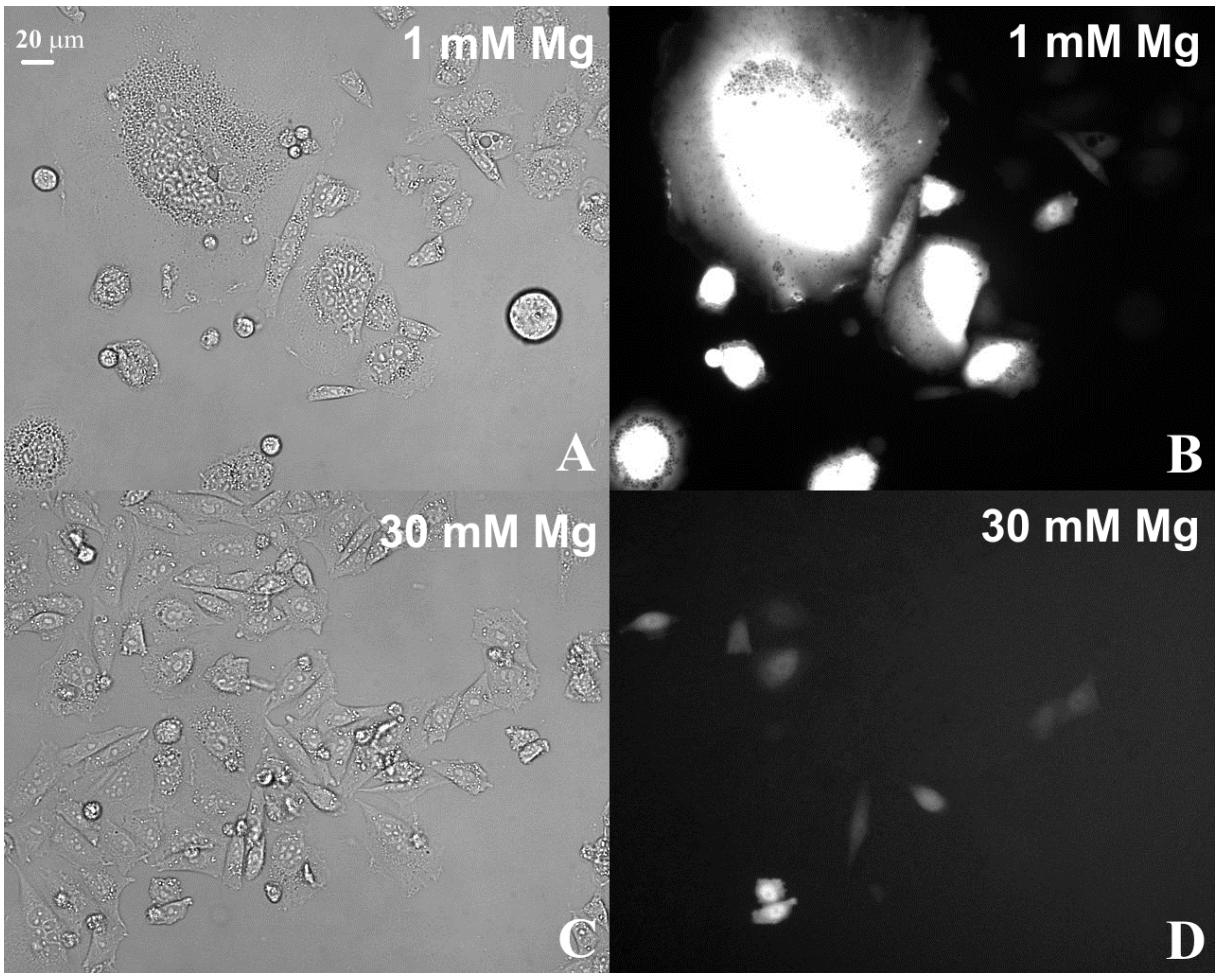

Figure 2. Gene electrotransfer of plated CHO cell 24 h after pulse application in 1 mM Mg or 30 mM Mg media. 8 x 1 ms (stainless steel wire electrodes with inter-electrode distance d = 2 mm; applied voltage U = 140 V resulting in electric field strength E = 0.7 kV/cm) pulses were applied with repetition frequency of 1 Hz to deliver pEGFP-N_1 (concentration of DNA in electroporation media was 10 μg/ml) into the cells. Phase contrast images of treated cells for (A) 1 mM Mg and (C) 30 mM Mg media and fluorescence images of treated cells for (B) 1 mM Mg and (D) 30 mM Mg media are presented. To visualize transfection 20x objective magnification was used.

Protocol 1/2 (Gene electrotransfer with different electroporation media): CHO cells will be grown in multiwells as a monolayer culture in Ham's tissue culture medium for mammalian cells with 10% fetal bovine serum (Sigma-Aldrich Chemie GmbH, Deisenhofen, Germany) at 37º C. Cells will be plated 24 h before the experiment in concentration 5 x 10^4 cells per well.

Just before the experiment remove culture media and replace it with 150 µl of electroporation media containing plasmid DNA with concentration 10 µg/ml. Use 1 mM or 30 mM electroporation media. Sucrose molarity has also been changed in order to attain the molarity of the media:

a) **1 mM Mg media** (10 mM phosphate buffer Na_2HPO_4/NaH_2PO_4, 1 mM $MgCl_2$, 250 mM sucrose; pH = 7.2)
b) **30 mM Mg media** (10 mM phosphate buffer Na_2HPO_4/NaH_2PO_4, 30 mM $MgCl_2$, 160 mM sucrose; pH = 7.2)

Incubate cells with plasmid DNA for 2-3 minutes at room temperature. Then apply a train of eight rectangular pulses with duration of 1 ms, U = 140 V resulting in electric field strength E = 0.7 kV/cm and repetition frequency 1 Hz to deliver plasmid DNA into the cells. Use stainless steel wire electrodes with inter-electrode distance d = 2 mm.
Cells in the control are not exposed to electric pulses.
Immediately after exposure of cells to electric pulses add 37.5 µl of fetal calf serum (FCS-Sigma, USA). Incubate treated cells for 5 minutes at 37ºC and then add 1 ml of culture media.

Protocol 2/2 (Determining gene electrotransfer efficiency and cell viability): After 24 h incubation at 37ºC determine the difference in gene electrotransfer efficiency and cell viability for both electroporation media by fluorescent microscopy (Leica, Wetzlar, Germany) at 20x magnification using GFP filter with excitation at 488 nm.

You will determine gene electrotransfer efficiency from the ratio between the number of green fluorescent cells (successfully transfected) and the total number of viable cells counted under the phase contrast. You will obtain cell survival from phase contrast images as the ratio between the number of viable cells in the treated sample and the number of viable cells in the control sample.

FURTHER READING:

Haberl S., Pavlin M., Miklavčič D. Effect of Mg ions on efficiency of gene electrotransfer and on cell electropermeabilization. *Bioelectrochemistry* 79: 265-271, 2010
Haberl S., Kandušer M., Flisar K., Bregar V.B., Miklavčič D., Escoffre J.M., Rols M.P., Pavlin M. Effect of different parameters used for in vitro gene electrotransfer on gene expression efficiency, cell viability and visualization of plasmid DNA at the membrane level. *J Gene Med* 15: 169-181, 2013
Rosazza C., Haberl Meglič S., Zumbusch A., Rols M.P., Miklavčič D. Gene electrotransfer: a mechanistic perspective. *Curr Gene Ther* 16: 98-129, 2016

NOTES & RESULTS

Electroporation media	Treated viable cells	Viable cells in control	Green fluorescent cells	Gene electrotransfer efficiency [%]	Viability [%]
1 mM Mg media					
30 mM Mg media					

NOTES & RESULTS

Monitoring cell membrane electroporation with ratiometric fluorescent dye Fura-2AM

L2

Gorazd Pucihar
University of Ljubljana, Faculty of Electrical Engineering

Duration of the experiments: 60 min
Max. number of participants: 4
Location: Cell Culture Laboratory 1
Level: Advanced

PREREQUISITES

Participants should be familiar with Laboratory safety (S1). The basic knowledge of handling with cells is required for this laboratory practice.

THEORETICAL BACKGROUND

Exposure of a biological cell to a sufficiently strong external electric field leads to a detectable increase of membrane permeability, a phenomenon termed electropermeabilization. Because it is assumed that an increased permeability is related to the occurrence of hydrophilic pores in the membrane, the phenomenon is often termed electroporation. Provided that the parameters of the electric field (amplitude, duration, number of pulses, frequency) are moderate, the increased permeability is reversible, and cells recover within a few minutes after the exposure. During the state of high permeability the molecules for which the membrane is otherwise impermeable (e.g. drugs, DNA) can be transported across the membrane. Electroporation is nowadays used in food processing, biotechnology, molecular biology, and different fields of medicine. It has already become an established method in oncology for electrochemotherapy of tumors, and holds great promises in gene therapy.

The efficiency of electroporation is influenced by the parameters of the electric field, cell size and geometry, and physiological characteristics of the medium surrounding the cell. Different fluorescent dyes (e.g. Propidium Iodide, Lucifer Yellow, Fura-2, Fura-3,…) can be employed to investigate the influence of these parameters on electroporation and the same dyes can be used to monitor electroporation.

The aim of this laboratory practice is to monitor electroporation with fluorescent dye and to determine the effect of cell size, shape and orientation on the efficiency of electroporation.

EXPERIMENT

We will monitor cell membrane electroporation using a fluorescent calcium sensitive indicator Fura-2AM. Calcium ions, present in the extracellular medium, do not readily cross an intact (nonporated) cell membrane and the intracellular Ca^{2+} concentration is low. Once the membrane becomes permeable due to electroporation, Ca^{2+} ions enter the cells, where they bind to the dye and change its excitation and emission spectrum (Figure 1).

This labwork is conducted by

TINA BATISTA NAPOTNIK

A B

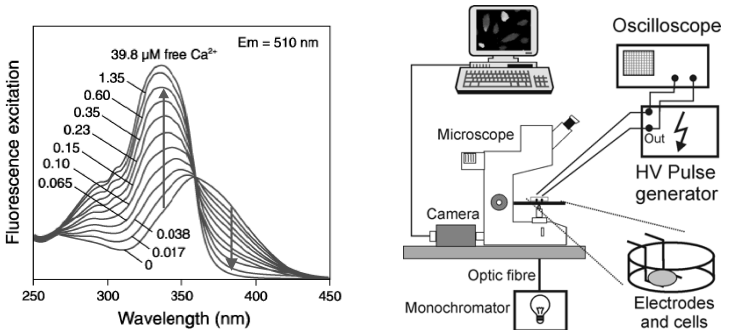

Figure 1: (A) Fluorescence excitation spectra of Fura-2 for different concentrations of Ca^{2+} (image from *http://probes.invitrogen.com/handbook/figures/0554.html*). (B) Schematic of the experiment.

Protocol: The experiments will be performed on Chinese hamster ovary cells (CHO) grown in Lab-Tek chambers (Nunc, Germany) in culture medium HAM-F12 supplemented with 10% fetal bovine serum, L-glutamine (all three from Sigma-Aldrich) and antibiotics. Plate 1.5×10^5 cells on cover glass of Lab-Tek chamber and keep them for 12-16 hours in the incubator. Before experiments, replace the culture medium with fresh medium containing 2 µM Fura-2 AM (Life Technologies). After 25-30 minutes of incubation at 37°C wash the excess dye and leave 1.5 ml of culture medium in the chamber.

Place the chamber under a fluorescence microscope (Zeiss AxioVert 200) and use ×63LD objective. Insert two parallel Pt/Ir wire electrodes with a 4 mm distance between them to the bottom of the chamber. Acquire the images using a cooled CCD camera (VisiCam 1280) and MetaFluor 7.7.5 software (Molecular Devices).

Using a ELECTRO cell B10 (BetaTech, France) device, deliver one electric pulse of 100 µs with voltages varying from 150 to 300 V. Immediately after the pulse, acquire two fluorescence images of cells at 540 nm, one after excitation with 340 nm and the other after excitation with 380 nm. Divide these two images in MetaFluor to obtain the ratio image ($R = F_{340}/F_{380}$). Wait for 5 minutes and apply pulse with a higher amplitude. After each pulse, determine which cells are being electroporated (Figure 2). Observe, which cells become electroporated at lower and which at higher pulse amplitudes.

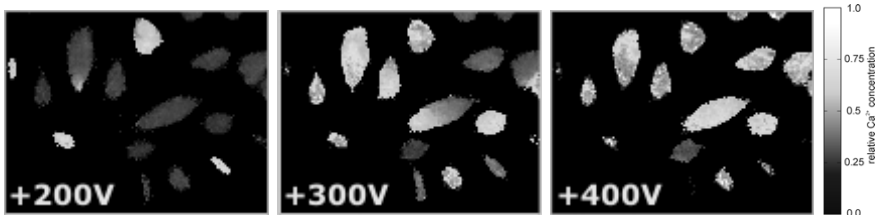

Figure 2: Cells stained with Fura-2AM and exposed to electric pulse with increasing amplitude.

FURTHER READING:

Neumann, E., S. Kakorin, and K. Toensing. Fundamentals of electroporative delivery of drugs and genes. *Bioelectrochem. Bioenerg.* 48:3-16, 1999.

Teissié, J., and M. P. Rols. An experimental evaluation of the critical potential difference inducing cell membrane electropermeabilization. *Biophys. J.* 65:409-413, 1993.

Grynkiewicz, G., M. Poenie, and R.Y. Tsien. A new generation of Ca^{2+} indicators with greatly improved fluorescence properties. *J. Biol. Chem.* 260:3440-3450, 1985.

Teruel M.N., and T. Meyer. Electroporation-induced formation of individual calcium entry sites in the cell body and processes of adherent cells. *Biophys. J.* 73:1785-1796, 1997.

Valič B., Golzio M., Pavlin M., Schatz A., Faurie C., Gabriel B., Teissié J., Rols M.P., and Miklavčič D. Effect of electric field induced transmembrane potential on spheroidal cells: theory and experiment. *Eur. Biophys. J.* 32: 519-528, 2003.

Towhidi L., Kotnik T., Pucihar G., Firoozabadi S.M.P., Mozdarani H., Miklavčič D. Variability of the minimal transmembrane voltage resulting in detectable membrane electroporation. *Electromagn. Biol. Med.* 27: 372-385, 2008.

Pucihar G., Krmelj J., Reberšek M., Batista Napotnik T., Miklavčič D. Equivalent pulse parameters for electroporation. *IEEE T. Biomed. Eng.* 58: 3279-3288, 2011.

NOTES & RESULTS

NOTES & RESULTS

Visualization of local ablation zone distribution between two needle electrodes L3

Tjaša Potočnik, Alenka Maček Lebar
University of Ljubljana, Faculty of Electrical Engineering

Duration of the experiments: 60 min
Max. number of participants: 4
Location: Cell Culture Laboratory 2 or Cell Culture Laboratory 3
Level: basic

PREREQUISITES

Participants should be familiar with Laboratory safety (S1) and Electroporation hardware safety (S2). No other specific knowledge is required for this laboratory practice.

THEORETICAL BACKGROUND

Electroporation is the method in which by applying external electric field of sufficient amplitude and duration membrane of exposed cells becomes permeabilized for molecules that otherwise cannot pass cell membrane. After reversible electroporation cell membrane reseals. With increasing amplitude of electric field the level of cell membrane permeabilization and the number of cells that are permeabilized increases. When pulses with sufficient magnitude and duration are applied, cell death is achieved and the process is defined as irreversible electroporation (IRE). IRE is an emerging ablation technique inducing apoptosis in successfully treated cells or tissues. Usually there is a sharp border between treated and untreated tissue regions because only the cells that are exposed to high enough electric field are ablated. Effective prediction of electric field can be obtained by numerical modeling, which includes the shape and position of the electrodes and parameters of electric pulses (amplitude, duration, number, frequency) used as well as electrical properties of the tissue. Using treatment planning, IRE offers benefits over other cancer therapies because it can be performed near large blood vessels, nerves, and ducts without causing damage to these structures, sparing extracellular matrix.

Electroporation can be detected by measuring increased transport of molecules across the membrane. Cell uptake of dyes, either fluorescent molecules (lucifer yellow, yo-pro-1, propidium iodide) or colour stains (such as trypan blue), is most often used for *in vitro* electroporation detection. Trypan blue can be used as an indicator of plasma membrane integrity and of cell viability. Trypan blue is normally impermeant to healthy cells. When cell membrane integrity is compromised, the dye is able to enter the cell and stains cellular structures blue, especially nuclei, making the cell appear blue. Cells that take up this dye several hours after exposure to electrical pulses are usually considered dead or dying.

The aim of this laboratory practice is to visualize local ablation zone distribution between two needle electrodes with increasing pulse amplitude using trypan blue.

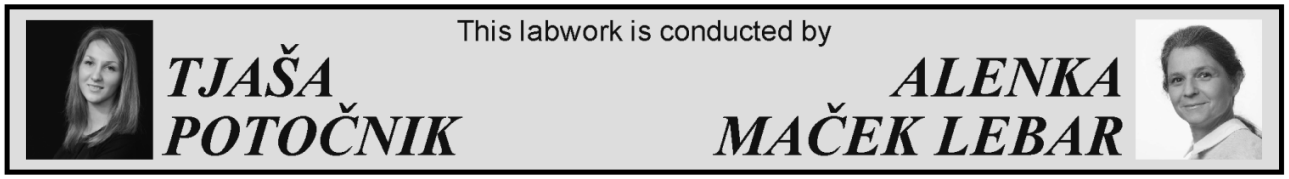

EXPERIMENT

We will visualize local ablation zone distribution between two needle electrodes using trypan blue. The effect of the pulse amplitude on the local ablation zone distribution between two needle electrodes will be determined for a train of eight 100 µs rectangular pulses delivered with the repetition frequency 1 Hz. The area of blue cells that is a consequence of efficient ablation increases with increasing pulse amplitude is presented in Figure 1.

Protocol: You will use Chinese hamster ovary cells (CHO), plated 48 h before experiment in concentration 2.5 x 10^5 cells per tissue culture dish. Cells are attached to the culture dish surface. Immediately before electric pulses are applied replace the growth medium with electroporation buffer. As electroporation buffer you will use isotonic 10 mM K_2HPO_4/KH_2PO_4 containing 1 mM $MgCl_2$ and 250 mM sucrose with pH 7.4. You will use needle electrodes 1 mm apart. For pulse delivery Gemini X2 electroporator (Hardvard apparatus BTX, USA) will be used. It can produce square and exponential pulses. During the experiment current will be monitored with an oscilloscope and a current probe. Electric field in the needle surrounding can be calculated numerically.

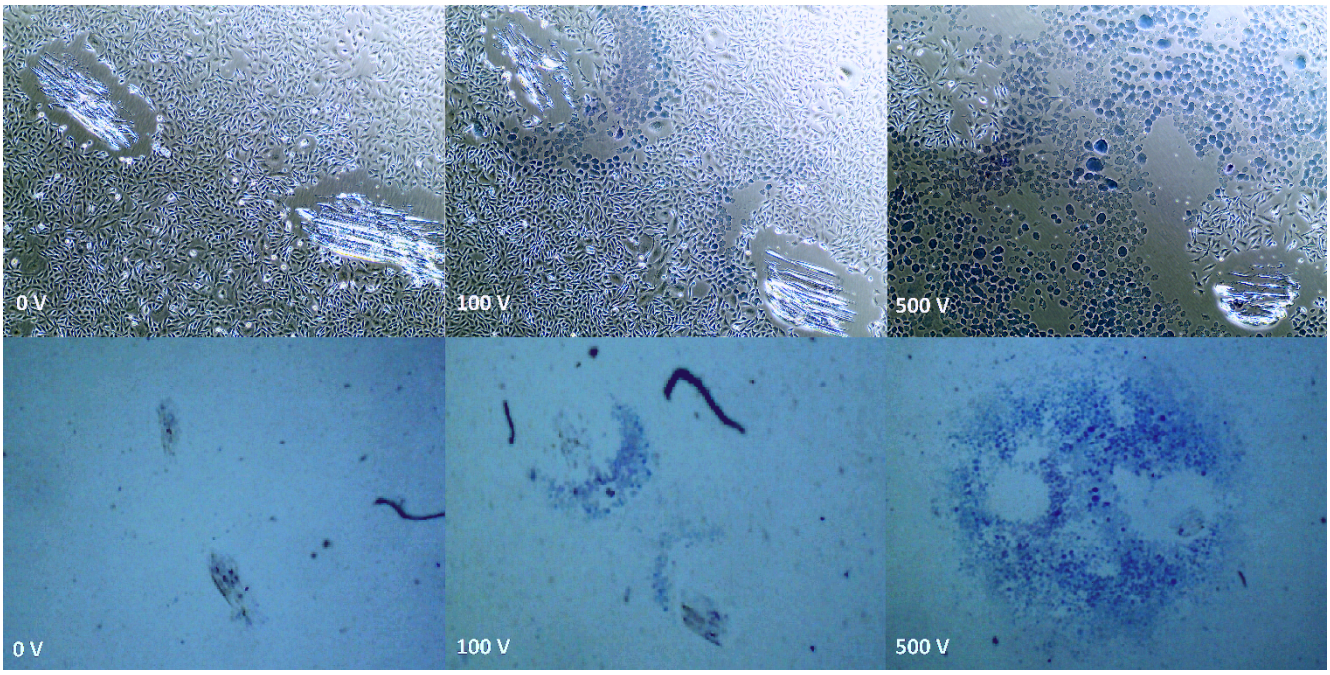

Figure 1: The sequence of the images of local ablation zone after cells were exposed to electric pulses with increasing pulse amplitude. The images were obtained by light microscopy under 10 × objective magnifications (top row) and under 5 × objective magnifications (bottom row).

Remove the tissue culture dish from the incubator and replace the growth medium with 500 µl of electroporation buffer. Carefully place needle electrodes on edge of tissue culture dish and apply electric pulses. Electric pulse parameters used are: 8 pulses, 100 µs duration and pulse repetition frequency 1 Hz, while pulse amplitude increases gradually. Increase the pulse amplitude from 0 V to 100 V, 300 V, 500 V and 700 V. After electroporation leave cells for 10 minutes at room temperature. Remove electroporation buffer and add 500 µl of trypan blue to tissue culture dish. Leave the cells for 5 minutes at room temperature then replace the trypan blue with 500 µl of fresh electroporation buffer. For visualization of local ablation zone, EVOS XL Core Imaging System (Invitrogen™) will be used.

FURTHER READING:

Batista Napotnik T, Miklavčič D. In vitro electroporation detection methods – An overview. Bioelectrochemistry 120: 166-182, 2018.
Čemažar, M, Jarm T., Miklavčič D, Maček Lebar A., Ihan A., Kopitar N.A., Serša G. Effect of electric field intensity on electropermeabilization and electrosensitivity of various tumor cell lines in vitro. *Electro and Magnetobiology* 17: 263-272, 1998.
Čorović S, Pavlin M, Miklavčič D. Analytical and numerical quantification and comparison of the local electric field in the tissue for different electrode configurations. Biomed. Eng. Online 6: 37, 2007.
Davalos RV, Mir IL, Rubinsky B. Tissue ablation with irreversible electroporation. Ann Biomed Eng 33(2):223-31, 2005.
Dermol J, Miklavčič D. Predicting electroporation of cells in an inhomogeneous electric field based on mathematical modeling and experimental CHO-cell permeabilization to propidium iodide determination. Bioelectrochemistry 100: 52-61, 2014.
Puc M., Kotnik T., Mir L.M., Miklavčič D. Quantitative model of small molecules uptake after in vitro cell electropermeabilization. Bioelectrochemistry 60: 1 – 10, 2003.
Rols M.P. Electropermeabilization, a physical method for the delivery of therapeutic molecules into cells. Biochim. Biophys Acta 1758: 423-428, 2006

NOTES & RESULTS

NOTES & RESULTS

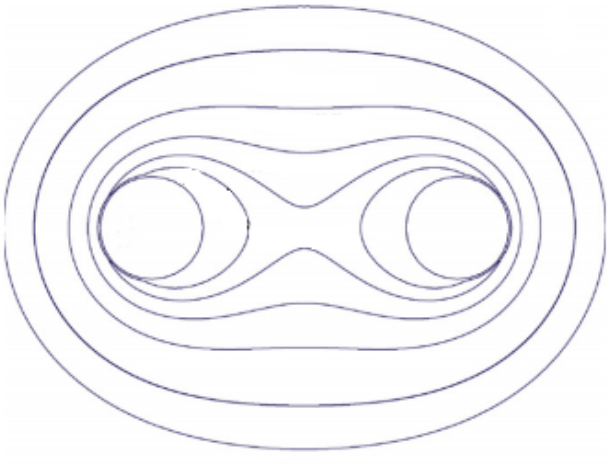

100 V

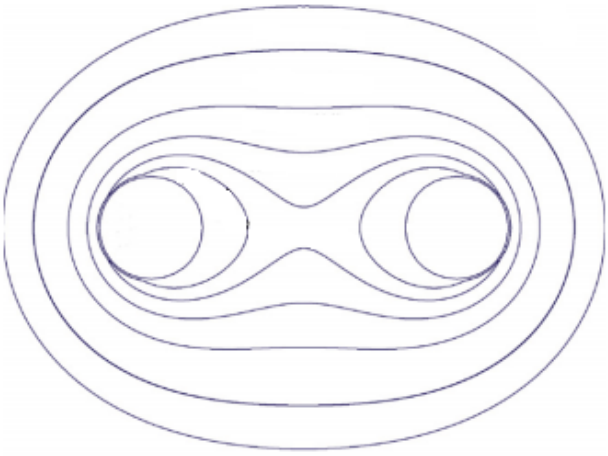

500 V

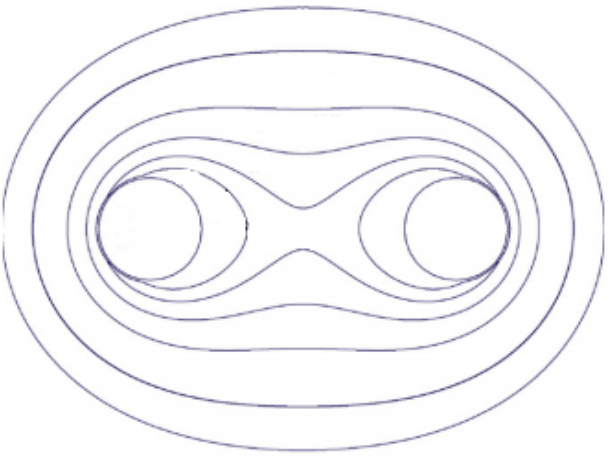

700 V

Effect of short high-frequency bipolar pulses on plasma membrane permeabilization L4

Janja Dermol-Černe, Lea Vukanović
University of Ljubljana, Faculty of Electrical Engineering

Duration of the experiments: 60 min
Max. number of participants: 4
Location: Cell Culture Laboratory 2
Level: basic

PREREQUISITES

Participants should be familiar with Laboratory safety (S1) and Electroporation Hardware Safety (S2). No other specific knowledge is required for this laboratory practice.

THEORETICAL BACKGROUND

In electrochemotherapy and irreversible electroporation as ablation technique, square 50-100 µs long monopolar pulses are usually applied at repetition frequency 1 Hz. The main drawbacks to the treatment of tissues with these monopolar pulses are discomfort and pain, the need to administer muscle relaxants and anesthesia, need for synchronization of the pulse delivery with the electrocardiogram and inhomogeneous tissue impedance. One of the possibilities to overcome these obstacles is high-frequency irreversible electroporation (HF-IRE). In HF-IRE, long monopolar pulses are replaced with bursts of a few µs long bipolar pulses, which mitigate muscle contractions, however at the expense of delivering higher energy.

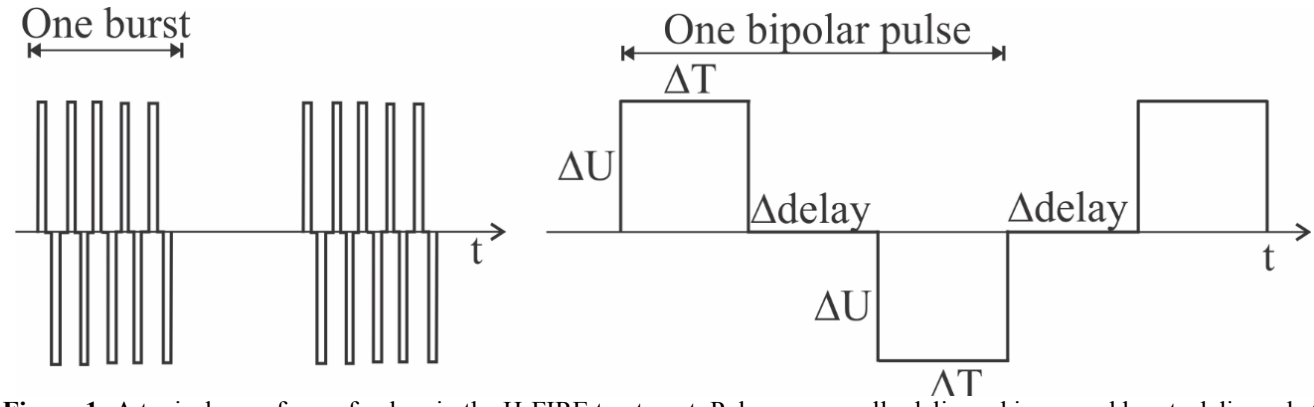

Figure 1: A typical waveform of pulses in the H-FIRE treatment. Pulses are usually delivered in several bursts delivered at repetition frequency 1 Hz. One pulse consists of a positive and a negative pulse and the delay between them.

The aim of this laboratory practice is the comparison of the effect of HF-IRE pulses and longer monopolar pulses on permeabilization of the plasma membrane as determined by spectrofluorometric measurements.

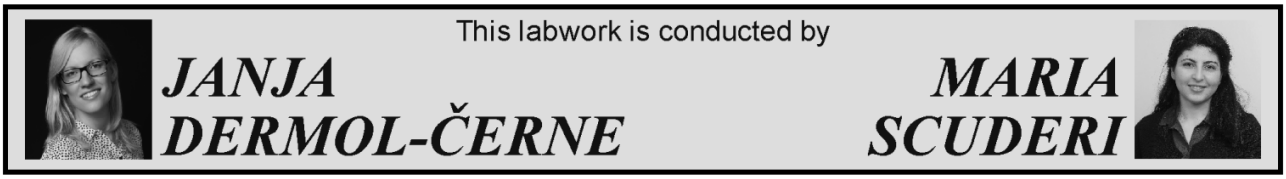

EXPERIMENT

We will detect electropermeabilization on spectrofluorometer using propidium iodide. Propidium iodide (PI) is a red-fluorescent dye. It is not permeant to live cells and is commonly used to detect dead cells in a population. After plasma membrane permeabilization, however, PI can diffuse into cells. It binds to DNA with little sequence preference. After binding, its fluorescence is increased 20- to 30-fold, with excitation maximum at 535 nm and emission maximum at 617 nm.

We will determine the effect of the pulse amplitude of HF-IRE pulses on the degree of cell membrane permeabilization. We will deliver 50 bipolar pulses consisting of 1 µs long positive 1 µs long negative pulse with 1 µs delay between them, delivered in 8 bursts at repetition frequency 1 Hz. We will compare the effect of the HF-IRE pulses on plasma membrane permeabilization with the monopolar pulses of parameters traditionally used in electrochemotherapy (8x100 µs pulses, 1 Hz repetition frequency). Thus, the duration of all pulses of HF-IRE pulses as well as of monopolar pulses is 800 µs.

We will use attached Chinese hamster ovary cells, $2.5x10^5$ cells per well plated 24 hours in advance in 24 well plate. As the electroporation buffer, we will use 10 mM K_2HPO_4/KH_2PO_4, 1 mM $MgCl_2$, 250 mM sucrose with 1.78 mS/cm, 292 mOsm/kg, and pH 7.4. We will use Pt/Ir wire electrodes with 0.8 mm diameter and 4 mm inter-electrode distance positioned at the bottom of the well. Between the electrodes, the electric field is approximately homogeneous and can be calculated as the ratio of the applied voltage and the inter-electrode distance.

For the application of pulses, we will use a laboratory prototype pulse HF-IRE pulse generator (University of Ljubljana) based on H-bridge digital amplifier with 1 kV MOSFETs (DE275-102N06A, IXYS, USA). We will monitor the delivered voltage and current by an oscilloscope, a differential probe and a current probe.

Protocol:

Remove the 24 well plate from the incubator and replace the growth medium with 300 µl per well of electroporation buffer containing 0.15 mM PI. Apply electric pulses and leave the cells for 3 minutes at room temperature to allow PI to diffuse into cells then replace the buffer with 1 ml of fresh electroporation buffer to stop PI influx. Increase the pulse amplitude of the bipolar pulses from 400 V to 1000 V. For the comparison with monopolar pulses, deliver 8x100 µs pulses with a repetition frequency of 1 Hz at 1000 V. As a negative control, apply no pulses to one well.

We will determine the fluorescence intensity spectrofluorometrically (Tecan, Infinite 200). Set the appropriate excitation and emission wavelengths for PI (535/617 nm). Plot a figure of fluorescence as a function of the electric field. Compare the fluorescence, obtained with the bipolar pulses, to the fluorescence, obtained with monopolar pulses of the same voltage.

FURTHER READING:

D. C. Sweeney, M. Reberšek, J. Dermol, L. Rems, D. Miklavčič, and R. V. Davalos, "Quantification of cell membrane permeability induced by monopolar and high-frequency bipolar bursts of electrical pulses," *Biochim. Biophys. Acta BBA - Biomembr.*, vol. 1858, no. 11, pp. 2689–2698, Nov. 2016.

C. B. Arena, M. B. Sano, M. N. Rylander, and R. V. Davalos, "Theoretical Considerations of Tissue Electroporation With High-Frequency Bipolar Pulses," *IEEE Trans. Biomed. Eng.*, vol. 58, no. 5, pp. 1474–1482, May 2011.

C. Yao *et al.*, "Bipolar Microsecond Pulses and Insulated Needle Electrodes for Reducing Muscle Contractions During Irreversible Electroporation," *IEEE Trans. Biomed. Eng.*, vol. 64, no. 12, pp. 2924–2937, Dec. 2017.

S. P. Bhonsle, C. B. Arena, D. C. Sweeney, and R. V. Davalos, "Mitigation of impedance changes due to electroporation therapy using bursts of high-frequency bipolar pulses," *Biomed. Eng. OnLine*, vol. 14, no. Suppl 3, p. S3, 2015.

NOTES & RESULTS

Bipolar/Monopolar	Bipolar	Bipolar	Bipolar	Bipolar	Bipolar	Monopolar
Voltage (V)	0	400	600	800	1000	1000
Pulse duration ΔT (μs)	0	1	1	1	1	100
Raw data (a.u.)						

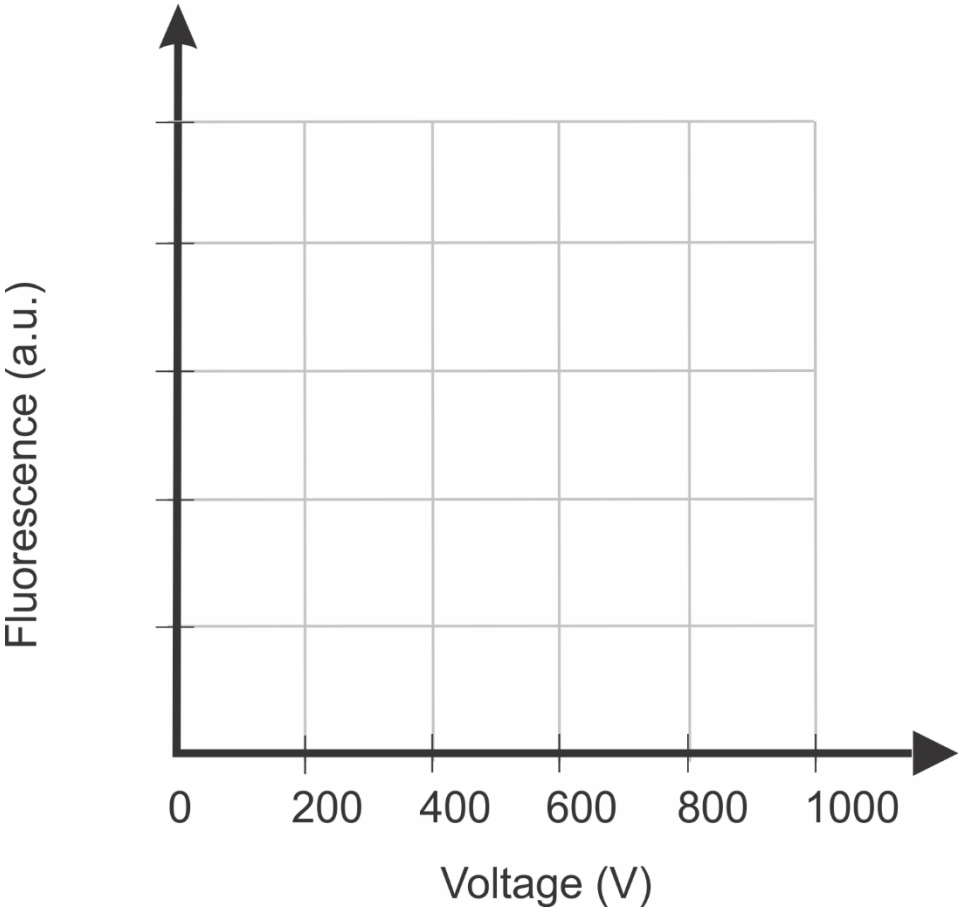

NOTES & RESULTS

Electrotransformation of *Escherichia coli* with plasmid DNA L5

Duša Hodžić, Saša Haberl Meglič
University of Ljubljana, Faculty of Electrical Engineering

Duration of the experiments: day 1: 90 min; day 2: 30 min
Max. number of participants: 4
Location: Microbiological laboratory 1
Level: Basic

PREREQUISITES

Participants should be familiar with Laboratory Safety (S1). No other specific knowledge is required for this laboratory practice.

THEORETICAL BACKGROUND

The ability to introduce plasmid DNA into bacterial cells is of great practical importance in molecular biology, genetic engineering, biotechnology etc. For example, bacteria with introduced plasmid DNA can have new pathways for production of proteins or are able to degrade organic pollutants (bioremediation). Since majority of bacterial species does not show a naturally occurring ability to take up DNA (competence) it is convenient to have methods that allow us such genetic manipulation of bacteria. The well-known methods are: chemical transformation, electrotransformation, biolistic transformation and sonoporation. Main advantages of electroporation compared to other methods are shorter time needed, easy application and no need of toxic chemicals. Nevertheless, optimization of electric pulses and other parameters is necessary for high yields of transformants.

Electrotransformation is transformation of bacteria by means of electroporation, a phenomenon that occurs when the cell is exposed to the external electric field of sufficient amplitude and duration which leads to permeabilization of the membrane. Increasing electric field amplitude or duration of pulses increases the level of cell membrane permeabilization and thus transformation effectiveness. When electric field parameters used are below the critical value, cell membrane can reseal and treated bacteria survive. This is also known as reversible electroporation.

The aim of this laboratory practice is to demonstrate transformation of *Escherichia coli* with plasmid DNA using reversible electroporation.

EXPERIMENT

Our experimental organism will be competent bacteria *E.coli* DH5α and the plasmid pSEUDO-GFP. We will detect transformed and surviving bacteria by counting colony forming units (CFU count) on LB agar plates with antibiotic erythromycin for selection.

Protocol 1/2 (Electroporation of bacteria): On the first day of experiment 200 µl of competent bacterial cells in 10% glycerol and water will be mixed with plasmid DNA (pSEUDO-GFP), incubated for 2 minutes on ice and exposed to electric field. Electric pulses will be applied with electric pulse generator Vitae HVP-VG (Igea, Italy). Samples for treatment are placed in electroporation cuvettes with integrated aluminium electrodes 2 mm apart (VWR, Belgium). Immediately after electroporation the recovery medium SOC will be added to bacterial suspension. After 60 minutes' incubation at 37 °C, bacteria will be plated on LB agar with selective antibiotic for transformants. Control sample will be the

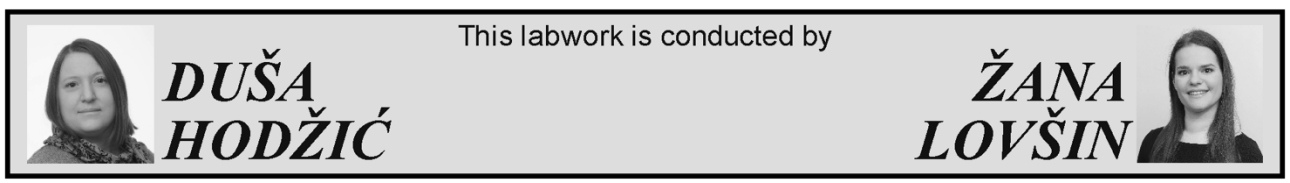

untreated suspension of bacteria. To determine the number of bacterial cells you will need to prepare serial dilutions of resuspended bacteria ranging from 10^{-1} to 10^{-6}. Dilute 100 µl of bacterial suspension in tubes containing 900 µl of sterile 0,9 % NaCl. Pipette 100 µl of suspension per LB agar plate and spread them evenly with a sterile Drigalski spatula. All agar plates will be incubated overnight at 37 °C.

Protocol 2/2 (Counting bacterial colonies): Determine electrotransformation efficiency and total cell count. The efficiency of reversible electroporation is expressed as number of transformants per microgram of DNA and can be monitored by plating the treated sample on nutrient agar with selective antibiotic and counting the number of CFU. Each colony may arise from one or a group of bacterial cells and they represent the cells that have successfully undergone the transformation.

FURTHER READING:

Calvin N.M., Hanavalt P.C. High-efficiency transformation of bacterial cells by electroporation. *Journal of Bacteriology* 170: 2796-2801, 1988.

Yoshida N., Sato M. Plasmid uptake by bacteria: a comparison of methods and efficiencies. *Applied Microbiology and Biotechnology* 83:791-798, 2009.

Kotnik T., Frey W., Sack M., Haberl Meglič S., Peterka M., Miklavčič D. Electroporation-based applications in biotechnology. *Trends in Biotechnology. Review* 33:480-488, 2015.

Munazza Gull and Sondos El-Baz (November 5th 2018). Introductory Chapter: Preface to Plasmids, Plasmid, Munazza Gull, IntechOpen, DOI: 10.5772/intechopen.78673. Available from: https://www.intechopen.com/books/plasmid/introductory-chapter-preface-to-plasmids

NOTES & RESULTS

Electric pulse parameters *n* x *t* (µs) *E* [kV/cm], *f* [Hz]	1 x 100 µs 7.5 kV/cm 1 Hz	1 x 100 µs 12.5 kV/cm 1 Hz	8 x 100 µs 12.5 kV/cm 1 Hz	1 x 1000 µs 12.5 kV/cm 1 Hz
Total cell count [*number of viable cells / ml*]				
Transformation efficiency [*number of transformants / µg pDNA*]				

NOTES & RESULTS

NOTES & RESULTS

Electroporation of planar lipid bilayers L6

Peter Kramar, Aljaž Velikonja, Alenka Maček Lebar
University of Ljubljana, Faculty of Electrical Engineering, Slovenia

Duration of the experiments: 120 min
Max. number of participants: 4
Location: Laboratory for skin and planar lipid bilayers
Level: Basic

PREREQUISITES

Participants should be familiar with Laboratory safety (S1). No other specific knowledge is required for this laboratory practice.

THEORETICAL BACKGROUND

A planar lipid bilayer can be considered as a small fraction of total cell membrane. As such it has often been used to investigate basic aspects of electroporation; especially because of its geometric advantage allowing chemical and electrical access to both sides of the lipid bilayer. Usually a thin bi-molecular film composed of specific phospholipids and organic solvent is formed on a small aperture separating two aqueous compartments. Electrodes immersed in these two aqueous compartments allow to measure current and voltage across the lipid bilayer (Figure 1).

Two different measurement principles of planar lipid bilayer's properties can be used: voltage or current clamp method. Planar lipid bilayer from an electrical point of view can be considered as imperfect capacitor, therefore two electrical properties, capacitance and resistance, mostly determine its behaviour.

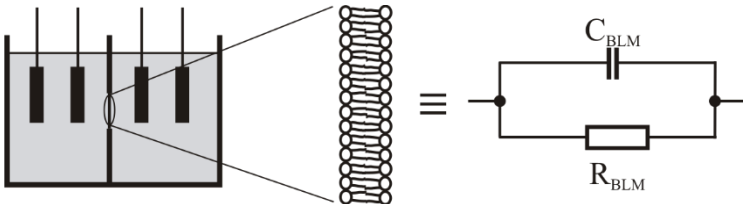

Figure 1: Equivalent circuit of a planar lipid bilayer.

The aim of this laboratory practice is to build a planar lipid bilayer by painting method (Muller - Rudin method) or/and foldig method (Montal – Mueller) and to determine capacitance and resistance of the planar lipid bilayer using LCR meter. Basic aspects of planar lipid bilayer electroporation will be given by observing formation of the pores and determining its breakdown voltage.

This labwork is conducted by

KATJA BALANTIČ

EXPERIMENT

Protocol:

Muller-Rudin method

Form a planar lipid bilayer by covering the surface of the aperture in a barrier separating two compartments of a measuring vessel with a lecithin solution (20 mg/ml of hexane). After evaporation of hexane, fill compartments with solution consisting of 0.1 mol KCl, 0.01 mol of HEPES, at pH=7.4. Connect the electrodes and apply a drop of lecithin dissolved in decane (20 mg/ml) to the aperture by the micropipette or paint it by a teflon brush. Measure capacitance and determine if the formation of planar lipid bilayer is appropriate.

Montal – Mueller method

Cover the surface of the aperture in a barrier separating two compartments of a measuring vessel with 1 µl lecithin solution (10 mg/ml of hexane and ethanol absolute in ratio 9:1). After evaporation of hexane and ethanol, add on the aperture 1,5 µl solution of pentan and hexadecane in ratio 7:3. Fill compartments with solution consisting of 0.1 mol NaCl, 0.01 mol of HEPES, at pH=7.4. On the solution surface apply 2 µl of lecithin solution in each compartment. Wait approximately 15 minutes that lipid molecules are equally spread on the solution surface. Then rise the solution surface above aperture synchronously in both compartments by pumps. Measure capacitance and determine if the formation of planar lipid bilayer is appropriate.

Measuring methods: When the planar lipid layer is formed, we apply the current or voltage to the planar lipid bilayer. In the current clamp method the current is applied to the planar lipid bilayer and we measure voltage across the bilayer. Apply a linearly increasing current and record a voltage across the bilayer. During the experiment you will obtain the time course of the voltage across the bilayer and the plot of the programmed current flowing between two current electrodes. In the voltage clamp method the voltage across the planar lipid bilayer is applied and current, which flows through planar lipid bilayer, is measured. To the planar lipid bilayer apply a linearly increasing voltage and record a flowing current. Like at the current clamp method you will obtain the time course of the flowing current and the plot of the programmed voltage across the planar lipid bilayer.

From collected data determine the breakdown voltage (U_{br}) and the lifetime (t_{br}) of planar lipid bilayer.

FURTHER READING:

Kalinowski S., Figaszewski Z., A new system for bilayer lipid membrane capacitance measurements: method, apparatus and applications, *Biochim. Biophys. Acta* 1112:57-66, 1992.

Pavlin M, Kotnik T, Miklavcic D, Kramar P, Macek-Lebar A. Electroporation of planar lipid bilayers and membranes. In Leitmanova Liu A (ed.), *Advances in Planar Lipid Bilayers and Liposomes*, *Volume 6*, Elsevier, Amsterdam, pp. 165-226, 2008.

Koronkiewicz S., Kalinowski S., Bryl K., Programmable chronopotentiometry as a tool for the study of electroporation and resealing of pores in bilayer lipid membranes. *Biochim. Biophys. Acta*, 1561:222–229, 2002.

Kotulska M., Natural fluctuationsof an electropore show fractional Lévy stable motion, *Biophys. J.*, 92:2412-21, 2007.

Montal M., Mueller, P., Formation Of Bimolecular Membranes From Lipid Monolayers And A Study of their Electrical Properties, *PNAS*, 69:3561-3566, 1972.

Kramar P, Miklavčič D, Maček-Lebar A. Determination of the lipid bilayer breakdown voltage by means of a linear rising signal. *Bioelectrochemistry* 70: 23-27, 2007.

NOTES & RESULTS

NOTES & RESULTS

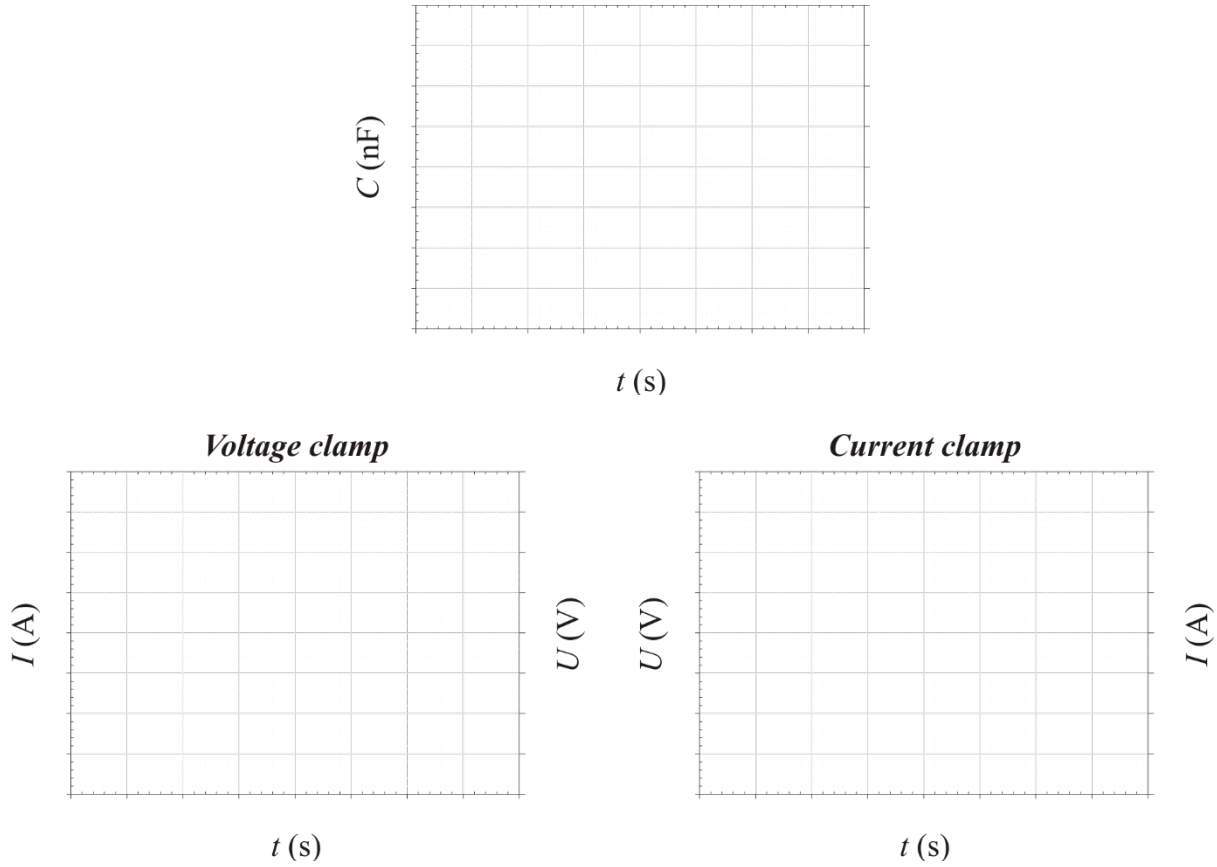

NOTES & RESULTS

E. coli inactivation by pulsed electric fields in a continuous flow system L7

Saša Haberl Meglič, Karel Flisar
University of Ljubljana, Faculty of Electrical Engineering

Duration of the experiment: day 1: 90 min; day 2: 60 min
Max. number of participants: 4
Location: Microbiological laboratory 2
Level: Basic

PREREQUISITES

Participants should be familiar with the Safety rules and Rules for sterile work in cell culture laboratory. No other specific knowledge is required for this laboratory practice.

THEORETICAL BACKGROUND

The first description of the profound effect of electrical pulses on the viability of a biological cell was given in 1958. If a cell is exposed to a sufficiently high electric field, its membrane becomes permanently permeable, resulting in leakage of cellular components, which leads to cell death. The method gained ground as a tool for microbial inactivation and the influence of different pulsed electric fields (PEF) on microbial viability was extensively studied on various microorganisms.

Since PEF microbial inactivation in controlled laboratory conditions showed promise, the idea arose of also removing pathogenic microorganisms from various water sources, hospital wastewaters and liquid food, without destroying vitamins or affecting the food's flavour, colour or texture. In order to facilitate PEF application on a large scale, the development of flow processes has been pursued. A standard PEF treatment system therefore consists of a pulse generator that enables continuous pulse treatment, flow chambers with electrodes and a fluid-handling system.

Several parameters have been described, which can influence inactivation of microbial cells. Specifically in a continuous flow system the flow rate of a liquid must be adjusted in order for each bacterial cell to be exposed to appropriate pulse conditions.

The aim of this laboratory practice is to demonstrate how different pulse parameters in a continuous flow system affect bacterial inactivation.

EXPERIMENT

We will inactivate *Escherichia coli* K12 TOP10 cells carrying plasmid pEGFP-N1, which encodes kanamycin resistance (Clontech Laboratories Inc., Mountain View, CA, USA) in a continuous flow system (see Figure 1) using different electric pulse parameters. To generate electric pulses square wave prototype pulse generator will be used. Pulses will be monitored on osciloscope (LeCroy 9310C). The inactivation level will be determined by plate count method.

Bacterial cells will be grown prior experiment for 17 hours at 37°C in Luria Broth (LB) medium (Sigma-Aldrich Chemie GmbH, Deisenhofen, Germany) with shaking.

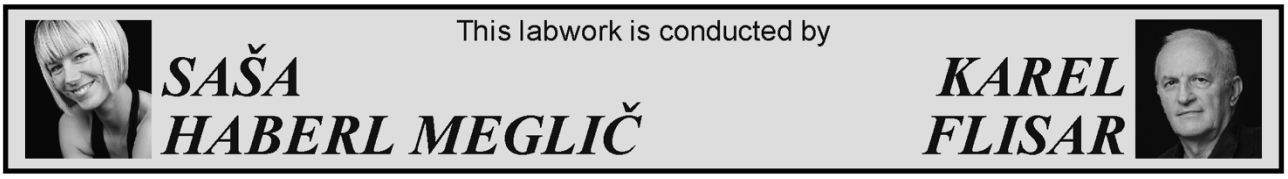

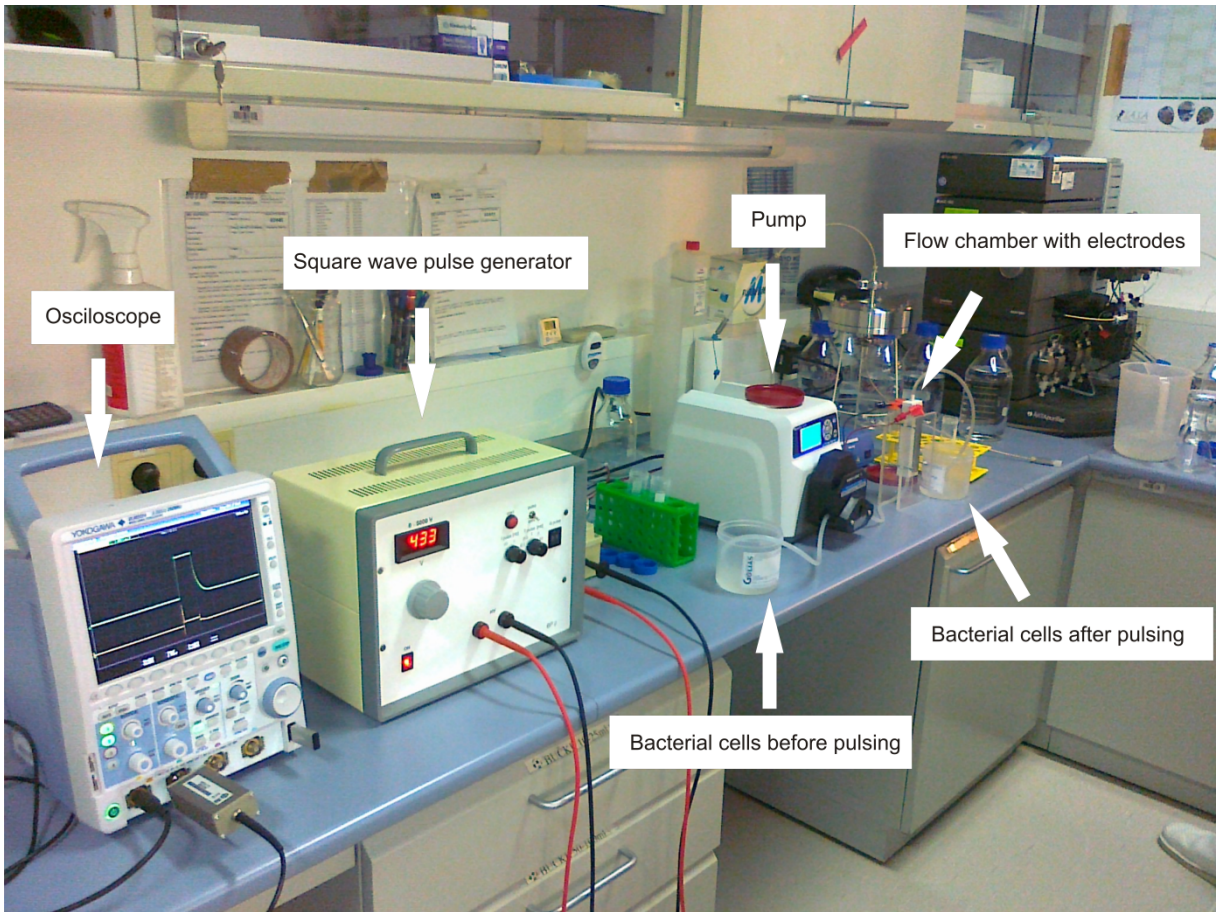

Figure 1. Continuous flow electroporation system. The circuit system includes a flow chamber with electrodes and a prototype square wave pulse generator. Voltage and current are both monitored throughout the experiment.

Protocol 1/2 (Electroporation of bacteria in a continuous flow system): On the first day of experiment *E. coli* cells will be centrifuged (4248 g, 30 min, 4°C) and the pellet will be re-suspended in 10 ml of distilled water and 100x diluted. The total volume of prepared bacterial cells for the treatment will be 0.3 L.

In order to determine the number of bacterial cells in our sample, you will prepare serial dilutions of bacterial sample ranging from 10^{-1} to 10^{-6} (in 900 µl of sterile distilled water you will dilute 100 µl of bacterial sample). You will pipette 100 µl of dilutions 10^{-5} and 10^{-6} on LB agar containing kanamycin antibiotic and evenly spread the liquid with sterile plastic rod.

The exposure of cells to electric pulses in flow through chamber in a continuous flow system depends on the geometry of the chamber, the frequency of pulses at which electroporator operates. The number of pulses is given by equation 1. At that flow, the desired number of pulses are applied to the liquid and thus to the cells in the flow-through chamber. Because the volume of our cross-field chamber between the electrodes (Q = 0.0005 L) and the frequency (10 Hz in our case) are constant, the flow through the chamber can be determined:

$$q = \frac{f}{n} \cdot Q \qquad (1)$$

where q (L/min) is the flow rate, Q (L) the volume between the two electrodes and n is the number of pulses received by the fluid in the chamber in residence time. For a frequency of 10 Hz, you will calculate

the flow rate (q) at which the whole liquid will be subjected to at least one pulse. For PEF flow through treatment you will use 0.3 L (10^{-2} dilution) of prepared bacterial cells. Bacterial cells will be pumped through the system at the calculated flow rate and pulses will be applied by prototype pulse generator.

After PEF treatment take 100 µl of treated sample and prepare dilutions ranging from 10^{-1} to 10^{-6}. You will pipette 100 µl of dilutions 10^{-4}, 10^{-5} and 10^{-6} on LB agar with kanamycin antibiotic and evenly spread the liquid with sterile plastic rod.

Protocol 2/2 (Determining bacterial viability): After 24 h incubation at 37ºC count colony forming units. Express the viability as log (N/N_0), where N represents the number of colony forming units per ml in a treated sample (bacterial cells exposed to electric pulses) and N_0 the number of colony forming units per ml in an untreated sample (bacterial cells not exposed to electric pulses).

Example of determining bacterial viability:
You counted 70 CFU in a control sample (dilution 10^{-7}) and 30 CFU in a treated sample (dilution 10^{-5}).

Number of bacterial cells per ml (control sample) = 70 x 10^7 (dilution factor of sample) x 10 (dilution factor of plating) = 7 x 10^9 bacterial cells/ml

Number of bacterial cells per ml (treated sample) = 30 x 10^5 (dilution factor of sample) x 10 (dilution factor of plating) = 3 x 10^7 bacterial cells/ml

log N/N_0 = log (3 x 10^7/ 7 x 10^9) = ***-2.368***

FURTHER READING:

Flisar K., Haberl Meglic S., Morelj J., Golob J., Miklavčič D. Testing a prototype pulse generator for a continuous flow system and its use for E. coli inactivation and microalgae lipid extraction. *Bioelectrochemistry* doi: 10.1016/j.bioelechem.2014.03.008, 2014
Gerlach D., Alleborn N., Baars A., Delgado A., Moritz J., Knorr D. Numerical simulations of pulsed electric fields for food preservation: A review. *Innov Food Sci Emerg Technol* 9: 408-417, 2008
Gusbeth C., Frey W., Volkmann H., Schwartz T., Bluhm H. Pulsed electric field treatment for bacteria reduction and its impact on hospital wastewater. *Chemosphere* 75: 228-233, 2009
Pataro G., Senatore B., Donsi G., Ferrari G. Effect of electric and flow parameters on PEF treatment efficiency. *J Food Eng* 105: 79-88, 2011

NOTES & RESULTS

NOTES & RESULTS

Analysis of electric field orientations on gene electrotransfer – visualization at the membrane level L8

Saša Haberl Meglič, Matej Reberšek
University of Ljubljana, Faculty of Electrical Engineering

Duration of the experiment: 90 min
Max. number of participants: 4
Location: Cell Culture Laboratory 1
Level: Advanced

PREREQUISITES

Participants should be familiar with Laboratory safety (S1). The basic knowledge of handling with cells is required for this laboratory practice.

THEORETICAL BACKGROUND

Gene electrotransfer is a non-viral method used to transfer genes into living cells by means of high-voltage electric pulses. An exposure of a cell to an adequate amplitude and duration of electric pulses leads to transient increase of cell membrane permeability for molecules which are otherwise deprived of membrane transport mechanisms. This allows various nonpermeant molecules, including DNA, to be transported across the membrane and enter the cell. Although mechanisms of the process are not yet fully elucidated, it was shown that several steps are crucial for gene electrotransfer: interaction of plasmid DNA (pDNA) with the cell membrane, translocation of pDNA across the membrane, migration of pDNA towards the nucleus, transfer of pDNA across the nuclear envelope and gene expression.

Many parameters (such as electric pulse protocol) can influence the first step (interaction of DNA with the cell membrane) and by that gene electrotransfer efficiency. Therefore, different electric pulse protocols are used in order to achieve maximum gene transfection, one of them is changing the electric field orientation during the pulse delivery. Since DNA is a negatively charged molecule and it is dragged towards the cell with the electrophoretic force in the opposite direction of the electric field, changing electric field orientation increases the membrane area competent for DNA entry into the cell.

The aim of this laboratory practice is to demonstrate how different pulse polarity affects formation of DNA – membrane complex after electric pulse application.

EXPERIMENT

We will focus on the interaction of DNA with the cell membrane by using TOTO-1 dye. For the experiment, we will use Chinese hamster ovary cells (CHO-K1) and plasmid DNA (pEGFP-N_1) that codes for GFP (green fluorescent protein). To generate and deliver electric pulses a βtech electroporator (Electro cell B10, Betatech, France) and electrodes with 4 mm inter-electrode distance will be used. Pulses will be monitored on osciloscope (LeCroy 9310C).

This labwork is conducted by

TAMARA POLAJŽER

Pulse protocols (see also Figure 1):

a) SP (single polarity): the direction of electric field is the same for all pulses
b) BP (both polarities): the direction of the electric field is changed between the pulses

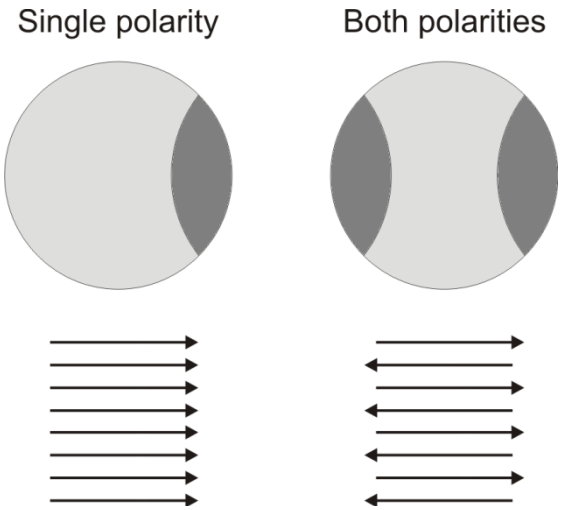

Figure 1: Two different pulse protocols will be used: single polarity (SP) and both polarities (BP).

Protocol:

Interaction of DNA with the cell membrane: CHO cells will be grown in Lab-Tek chambers as a monolayer culture in Ham's tissue culture medium for mammalian cells with 10% fetal bovine serum (Sigma-Aldrich Chemie GmbH, Deisenhofen, Germany) at 37º C. Cells will be plated 1 h before the experiment in concentration 1 x 10^5 cells per chamber.

To visualize DNA interaction with cell membrane TOTO-1 nucleic acid stain (Molecular Probes-Invitrogen, Carlsbad, California, USA) will be used. The plasmid pEGFP-N1 will be labelled on ice with 2.3 x 10^{-4} M TOTO-1 DNA intercalating dye 1 h before the experiment. Plasmid concentration will be 1 µg/µl, which yields an average base pair to dye ratio of 5.

Just before the experiment remove culture medium and rinse the cells with 1 ml of electroporation buffer (10 mM phosphate buffer K_2HPO_4/KH_2PO_4, 1 mM $MgCl_2$, 250 mM sucrose; pH = 7.4). Afterwards add 500 µl of electroporation buffer containing 5 µg of labelled plasmid DNA. Then apply a train of eight pulses with amplitude of 350 V, duration of 1 ms and repetition frequency 1 Hz using single polarity or both polarities (see Pulse protocols).

Immediately after exposure of cells to electric pulses rinse the cells three times with 1 ml of electroporation buffer. Add again 500 µl of electroporation buffer and observe the interaction of DNA with the cell membrane with fluorescent microscopy (Zeiss 200, Axiovert, Germany) using 100x oil immersion objective using TOTO filter with excitation at 514 nm.

FURTHER READING:

Faurie C., Reberšek M., Golzio M., Kandušer M., Escoffre J. M., Pavlin M., Teissie J., Miklavčič D., Rols M. P. Electro-mediated gene transfer and expression are controlled by the life-time of DNA/membrane complex formation. *J Gene Med* 12: 117-125, 2010

Golzio M., Teissié J., Rols M. P. Direct visualization at the single-cell level of electrically mediated gene delivery. *PNAS* 99: 1292-1297, 2002.

Reberšek M., Faurie C., Kandušer M., Čorović S., Teissié J., Rols M.P., Miklavčič D. Electroporator with automatic change of electric field direction improves gene electrotransfer *in vitro*. *Biomed Eng Online* 6: 25, 2007.

Reberšek M., Kandušer M., Miklavčič D. Pipette tip with integrated electrodes for gene electrotransfer of cells in suspension: a feasibility study in CHO cells. *Radiol Oncol* 45: 204-208, 2011.

Video Article:

Pavlin M., Haberl S., Reberšek M., Miklavčič D., Kandušer M. Changing the direction and orientation of electric field during electric pulses application improves plasmid gene transfer in vitro. *J Vis Exp*, 55: 1-3, 2011.

NOTES & RESULTS

NOTES & RESULTS

Comparison of flow cytometry and spectrofluorometric measurements in cell permeabilization experiments L9

Janja Dermol, Lea Vukanović
University of Ljubljana, Faculty of Electrical Engineering

Duration of the experiments: 90 min
Max. number of participants: 4
Location: Cell Culture Laboratory 2
Level: advanced

PREREQUISITES

Participants should be familiar with Laboratory safety (S1). The basic knowledge of handling with cells is required for this laboratory practice.

THEORETICAL BACKGROUND

When cells are exposed to high electric fields, otherwise non-permeant molecules can cross the cell membrane. A commonly used way of detecting cell membrane permeabilization is by using fluorescent dyes such as propidium iodide. When the cell is permeabilized, the propidium ion enters the cell, binds to nucleic acids in the cytosol and nucleus, and upon excitation starts to emit 20-times higher fluorescence than in the unbound state. Cell membrane permeabilization can be determined using different methods, e.g. fluorescent microscopy, spectrofluorometric measurements, flow cytometry, or clonogenic test after electroporation with chemotherapeutics. In this lab work, we will compare spectrofluorometric measurements and flow cytometry.

Spectrofluorometric measurements allow for the analysis of a large number of cells at different wavelengths, but the exact number of permeabilized cells cannot be extracted. Namely, as a result, we obtain the sum of the fluorescence intensities of all cells which can conceal subpopulations of differently permeabilized or even non-permeabilized cells.

Flow cytometry, on the other hand, gives information on the shape, size, internal structure, and fluorescence of each separate cell, and thus offers possibility to detect subpopulations which differ in any of the measured parameters. Cells (or any other particle) move through a laser beam and refract or scatter light in all directions. Forward scatter (FSC) is the light that is scattered in the forward direction as laser strikes the cell while side scatter (SSC) is the light that is scattered at larger angles. The magnitude of FSC is roughly proportional to the size of the particle and SSC is indicative of the granularity and the internal structural complexity. Fluorescence can be measured at different wavelengths, and the measured signal is proportional to the amount of the emitted fluorescence. After measurements, the analysis is done by gating to separate different cell subpopulations (Figure 1).

The aim of this laboratory practice is the comparison of two different methods of permeabilization detection using fluorescent dye propidium iodide.

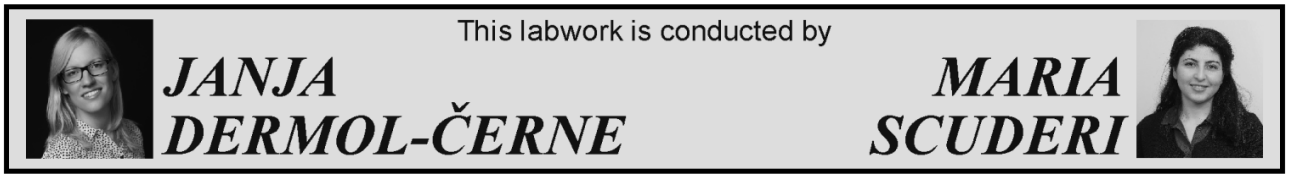

EXPERIMENT

We compare the fluorescence detected by flow cytometry (Life Technologies, Attune NxT, USA) and by the spectrofluorometer (Tecan Infinite 200, Tecan, Austria) after standard electroporation protocol (8, 100 µs pulses of different voltage applied at 1 Hz). To apply the pulses, we use the Gemini X2 electroporator (Harvard apparatus BTX, USA), and we monitor the pulses by an oscilloscope and current probe (both LeCroy, USA).

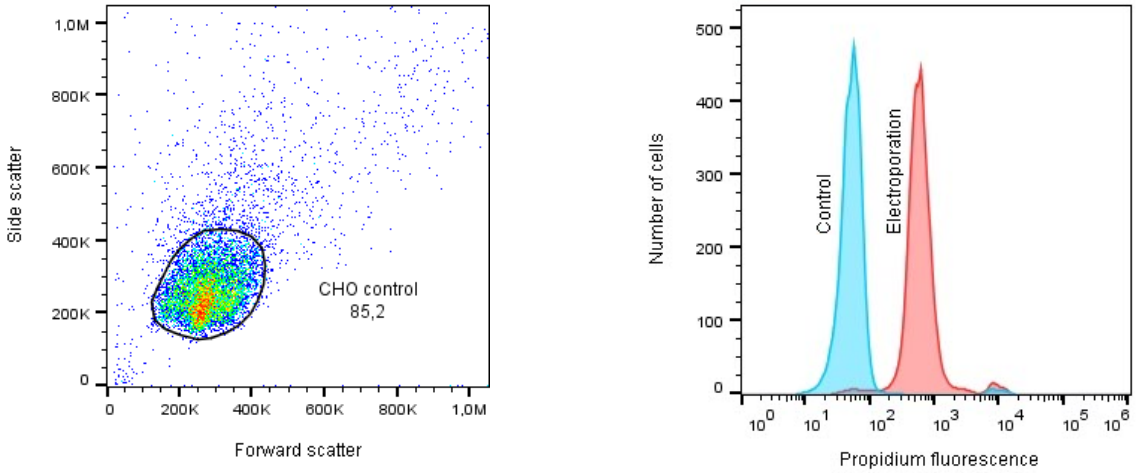

Figure 1: The analysis of the permeabilization data obtained by flow cytometry measurements in the software FlowJo (TreeStar, USA). Left: the viable cells are determined from the FSC-A and SSC-A dot diagram by gating. Right: histogram of measured fluorescence for control and pulsed cells. After electroporation, the cell fluorescence shifts for two decades which allows the discrimination between permeabilized and non-permeabilized cells. The peak at 10^4 are the dead and/or irreversibly permeabilized cells.

Protocol:

The experiments are performed on Chinese Hamster Ovary (CHO) cells. First, cells are detached by 10x trypsin-EDTA (Sigma-Aldrich, Germany), diluted 1:9 in Hank's basal salt solution (Sigma-Aldrich, Germany). Then, they are centrifuged (180g, 21°C, 5 min), the supernatant is removed and replaced with the low-conductivity KPB buffer (10 mM KH_2PO_4/K_2HPO_4, 1 mM $MgCl_2$, 250 mM sucrose) in concentration 10^7 cells/ml. 100 µl of cell suspension is dispensed in 1.5 ml microcentrifuge tubes (Isolab, Germany). Immediately before pulse application, 10 µl of 1.5 mM propidium iodide (Life Technologies, USA) is added to the tube. Then, 100 µl of cell suspension with propidium iodide is pipetted between 2 mm stainless-steel electrodes. Using Gemini X2 electroporator, 8, 100 µs pulses of different voltage at 1 Hz are applied. After the pulse application, 80 µl of cell suspension is transferred from between the electrodes to a new 1.5 ml tube. Two minutes after pulse application, the sample is centrifuged (1 min, 2000g, room temperature), the supernatant is removed and replaced by 500 µl of KPB buffer. The change of the buffer stops propidium influx in the cells and allows us to compare different parameters at the same time point. From each tube, 100 µl of the cell suspension is transferred to a 96-well plate in triplicates. 100 µl of the cell suspension is transferred to a 5 ml tube. Then, the protocol is repeated for the next sample. When all samples are prepared, we start with the measurements.

First, the fluorescence intensity is determined spectrofluorimetrically. We set the appropriate excitation (535 nm) and emission (617 nm) wavelengths. We measure at an optimal gain which prevents from signal saturation. The optimal gain is automatically determined by the software based on sensor sensitivity and the maximum signal intensity we are measuring. The average fluorescence intensity is calculated for each voltage from the triplicates. We plot the fluorescence intensity in dependence on the applied voltage.

Second, we determine the number of fluorescent cells by flow cytometry. On the control cells, we set up the optimal measuring parameters at the lowest flow rate (12.5 µl/min). When optimal parameters are determined, we measure 10,000 events for each voltage with higher flow rate (200 µl/min). By gating, living cells and the percentage of permeabilized cells are determined for each voltage. We plot the cell permeabilization in dependence on the applied voltage for both measurements (spectrofluorometric and flow cytometry) and compare the results.

FURTHER READING:

Kotnik T, Maček Lebar A, Miklavčič D, Mir, LM. Evaluation of cell membrane electropermeabilization by means of nonpermeant cytotoxic agent. Biotechniques. 2000;28**:** 921–926.
Marjanovič I, Kandušer M, Miklavčič D, Keber MM, Pavlin M. Comparison of Flow Cytometry, Fluorescence Microscopy and Spectrofluorometry for Analysis of Gene Electrotransfer Efficiency. J Membr Biol. 2014;247: 1259–1267. doi:10.1007/s00232-014-9714-4
Michie, J., Janssens, D., Cilliers, J., Smit, B. J., Böhm, L. Assessment of electroporation by flow cytometry. Cytometry 2000:41: 96–101.
Rols MP, Teissié J. Flow cytometry quantification of electropermeabilization. Methods Mol Biol Clifton NJ. 1998;91: 141–147.
Shapiro, H. M. *Practical flow cytometry*. (Wiley-Liss, 2003).

NOTES & RESULTS

Voltage (V)	0	100	150	200	250	0 and 250
Fluorescence intensity as measured with spectrofluorometer (a.u.)						
Percentage of fluorescent cells as determined by the flow cytometry (%)						

NOTES & RESULTS

Monitoring of electric field distribution in biological tissue by means of magnetic resonance electrical impedance tomography L10

Matej Kranjc[1], Igor Serša[2]
[1]University of Ljubljana, Faculty of Electrical Engineering
[2]Institut "Jožef Stefan"

Duration of the experiment: day 1: 90 min
Max. number of participants: 4
Location: MRI Laboratory (Jožef Stefan Institute)
Level: Basic

PREREQUISITES

Participants should be familiar with Laboratory safety (S1). No other specific knowledge is required for this laboratory practice.

THEORETICAL BACKGROUND

A method capable of determining electric field distribution during the pulse delivery has a practical value as it can potentially enable monitoring of the outcome of electroporation which strongly depends on the local electric field. Measurement of electric field distribution enables detection of insufficient electric field coverage before the end of either reversible or irreversible electroporation treatment, thus enabling corrections of field coverage during the treatment and consequently increasing and assuring its effectiveness. As there are no available approaches for measurement of electric field distribution *in situ*, an indirect approach using magnetic resonance techniques was suggested. Magnetic resonance electrical impedance tomography (MREIT) enables reconstruction of electric field distribution by measurement of electric current density distribution, first, and calculation of electrical conductivity of the treated subject during application of electric pulses using MRI data as an input to numerical algorithms, second. This method enables determination of electric field distribution *in situ* also accounting for changes that occur in the tissue due to electroporation.

MREIT is a relatively new medical imaging modality based on numerical reconstruction of electrical conductivity inside a tissue by means of current density distribution measured by current density imaging (CDI) sequence. The MREIT algorithm applied for reconstruction of electrical conductivity of the tissue is based on solving Laplace's equation through iterative calculation. Electrical conductivity is updated after each iteration (k+1):

$$\sigma^{k+1} = \frac{|\mathbf{J}_{\mathrm{CDI}}|}{|\nabla u^k|}.$$

where $\mathbf{J}_{\mathrm{CDI}}$ is current density obtained by CDI and u^{k} is electric potential obtained as a solution of Laplace's equation. When difference between two successive conductivities falls below certain value electric field distribution can be calculated using:

$$\mathbf{E} = \frac{\mathbf{J}_{\mathrm{CDI}}}{\sigma}.$$

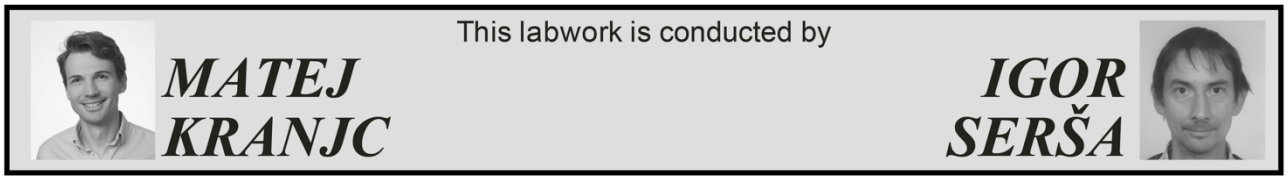

The aim of this laboratory practice is to demonstrate monitoring of electric field distribution in a biological tissue using MREIT.

EXPERIMENT

We will monitor current density distribution and electric field distribution in biological tissue exposed to electric pulses by means of MREIT. We will then compare measured current density distribution and reconstructed electric field distribution with simulation results obtained by a numerical model of the tissue.

Protocol

The experiment will be performed on biological tissue (chicken liver) sliced in a disc-like sample measuring 21 mm in diameter and 2 mm in height (Fig. 1a). Electric pulses will be delivered via two cylindrically shaped electrodes inserted into the sample. After the insertion, the electrodes will be connected to an electric pulse generator connected to an MRI spectrometer. The sample will be placed in a 25 mm MR microscopy RF probe (Fig. 1b) inside a horizontal-bore superconducting MRI magnet (Fig. 1c). Electroporation treatment of the sample will be performed by applying two sequences of four high voltage electric pulses with a duration of 100 μs, a pulse repetition frequency of 5 kHz and with an amplitude of 500 V and 1000 V.

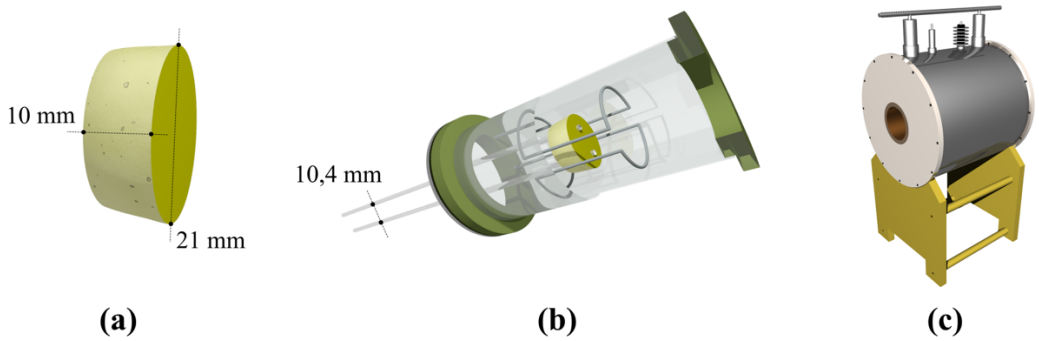

Figure 1: Biological sample (a) placed in a MR microscopy probe (b) inside a horizontal MRI magnet (c).

MR imaging will be performed on a MRI scanner consisting of a 2.35 T (100 MHz proton frequency) horizontal bore superconducting magnet (Oxford Instruments, Abingdon, United Kingdom) equipped with a Bruker micro-imaging system (Bruker, Ettlingen, Germany) for MR microscopy with a maximum imaging gradient of 300 mT/m and a Tecmag Apollo spectrometer (Tecmag, Houston TX, USA). Monitoring of electric field is enabled by CDI, which is an MRI method that enables imaging of current density distribution inside conductive sample. We will apply two-shot RARE version of the CDI sequence (Fig. 2).

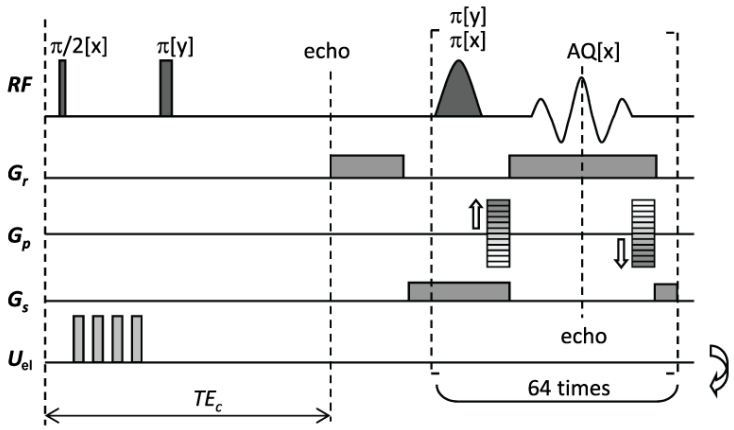

Figure 2: Two-shot RARE pulse sequence used for acquisition of current density distribution. The sequence consists of a current encoding part with a short (100 μs long) high-voltage electroporation pulse (U_{el}) delivered immediately after the nonselective 90° radiofrequency (RF) excitation pulse. In the second part of the sequence signal acquisition is performed using the single-shot RARE signal acquisition scheme that includes standard execution of readout (G_r), phase-encoding (G_p) and slice-selection (G_s) magnetic field gradients. Due to auxiliary phase encoding induced by the electric pulse, the RARE sequence is repeated twice, each time with a different phase of the refocusing pulses (0°and 90°), and the corresponding signals are co-added.

Electric field distribution in the sample will be reconstructed by iteratively solving Laplace's equation using J-substitution mathematical algorithm and finite element method with the numerical computational environment MATLAB on a desktop PC. We will compare measured current density distribution obtained by means of CDI and reconstructed electric field distribution obtained by means of MREIT in the sample with simulation results obtained by a numerical model of the sample.

FURTHER READING

Kranjc M., Bajd F, Sersa I., Miklavcic D., Magnetic resonance electrical impedance tomography for monitoring electric field distribution during tissue electroporation. *IEEE Trans Med Imaging* 30:1771–1778, 2011.

Kranjc M., Bajd F., Serša I., Miklavčič D., Magnetic resonance electrical impedance tomography for measuring electrical conductivity during electroporation. *Physiol Meas* 35:985–96, 2014.

Kranjc M, Markelc B, Bajd F, Čemažar M, Serša I, Blagus T, Miklavčič D. In situ monitoring of electric field distribution in mouse tumor during electroporation. Radiology 274: 115-123, 2015.

Kranjc M., Bajd F., Serša I. de Boevere M., Miklavcic D., Electric field distribution in relation to cell membrane electroporation in potato tuber tissue studied by magnetic resonance techniques. *Innov Food Sci Emerg Technol*, 2016.

Woo E. J. and Kranjc M. Principles and use of magnetic resonance electrical impedance tomography in tissue electroporation in *Handbook of Electroporation* (ed. Miklavcic, D.) 1–18 Springer, 2016.

Seo J.K., Woo E.J., Magnetic Resonance Electrical Impedance Tomography (MREIT). *SIAM Rev* 53:40–68, 2011.

Sersa I. Auxiliary phase encoding in multi spin-echo sequences: application to rapid current density imaging. *J Magn Reson*, 190(1):86–94, 2008

NOTES & RESULTS

NOTES & RESULTS

Measurements of the induced transmembrane voltage with fluorescent dye di-8-ANEPPS

L11

Gorazd Pucihar
University of Ljubljana, Faculty of Electrical Engineering

Duration of the experiments: 60 min
Max. number of participants: unlimited
Location: Online ONLY
Level: Advanced

PREREQUISITES

Participants should be familiar with Laboratory safety (S1). The basic knowledge of handling with cells is required for this laboratory practice.

THEORETICAL BACKGROUND

When a biological cell is placed into an external electric field the induced transmembrane voltage (ITV) forms on its membrane. The amplitude of the ITV is proportional to the amplitude of the applied electric field, and with a sufficiently strong field, this leads to an increase in membrane permeability - electroporation. Increased permeability is detected in the regions of the cell membrane where the ITV exceeds a sufficiently high value, in the range of 250 – 1000 mV, depending on the cell type. In order to obtain an efficient cell electroporation it is therefore important to determine the distribution of the ITV on the cell membrane. The ITV varies with the position on the cell membrane, is proportional to the electric field, and is influenced by cell geometry and physiological characteristics of the medium surrounding the cell. For simple geometric shapes the ITV can be calculated analytically (e.g. for a spherical cell, using Schwan's equation). For more complicated cell shapes experimental and numerical methods are the only feasible approach to determine the ITV.

The aim of this laboratory practice is to measure the ITV on a spherical cell by means of a fluorescent potentiometric dye di-8-ANEPPS.

EXPERIMENT

Potentiometric fluorescent dyes allow observing the variations of the ITV on the membrane and measuring its value. Di-8-ANEPPS is a fast potentiometric fluorescent dye, which becomes fluorescent when it binds to the cell membrane, with its fluorescence intensity varying proportionally to the change of the ITV. The dye reacts to the variations in the ITV by changing the intramolecular charge distribution that produce corresponding changes in the spectral profile or intensity of the dye's fluorescence.

Protocol: The experiments are performed on Chinese hamster ovary cells (CHO) grown in Lab-Tek chambers (Nunc, Germany) in culture medium HAM-F12 supplemented with 10% fetal bovine serum, L-glutamine (all three from Sigma-Aldrich) and antibiotics. When cells attach to the cover glass of a Lab-Tek chamber (usually after 2 to 3 hours to obtain attached cells of spherical shape), carefully replace the culture medium with 1 ml of SMEM medium (Spinner's modification of the MEM, Sigma-Aldrich) containing 30 μM of di-8-ANEPPS and 0.05% of Pluronic (both Life Technologies). After staining for 12 min at 4°C, wash the cells thoroughly with pure SMEM to remove the excess dye. After washing leave 1.5 ml of SMEM in the chamber. Place the chamber under a fluorescence microscope (Zeiss

This labwork is conducted by

JANJA DERMOL-ČERNE

AxioVert 200, Germany) and use ×63 oil immersion objective. Position two parallel Pt/Ir wire electrodes, with a 4 mm distance between them, to the bottom of the chamber. Set a single 40 V, 50 ms pulse on the programmable square wave electroporator TSS20 (Intracel). This will result in a voltage-to-distance ratio of ~100 V/cm. The pulse must be synchronized with the image acquisition. Set the excitation wavelength to 490 nm and use ANEPPS filter to detect fluorescence (emission 605 nm).
Find the cells of interest. Acquire the control fluorescence image and subsequently the image with a pulse, using a cooled CCD camera (VisiCam 1280, Visitron) and MetaFluor 7.7.5 (Molecular Devices). Apply four pulses with a delay of 4 s between two consecutive pulses. For each pulse, acquire a pair of images, one immediately before (control image) and one during the pulse (pulse image) (Figures 1A and B).
Open the images in MetaMorph 7.7.5 (Molecular Devices). To *qualitatively* display the ITV on the cell membrane, convert the acquired 12-bit images to 8-bit images. For each pulse, obtain the difference image by subtracting (on a pixel-by-pixel basis) the control image from the pulse image. Add 127, so that 127, i.e. mid-gray level, corresponds to 0 V, brighter levels to negative voltages, and darker levels to positive ones (Figure 1C). Average the three difference images to increase the signal-to-noise ratio.
To *quantitatively* determine the ITV, open the acquired, unprocessed fluorescence images. Determine the region of interest at the site of the membrane and measure the fluorescence intensities along this region for the control and pulse image. Transform the values to the spreadsheet. Measure the background fluorescence in both images and subtract this value from the measured fluorescence. Calculate the relative changes in fluorescence ($\Delta F/F_C$) by subtracting the fluorescence in the control image F_C from the fluorescence in the pulse image F_P and dividing the subtracted value by the fluorescence in the control F_C; $\Delta F/F_C = (F_P - F_C) / F_C$. Average the relative changes calculated for all four acquired pairs of images. Transform the fluorescence changes to the values of the ITV (ΔF/F = -6% / 100 mV), and plot them on a graph as a function of the arc length (Figure 1D).

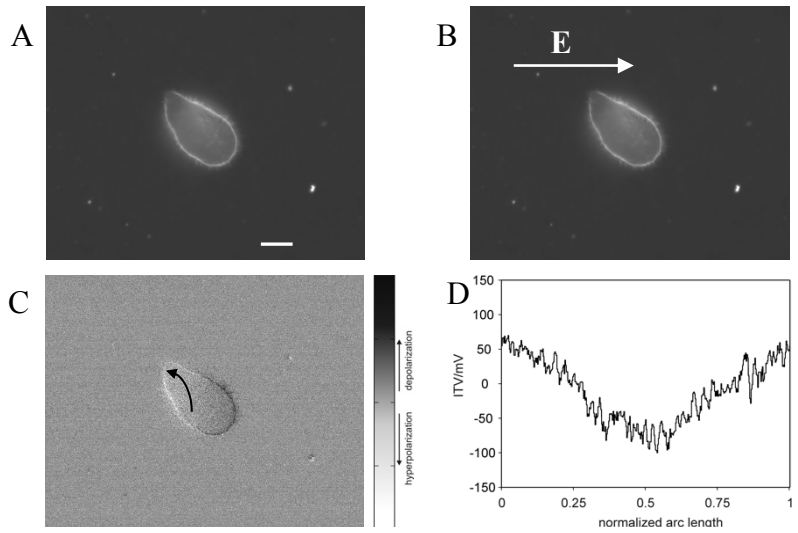

Figure 1: Measurements of the induced transmembrane voltage (ITV) on an irregularly shaped CHO cell. (A) A control fluorescence image of a cell stained with di-8-ANEPPS. Bar represents 10 µm. (B) Fluorescence image acquired during the exposure to a 35 V (~88 V/cm), 50 ms rectangular pulse. (C) Changes in fluorescence of a cell obtained by subtracting the control image A from the image with pulse B and shifting the grayscale range by 50%. The brightness of the image was automatically enhanced. (D) ITV measured along the path shown in C.

FURTHER READING:

Teissié J., and Rols M. P. An experimental evaluation of the critical potential difference inducing cell membrane electropermeabilization. *Biophys. J.* 65:409-413, 1993.

Gross D., Loew L. M, and Webb W. Optical imaging of cell membrane potential changes induced by applied electric fields *Biophys. J.* 50:339-348, 1986.

Montana V., Farkas D. L., and Loew L. M. Dual-wavelength ratiometric fluorescence measurements of membrane-potential. *Biochemistry* 28:4536-4539, 1989.

Loew L. M. Voltage sensitive dyes: Measurement of membrane potentials induced by DC and AC electric fields. *Bioelectromagnetics* Suppl. 1:179-189, 1992.

Hibino M., Itoh H., and Kinosita K. Time courses of cell electroporation as revealed by submicrosecond imaging of transmembrane potential. *Biophys. J.* 64:1789-1800, 1993.

Kotnik T., Bobanović F., and Miklavčič D. Sensitivity of transmembrane voltage induced by applied electric fields – a theoretical analysis. *Bioelectrochem. Bioenerg.* 43:285-291, 1997.

Pucihar G., Kotnik T., Valič B., Miklavčič D. Numerical determination of transmembrane voltage induced on irregularly shaped cells. *Annals Biomed. Eng.* 34: 642-652, 2006.

Video Article:

Pucihar G., Kotnik T., Miklavčič D. Measuring the induced membrane voltage with di-8-ANEPPS (Video Article). *J. Visual Exp.* 33: 1659, 2009.

NOTES & RESULTS

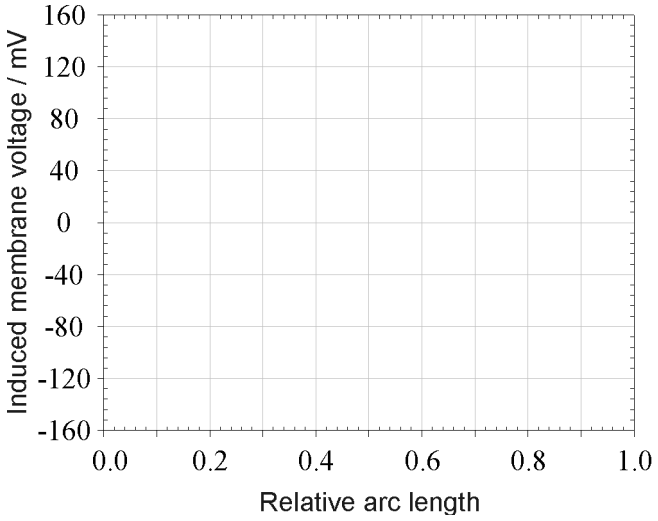

NOTES & RESULTS

Analysis of electric field orientations on gene electrotransfer efficiency L12

Saša Haberl Meglič, Matej Reberšek
University of Ljubljana, Faculty of Electrical Engineering

Duration of the experiment: 60 min
Max. number of participants: Unlimited
Location: Online ONLY
Level: Advanced

PREREQUISITES

Participants should be familiar with the Safety rules and Rules for sterile work in cell culture laboratory. The basic knowledge of handling with cells is required for this laboratory practice.

THEORETICAL BACKGROUND

Gene electrotransfer is a non-viral method used to transfer genes into living cells by means of high-voltage electric pulses. An exposure of a cell to an adequate amplitude and duration of electric pulses leads to transient increase of cell membrane permeability for molecules which are otherwise deprived of membrane transport mechanisms. This allows various nonpermeant molecules, including DNA, to be transported across the membrane and enter the cell. Although mechanisms of the process are not yet fully elucidated, it was shown that several steps are crucial for gene electrotransfer: interaction of plasmid DNA (pDNA) with the cell membrane, translocation of pDNA across the membrane, migration of pDNA towards the nucleus, transfer of pDNA across the nuclear envelope and gene expression.

Many parameters (such as electric pulse protocol) can influence the first step (interaction of DNA with the cell membrane) and by that gene electrotransfer efficiency. Therefore different electric pulse protocols are used in order to achieve maximum gene transfection, one of them is changing the electric field orientation during the pulse delivery. Since DNA is a negatively charged molecule and it is dragged towards the cell with the electrophoretic force in the opposite direction of the electric field, changing electric field orientation increases the membrane area competent for DNA entry into the cell.

The aim of this laboratory practice is to demonstrate how different pulse polarity affects the efficiency of gene electrotransfer and cell viability.

EXPERIMENT

For the experiment we will use Chinese hamster ovary cells (CHO-K1) and plasmid DNA (pEGFP-N_1) that codes for GFP (green fluorescent protein). To generate and deliver electric pulses a high-voltage prototype generator and electrodes with four cylindrical rods, which were developed at a Laboratory of Biocybernetics will be used. Pulses will be monitored on osciloscope (LeCroy 9310C).

Pulse protocols (see also Figure 1):

a) SP (single polarity): the direction of electric field is the same for all pulses

This labwork is conducted by

SAŠA HABERL MEGLIČ

b) OBP (orthogonal both polarities): the direction of the electric field is changed between the pulses

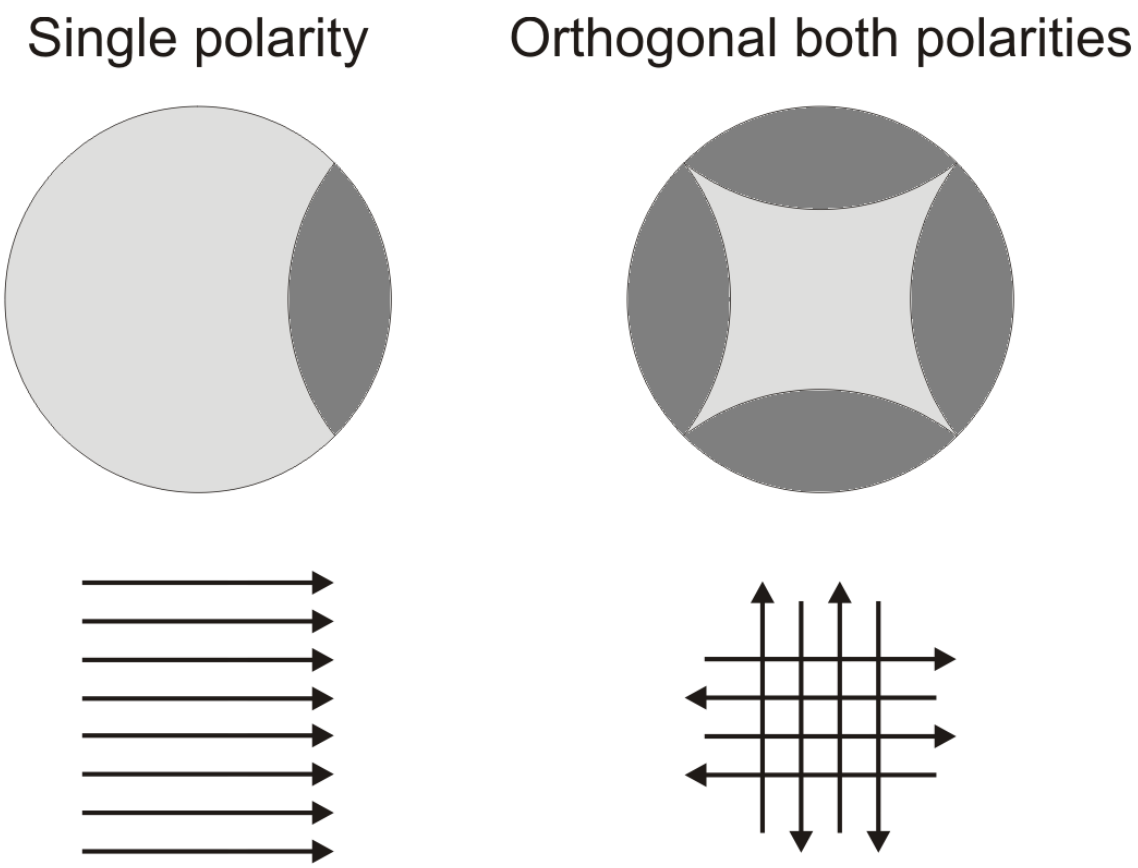

Figure 1: Two different pulse protocols will be used: single polarity (SP) and orthogonal both polarities (OBP)

Protocol 1/2 (Gene electrotransfer with different pulse parameters): CHO cells will be grown in multiwells as a monolayer culture in Ham's tissue culture medium for mammalian cells with 10% fetal bovine serum at 37º C. Cells will be plated 24h before the experiment in concentration 5 x 10^5 cells per well.
Just before the experiment remove culture medium and replace it with 150 µl of electroporation buffer containing plasmid DNA with concentration 10 µg/ml. Incubate cells with plasmid for 2-3 minutes at room temperature. Then apply a train of eight pulses with amplitude of 225 V, duration of 1 ms and repetition frequency 1 Hz using single polarity and orthogonal both polarities (see Pulse protocols) to deliver plasmid DNA into the cells.
Cells in the control are not exposed to electric pulses.
Immediately after exposure of cells to electric pulses add 37 µl of fetal calf serum (FCS-Sigma, USA). Incubate treated cells for 5 minutes at 37º C and then add 1 ml of culture medium.

Protocol 2/2 (Determining gene electrotransfer efficiency and cell viability): After 24 h incubation at 37º C determine the difference in gene electrotransfer efficiency and cell viability for both pulse protocols by fluorescent microscopy (Leica, Wetzlar, Germany) at 20x magnification using GFP filter with excitation at 488 nm.

You will determine gene electrotransfer efficiency from the ratio between the number of green fluorescent cells (successfully transfected) and the total number of cells counted under the phase

contrast. You will obtain cell survival from phase contrast images as the ratio between the number of viable cells in the treated sample and the number of viable cells in the control sample.

FURTHER READING:

Faurie C., Reberšek M., Golzio M., Kandušer M., Escoffre J. M., Pavlin M., Teissie J., Miklavčič D., Rols M. P. Electro-mediated gene transfer and expression are controlled by the life-time of DNA/membrane complex formation. *J Gene Med* 12: 117-125, 2010
Golzio M., Teissié J., Rols M. P. Direct visualization at the single-cell level of electrically mediated gene delivery. *PNAS* 99: 1292-1297, 2002
Pavlin M., Haberl S., Reberšek M., Miklavčič D., Kandušer M. Changing the direction and orientation of electric field during electric pulses application improves plasmid gene transfer in vitro. *J Vis Exp*, 55: 1-3, 2011
Reberšek M., Faurie C., Kandušer M., Čorović S., Teissié J., Rols M.P., Miklavčič D. Electroporator with automatic change of electric field direction improves gene electrotransfer *in vitro*. *Biomed Eng Online* 6: 25, 2007
Reberšek M., Kandušer M., Miklavčič D. Pipette tip with integrated electrodes for gene electrotransfer of cells in suspension: a feasibility study in CHO cells. *Radiol Oncol* 45: 204-208, 2011

NOTES & RESULTS

Pulse parameters	Gene electrotransfer efficiency [%]	Cell viability [%]
Single polarity		
Orthogonal both polarities		

COMPUTER MODELING

Treatment planning for electrochemotherapy and irreversible electroporation: optimization of voltage and electrode position C1

Anže Županič[1], Bor Kos[2]
[1]Eawag - Swiss federal institute of aquatic science and technology, Switzerland
[2]University of Ljubljana, Faculty of Electrical Engineering

Duration of the experiments: 60 min
Max. number of participants: 6
Location: Laboratory of Biocybernetics
Level: Basic

PREREQUISITES

No specific knowledge is required for this laboratory exercise.

THEORETICAL BACKGROUND

Electrochemotherapy (ECT) is an efficient local treatment of cutaneous and subcutaneous tumors, which combines the delivery of nonpermeant, cytotoxic chemotherapeutics (e.g. bleomycin, cisplatin) and short high-voltage electric pulses. The pulses induce electric fields inside the tissue, thereby increasing cell membrane permeability in tissue (electropermeabilization) to otherwise nonpermeant chemotherapeutics. ECT requires the electric field inside the tumor to be higher than the threshold value needed for reversible electroporation (E_{rev}) while irreversible electroporation (E_{irrev}) in nearby critical structures should be limited. For IRE, the electric field in the entire tumor volume needs to be above the irreversible electroporation threshold. It is not necessary that the whole tumor is electropermeabilized by one pulse or pulse sequence - sometimes a combination of several pulse sequences or a combination of different electrodes is required.

The aim of this laboratory practice is to learn how to use optimization techniques to achieve suitable electric field distribution for electrochemotherapy experimental planning and treatment planning.

EXPERIMENT

A finite element based numerical modeling program package COMSOL Multiphysics version 5.4 (COMSOL AB, Stockholm, Sweden) will be used to optimize voltage between the electrodes and position of the electrodes on a simple 3D model of a spherical subcutaneous tumor and surrounding tissue (Figure 1a). Electrode positions and the applied voltage should be chosen, so that the following objectives are fulfilled:

- For electrochemotherapy: the tumor is permeabilized ($E_{tumor} > E_{rev} = 400\ V/cm$),
- For irreversible electroporation: the tumor is permeabilized above the irreversible threshold ($E_{tumor} > E_{irrev} = 600\ V/cm$),
- the damage to healthy tissue is kept to a minimum.

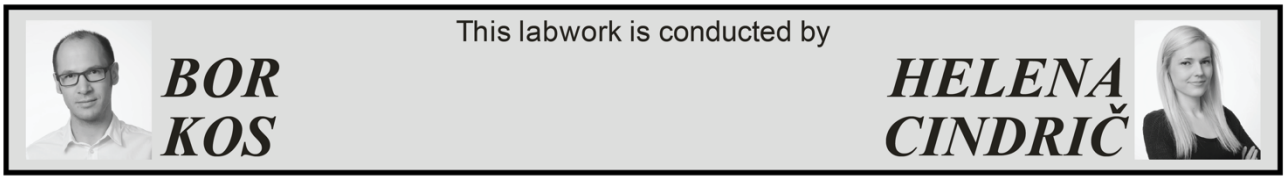

We will calculate the electric field distribution in the model after each change of the electrode placement or voltage. The final goal of this exercise is to achieve 100 % $E_{tumor} > E_{rev}$ (or 100 % $E_{tumor} > E_{irr}$ when planning for IRE) and minimize E_{irr} in healthy tissue.

Protocol: Build the 3-d model by following the lecturer's instructions and take into account your tissue-specific electric properties. Solve the model and evaluate the initial solution. In case, the initial solution is inappropriate (see e.g., Figure 1b), try to improve on the solution by changing electrode positions and voltage between the electrodes. Calculate the electric field distribution in the model after changing the electrode positions or voltage and then determine the coverage of tumor tissue with $E_{tumor} > (E_{rev}$ or $E_{irrev})$ and determine damage to healthy tissue due to irreversible electroporation. Repeat the process, until the quality of your solution reaches the set goals. Compare the results with others, who have used different tissue properties. Use a parametric study to find the lowest voltage which achieves the objective for the selected electrode geometry.

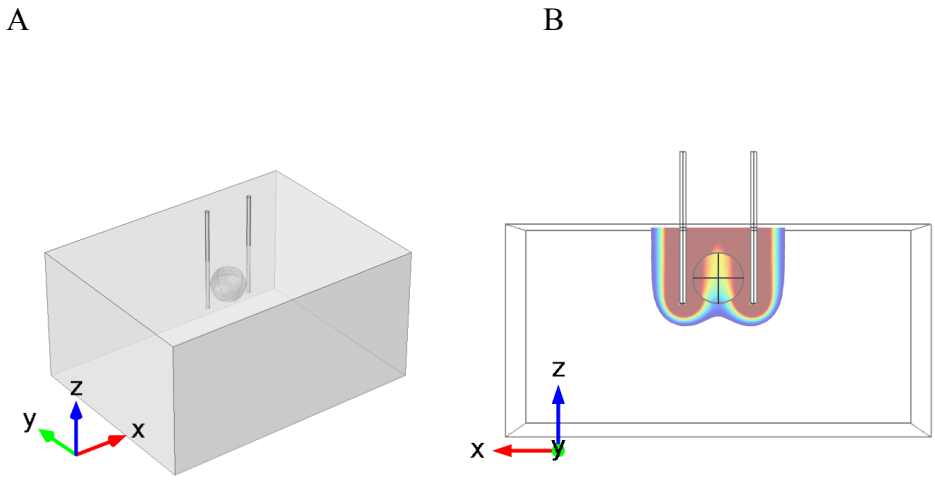

Figure 1: (A) Simple 3D model of tumor and needle electrodes in healthy tissue; (B) electric field over reversible threshold inside the healthy tissue and the tumor.

FURTHER READING:

Miklavčič D, Čorović S, Pucihar G, Pavšelj N. Importance of tumor coverage by sufficiently high local electric field for effective electrochemotherapy. *EJC Supplements*, 4: 45-51, 2006.

Čorović S, Županič A, Miklavčič D. Numerical modeling and optimization of electric field distribution in subcutaneous tumor treated with electrochemotherapy using needle electrodes. *IEEE Trans. Plasma Sci.,* 36: 1665-1672, 2008.

Županič A, Čorović S, Miklavčič D. Optimization of electrode position and electric pulse amplitude in electrochemotherapy. *Radiol. Oncol.,* 42: 93-101, 2008.

Edd JF, Davalos RV. Mathematical modeling of irreversible electroporation for treatment planning, *Technol. Cancer Res. Treat.,* 6: 275-286, 2007.

Kos B, Zupanic A, Kotnik T, Snoj M, Sersa G, Miklavcic D. Robustness of Treatment Planning for Electrochemotherapy of Deep-Seated Tumors, Journal of Membrane Biology 236: 147-153, 2010.

Cukjati, D, Batiuskaite D, Andre F, Miklavcic D, Mir L. Real Time Electroporation Control for Accurate and Safe in Vivo Non-viral Gene Therapy. *Bioelectrochemistry* 70: 501–507, 2007.

NOTES & RESULTS

NOTES & RESULTS

Numerical Modeling of Thermal Effects during Irreversible Electroporation Treatments

C2

Paulo A. Garcia[1] and Bor Kos[2]
[1]Virginia Tech – Wake Forest University
[2]University of Ljubljana, Faculty of Electrical Engineering

Duration of the experiment: 90 min
Max. number of participants: 6
Location: Laboratory of Biocybernetics
Level: Advanced

PREREQUISITES

Basic to advanced knowledge of finite element modeling

THEORETICAL BACKGROUND

Irreversible electroporation (IRE) is a new, safe, and effective minimally invasive ablation modality with the potential to treat many currently unresectable and/or untreatable tumors. The non-thermal mode of cell death in IRE is unique in that it does not rely on thermal changes from Joule heating to kill tumor cells thus allowing for successful treatment even in close proximity to critical structures and without being affected by the heat sink effect. Accurate modeling of the electrical and thermal responses in tissue is important to achieve complete coverage of the tumor and ensure that the thermal changes during a procedure do not generate thermal damage, especially in critical structures (e.g. bile ducts, nerves and sensitive blood vessels).

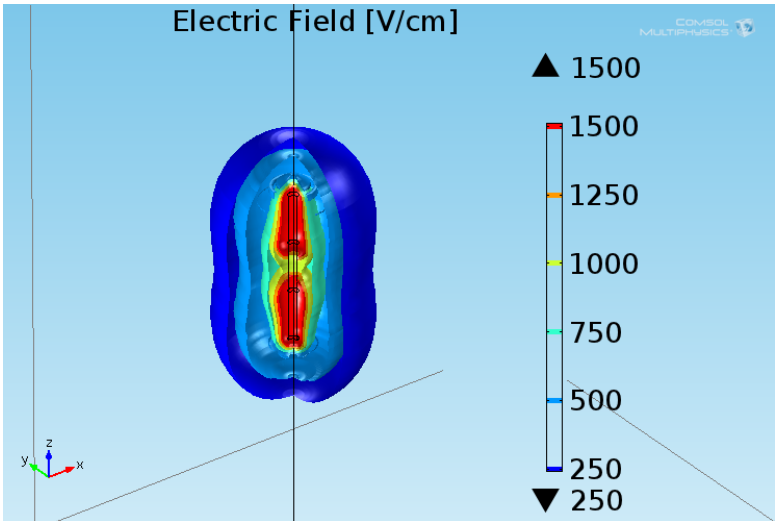

Figure 2: Electric Field distribution resulting from a bipolar electrode with an applied voltage of 1250 V.

The temperature distribution (T) within the tissue will be obtained by transiently solving a modified heat conduction equation with the inclusion of the Joule heating source term $Q = \sigma|\nabla\varphi|^2$

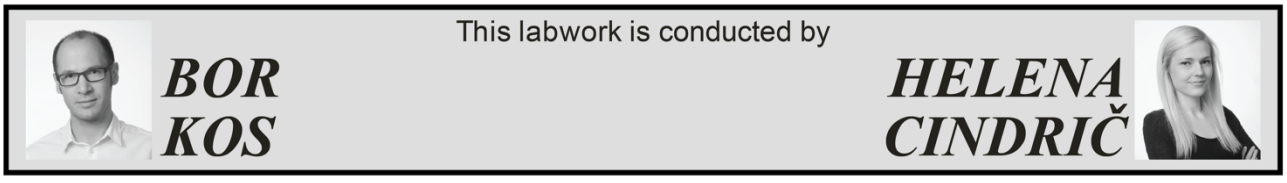

$$\rho C \frac{\partial T}{\partial t} = \nabla \cdot (k \nabla T) + Q \qquad (1)$$

where σ is the electrical conductivity, φ the electric potential, k is the thermal conductivity, C is the specific heat capacity, and ρ is the density of the tissue. At each time step, the current density and electric field distribution are determined and updated in the Joule heating term to capture the electrical conductivity changes in liver tissue from electroporation and temperature.

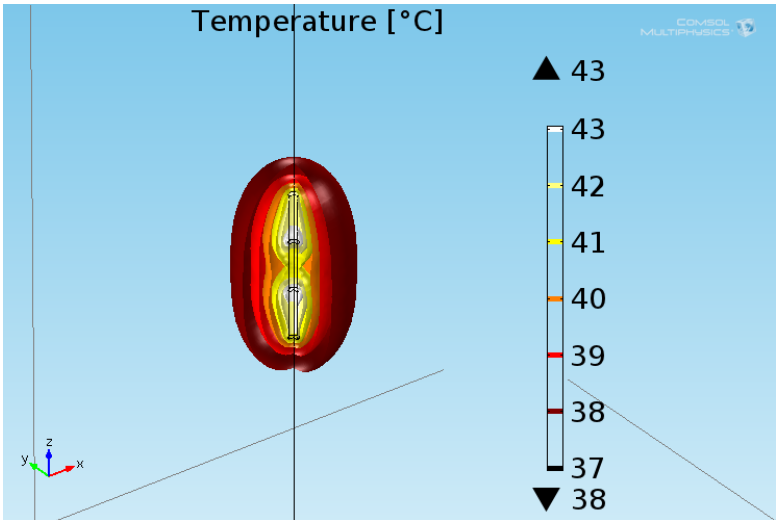

Figure 3: Temperature distribution after a ninety 100-µs pulse IRE treatment in liver tissue at 1 pulse per second.

Thermal damage is a process that depends on temperature and time. If the exposure is long, damage can occur at temperatures as low as 42°C, while 50°C is generally chosen as the target temperature for instantaneous damage. The damage can be calculated based on the temperatures to assess whether a particular set of pulse parameters and electrode configuration will induce thermal damage in superposition with IRE. The thermal damage will be quantified using the Arrhenius rate equation given by:

$$\Omega(t) = \int_{t=0}^{t=\tau} \zeta \cdot e^{\frac{-E_a}{R \cdot T(t)}} dt \qquad (2)$$

where R is the universal gas constant, 8.314 J/(mol·K); ζ is the pre-exponential factor, 7.39×10^{39} s^{-1}, a measure of the effective collision frequency between reacting molecules in bimolecular reactions; E_a the activation energy barrier that molecules overcome to transform from their "native state" to the "damaged state", 2.577×10^5 J/mol for liver tissue. It is important to note that the pre-exponential factor and activation energy are tissue specific parameters that describe different modes of thermal damage such as microvascular blood flow stasis, cell death, and protein coagulation. In terms of finite element modeling of thermal damage, an integral value $\Omega(t) = 1$ corresponds to a 63% probability of cell death and an integral value $\Omega(t) = 4.6$ corresponds to 99% probability of cell death due to thermal effects. In order to convert the damage integral to a probability of cell death, $P(\%)$, we will use:

$$P(\%) = 100 \cdot \left(1 - e^{-\Omega(t)}\right)$$

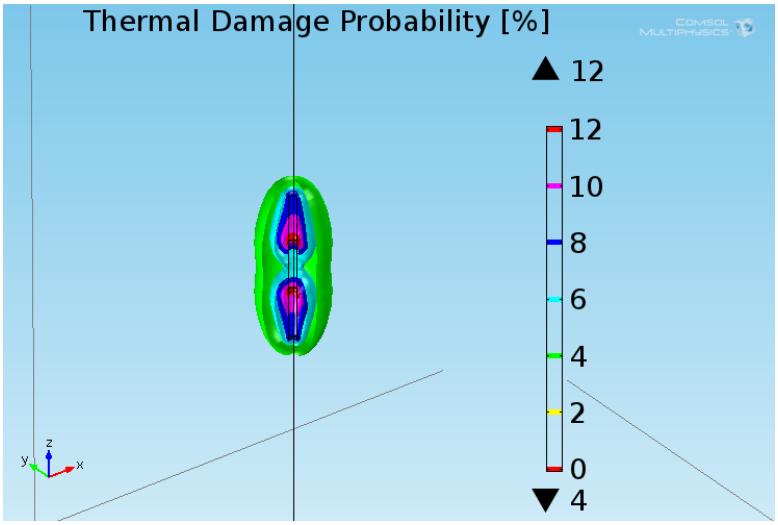

Figure 4: Thermal damage probability of cell death due to excessive thermal effects as a result of Joule heating.

The aim of this laboratory practice is to get familiar with the numerical simulation tools needed for capturing the electrical and thermal responses during a ninety 100-µs pulse IRE. We will accomplish this by coupling the Laplace, Heat Conduction, and Arrhenius equations using COMSOL Multiphysics 5.4 (Comsol AB, Stockholm, Sweden) to determine the IRE zones of ablation and evaluate if the increase in temperature due to Joule heating due to the pulses generates any potential thermal damage.

EXPERIMENT

In this exercise we will compare the effect of a static, σ_0, and dynamic, $\sigma(E)$, electrical conductivity functions in the resulting electrical and thermal effects during an entire IRE protocol in liver tissue. Initially we will determine the volume of tissue affected by IRE from the electric field distributions. We will then evaluate the temperature increase in liver tissue as a result of the Joule heating and determine if there was a probability of cell death due to thermal damage with the given IRE protocols employed. This exercise will provide the participants with accurate predictions of all treatment associated effects which is a necessity toward the development and implementation of optimized treatment protocols.

Specifically:
1) Simulate the electric field distribution using a static conductivity and 1000 V, 1500 V, and 2000 V.
2) Simulate the electric field distribution using a dynamic conductivity and 1000 V and 1500 V.
3) Include the Heat Conduction Equation by coupling with the Laplace Equation via Joule Heating.
4) Explore the resulting temperature distributions as a function of pulse number and frequency.
5) Incorporate the Arrhenius equation to assess potential thermal damage from the Joule Heating.
6) Investigate the effect of pulse frequency (1 Hz, 10 Hz, and 100 Hz) for ninety 100-µs pulses.

FURTHER READING:

Davalos RV, Rubinsky B, Mir LM. Theoretical analysis of the thermal effects during in vivo tissue electroporation. *Bioelectrochemistry* 61(1-2): 99-107, 2003

Chang, IA and Nguyen, UD., Thermal modeling of lesion growth with radiofrequency ablation devices. *Biomed Eng Online*, 3(1): 27, 2004

Davalos, R.V. and B. Rubinsky, Temperature considerations during irreversible electroporation. *International Journal of Heat and Mass Transfer*, 51(23-24): 5617-5622, 2008

Pavšelj N and Miklavčič D, Numerical modeling in electroporation-based biomedical applications. *Radiology and Oncology*, 42(3): 159-168, 2008

Lacković I, Magjarević R, Miklavčič D. Three-dimensional finite-element analysis of joule heating in electrochemotherapy and in vivo gene electrotransfer. *IEEE T. Diel. El. Insul.* 15: 1338-1347, 2009

Garcia, PA, et al., A Parametric Study Delineating Irreversible Electroporation from Thermal Damage Based on a Minimally Invasive Intracranial Procedure. *Biomed Eng Online*, 10(1): 34, 2010

Pavšelj N, Miklavčič D. Resistive heating and electropermeabilization of skin tissue during in vivo electroporation: A coupled nonlinear finite element model. *International Journal of Heat and Mass Transfer* 54: 2294-2302, 2011

Garcia PA, Davalos RV, Miklavčič D. A numerical investigation of the electric and thermal cell kill distributions in electroporation-based therapies in tissue. *PLOS One* 9(8): e103083, 2014.

NOTES & RESULTS

Molecular dynamics simulations of membrane electroporation C3

Mounir Tarek
CNRS- Université de Lorrains, Nancy France
Europeen Laboratory EBAM

Duration of the experiments: 90 min
Max. number of participants: 18
Location: Computer room (P18-A2)
Level: Basic

PREREQUISITES

No specific knowledge is required for this laboratory practice.

THEORETICAL BACKGROUND

The application of high electric fields to cells or tissues permeabilizes the cell membrane and is thought to produce aqueous-filled pores in the lipid bilayer. Electroporation is witnessed when the lipid membrane is subject to transmembrane voltages (TMV) of the order of few hundred millivolts, which results from the application of electrical pulses on a microsecond to millisecond time scale

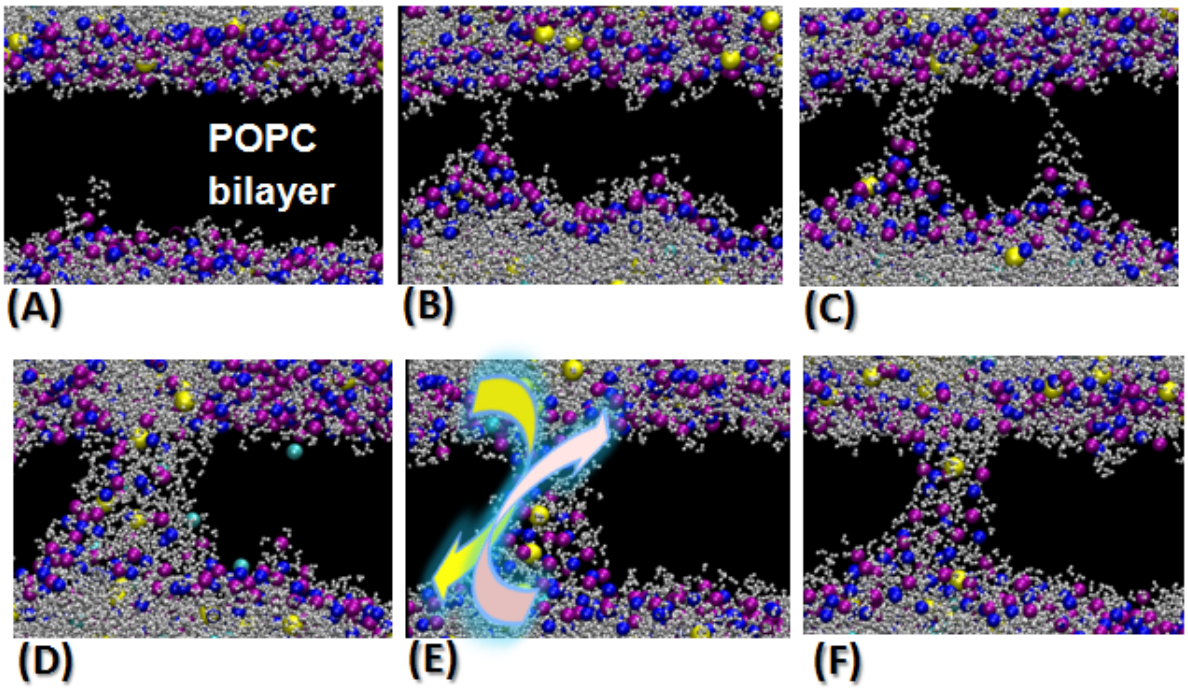

Figure 1: Configurations from the MD simulation for a large POPC subject to a transverse electric field (A) Bilayer at equilibrium. (B-C) Formation of water wires at the initial stage of the electroporation process (D-F) Formation at a later stage of large water pores that conduct ions across the membrane and that are stabilized by lipid head-group (yellow cyan). (Delemotte and Tarek. *J. Membr. Biol.* 2012).

This labwork is conducted by

MOUNIR TAREK

which are sufficient to produce a transient trans-membrane potential and an electrical field across the membrane of the order of ~ 10^8 V/m. This process is believed to involve (1) charging of the membrane due to ion flow, (2) rearrangement of the molecular structure of the membrane, (3) formation of pores, which perforate the membrane and are filled by water molecules (so-called aqueous, or hydrophilic, pores), (4) an increase in ionic and molecular transport through these pores, and, under appropriate conditions, membrane integrity recovery when the external field stress is removed.

Molecular Dynamics (**MD**) simulations belong to a set of computational methods in which the dynamical behaviour of an ensemble of atoms or molecules, interacting via approximations of physical pair potentials, is determined from the resolution of the equation of motions. MD simulations enable ones to investigate the molecular processes affecting the atomic level organization of membranes when these are submitted to voltage gradient of magnitude similar to those applied during electropulsation. The aim of this practical exercise is to characterize from MD simulations trajectories the electrostatic properties of membranes subject to a transmembrane potential (0 to 2 V).

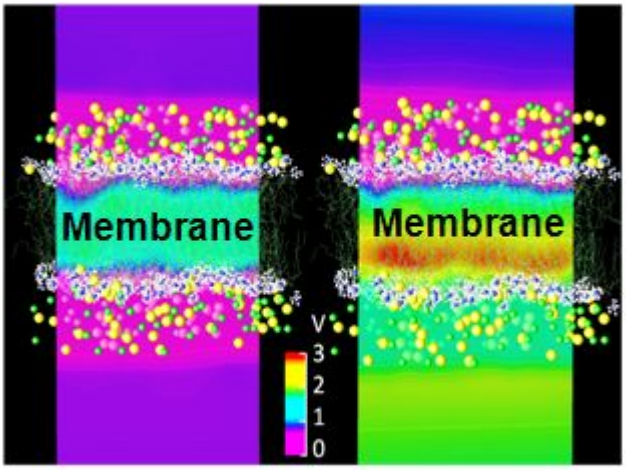

Figure 2: Electrostatic potential maps generated from the MD simulations of a POPC lipid bilayer (acyl chains, green; head groups, white) surrounded by electrolyte baths at 1 M NaCl (Na+ yellow, Cl- green, water not shown) terminated by an air/water interface. Left: net charge imbalance Q = 0 e (TMV=0 mV). Right: Q = 6 e (TMV=2 V).

The aim of this laboratory practice is to get familiar with the tools for molecular dynamics, possibilities to set on models and graphical presentation of atomistic models.

EXPERIMENT

Due to the limited time and large resources needed to generate MD trajectories of membranes, the latter will be provided to the students. The simulations concern pure planar phospholipid bilayers (membrane constituents) and water described at the atomic level. A set of long trajectories spanning few nanoseconds generated with or without a transmembrane voltage induced by unbalanced ionic concentrations in the extracellular and intracellular will be provided. The students will (1) determine the distribution of potential and electric field in model membrane bilayers (2) measure the membrane capacitance, (3) visualize at the molecular level the formation of membrane pores under the influence of a transmembrane voltage, and measure the intrinsic conductance of such pores.

FURTHER READING:

Tarek, M. Membrane Electroporation: A Molecular Dynamics Study *Biophys. J.* 88: 4045-4053, 2005.
Dehez, F.; Tarek, M.; and Chipot, C. Energetics of Ion Transport in a Peptide Nanotube *J. Phys. Chem. B* 111: 10633-10635, 2007
Andrey A. Gurtovenko, Jamshed Anwar, and Ilpo Vattulainen, Defect-Mediated Trafficking across Cell Membranes: Insights from in Silico Modeling, *Chem. Rev.* 110: 6077-6103, 2010.
Delemotte, L. and Tarek, M. Molecular Dynamics Simulations of Membrane Electroporation *J. Membr. Biol.* 245/9:531-543, 2012.
Polak A, Tarek M, Tomšič M, Valant J, Poklar Ulrih N, Jamnik A, Kramar P, Miklavčič D. Electroporation of archaeal lipid membranes using MD simulations. *Bioelectrochemistry* 100: 18-26, 2014.

NOTES & RESULTS

NOTES & RESULTS

HARDWARE
DEVELOPMENT AND MEASUREMENT

Measurement of electroporation pulses with oscilloscope, and voltage and current probes

H1

Matej Reberšek
University of Ljubljana, Faculty of Electrical Engineering

Duration of the experiment: 60 min
Max. number of participants: 10
Location: Laboratory of Biocybernetics
Level: Basic

PREREQUISITES

No specific knowledge is required for this laboratory exercise.

THEORETICAL BACKGROUND

Electroporation is initiated by the delivery of electrical pulses to biological cells. Electrical pulses may vary in pulse parameters such as pulse shape, amplitude, duration and polarity. We may deliver different number of pulses, use combination of different pulses or vary pulse repetition rates. We also may deliver pulses in bursts or in different directions relative to the cell. The process of the electroporation is strongly dependent on the pulse parameters of the delivered electrical pulses. In order to control the process of the electroporation and to exactly specify the experimental method, and thus enable the reproduction of experiments under the same conditions, we should exactly determine and describe these electrical parameters. When reporting electroporation methods we should: 1) describe exactly how the electric pulses were measured; 2) provide time-domain waveforms of the electric pulse at the electrodes; and 3) calculate or otherwise determine to what electric field the cells were exposed to.

The aim of this laboratory practice is to learn how to use standard measurement equipment to measure or monitor the delivery of electroporation pulses. During the laboratory practice we will also learn what are the electrical parameters of electroporation pulses, what should we report in our studies concerning the measurement and what are some possible complications during the pulse delivery or measurement.

EXPERIMENT

Oscilloscope, and voltage and current probes will be used to monitor the delivery of the electroporation pulses to the load. We will first learn how to set the three main controls (vertical, horizontal and trigger) for adequate data acquisition. We will learn how to use measuring tool to automatically measure the pulse parameters, how to use sequencing to measure several pulses with low pulse repetition rate and how to set acquire to measure bursts of pulses.

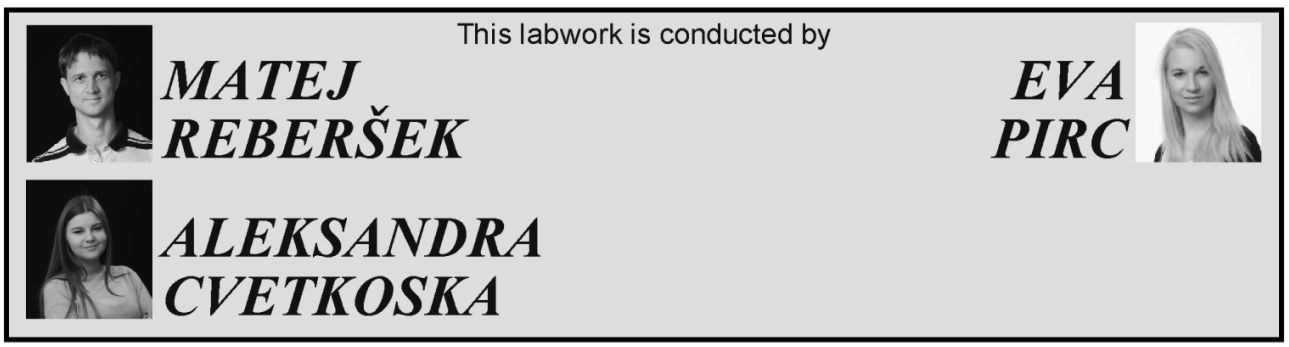

We will monitor the delivery of microsecond and nanosecond pulses to the load. Learn how to detect disconnection and improper impedance matching of the load, and how a point of measuring and improper wiring may affect the measuring and the delivery of the pulse.

Eight different commercial available electroporators: BTX (GEMINI X^2), IGEA (Cliniporator Vitae, GeneDrive), Invitrogen (Neon), Intracel (TSS20), Leroy(Beta-tech B10), Pulse Biosciences (CellFX), Societe Jouan (JOUAN) will be presented during the exercise and available for demonstrations at the end of the exercise. Additionally, also custom made prototype electroporaotrs designed and developed in our laboratory will be on display.

FURTHER READING:

Batista Napotnik T, Reberšek M, Vernier PT, Mali B, Miklavčič D. Effects of high voltage nanosecond electric pulses on eukaryotic cells (in vitro): A systematic review. *Bioelectrochemistry*, 110: 1-12, 2016.

Reberšek M, Miklavčič D, Bertacchini C, Sack M. Cell membrane electroporation –Part 3: The equipment. *IEEE Electr. Insul. M.,* 30(3): 8-18, 2014.

Silve A, Vézinet R, Mir LM. Nanosecond-Duration Electric Pulse Delivery *In Vitro* and *In Vivo*: Experimental Considerations. IEEE Trans. Instrum. Meas., 61(7): 1945-1954, 2012.

Kenaan M, El Amari S, Silve A, Merla C, Mir LM, Couderc V, Arnaud-Cormos D, Leveque P. Characterization of a 50-Ω Exposure Setup for High-Voltage Nanosecond Pulsed Electric Field Bioexperiments. *IEEE T. Biomed. Eng.* 58(1): 207-214, 2011.

Reberšek M, Miklavčič D. Concepts of Electroporation Pulse Generation and Overview of Electric Pulse Generators for Cell and Tissue Electroporation. In *Advanced Electroporation Techniques in Biology and Medicine*, *CRC Press*, 17:341-352, 2010.

Silve A, Villemejane J, Joubert V, Ivorra A, Mir LM. Nanosecond Pulsed Electric Field Delivery to Biological Samples: Difficulties and Potential Solutions. In *Advanced Electroporation Techniques in Biology and Medicine*, Pakhomov AG, Miklavcic D, Markov MS, *CRC Press*, 18: 353–368, 2010.

NOTES & RESULTS

NOTES & RESULTS

Development of pulsed power generators for electroporation H2

Matej Reberšek and Eva Pirc
University of Ljubljana, Faculty of Electrical Engineering

Duration of the experiment: 60 min
Max. number of participants: 4
Location: Laboratory for Physiological Measurements
Level: Advanced (Electrical Engineer)

PREREQUISITES

Basic to advanced knowledge of electrical engineering.

THEORETICAL BACKGROUND

Electroporation is initiated by the delivery of electrical pulses to biological cells. To generate electrical pulses for electroporation applications a pulsed power generator is required. Pulsed power generators operate in two phases: a charge and a discharge phase. During the charge phase, energy is accumulated over a long period of time in an energy storage element such as capacitor. In the discharge phase, stored energy is quickly released into the load. Several different concepts are used to generate electroporation pulses. The most common method of generating micro- and millisecond electroporation pulses is a square wave pulse generator, in which an on/off switch is used to connect and disconnect capacitor to the load. To generate nanosecond square wave electroporation pulses pulse forming networks or lines are used because high-voltage power switches cannot turn off in nanoseconds.

The aim of this laboratory practice is to learn how to develop milli-, micro- and nanosecond square wave pulse generators. During the laboratory practice we will learn how to choose or calculate the values of the electrical components for a given load and pulse duration.

EXPERIMENT

We will design and assemble two pulse generators: a square wave pulse generator and a Blumlein generator. The square wave pulse generator will enable generation of up to 1 kV micro- and millisecond electroporation pulses. And the Blumlein generator will enable generation of up to 1 kV nanosecond pulses. The output signals of the generators will be measured by oscilloscope, and voltage and current probes.

Square wave pulse generator: We will assemble this generator (Figure 1) by using: a high voltage power supply (V), high voltage capacitor (C), MOSFET switch (S), MOSFET driver (MD) and function generator (FG).

This labwork is conducted by

MATEJ REBERŠEK

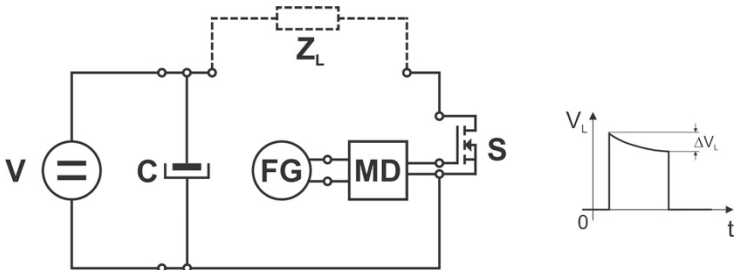

Figure 1. Schematics of the square wave pulse generator and its typical output waveform on load (Z_L).

To power the generator, we will use high voltage DC power supply MCP 350-1250 (FUG, Germany). To store enough energy in the capacitor for the pulse generation, we will calculate its minimal capacitance (equation 1). MOSFET switch will be chosen from the datasheets considering the pulse maximal output voltage and current, and rise, fall and turn off delay time. We will use 4422 (Microchip, USA) MOSFET driver circuit to drive the MOSFET switch and a function generator (HP, USA) to generate a control signal.

$$i_C = C\frac{dV_C}{dt};\ \ i_L = \frac{V_L}{Z_L} \xrightarrow{i_C=i_L;\ V=V_C=V_L;\ dV=\Delta V;\ dt=N\cdot t_P} C = \frac{N\cdot t_P}{\frac{\Delta V}{V}Z_L} \tag{1}$$

We will assemble the square wave pulse generator in four steps, by gradually increasing the requirements for pulse parameters and load (Table 1). We will vary pulse number (N), pulse duration (t_P), relative voltage drop ($\Delta V/V$) and resistance of the load (Z_L). In the first step, we will assemble the generator for one short (10 µs) fully square (1%) pulse on high resistive (1 kΩ) load. In the second step, we will lower the resistance of the load and observe the operation of MOSFET switch and output pulse waveform. In the third step, we will improve the pulse waveform. And in the final step, we will improve the pulse waveform for prolonged pulse duration and number of pulses.

Table 1. Parameters of the pulses that will be generated and resistance of the loads that will be used in specific assembly step.

Step	N	t_P [µs]	ΔV/V [%]	Z_L [Ω]	C [µF]	S
1	1	10	1	1000		
2	1	10		50	1	
3	1	10	1	50		
4	8	100	5	50		

Blumlein generator: We will assemble this generator (Figure 2) by using: a high voltage power supply (V), resistor (R), transmission lines (T_1 and T_2), radiofrequency MOSFET switch (S), MOSFET driver (MD) and function generator (FG).

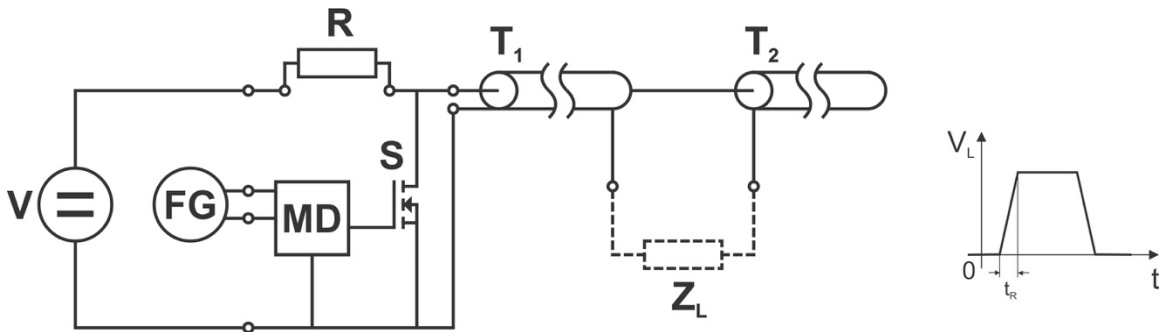

Figure 2. Schematics of the Blumlein generator and its typical output waveform on load (Z_L).

To power the generator, we will use high voltage DC power supply MCP 350-1250 (FUG, Germany). High-voltage and high-impedance resistor will be used to charge the transmission lines. The length of the transmission lines will be calculated (Equation 2) by propagation velocity (v_P) of the signal in transmission line. High-voltage, high- frequency and high-current MOSFET switch (IXYS, USA) will be used to quickly discharge the transmission lines. We will use 4422 (Microchip, USA) MOSFET driver circuit to drive the MOSFET switch and a function generator (HP, USA) to generate control signal.

$$v_P = \frac{1}{\sqrt{\varepsilon \cdot \mu}} \overset{\mu_r=1}{\Longrightarrow} \frac{c}{\sqrt{\varepsilon_r}} \overset{polyethylene}{\Longrightarrow} \frac{3 \cdot 10^8 \frac{m}{s}}{\sqrt{2.25}} = 0.2 \frac{m}{ns}; \quad l = \frac{v_P \cdot t_P}{2} \tag{2}$$

The Blumlein generator will be assembled to generate 1 kV, 20 ns square wave pulses on 100 Ω load.

FURTHER READING:

Reberšek M, Miklavčič D, Bertacchini C, Sack M. Cell membrane electroporation –Part 3: The equipment. *IEEE Electr. Insul. M.,* 30(3): 8-18, 2014.
Reberšek M, Miklavčič D. Advantages and disadvantages of different concepts of electroporation pulse generation. *Automatika (Zagreb)*, 52: 12-19, 2011.
Reberšek M, Miklavčič D. Concepts of Electroporation Pulse Generation and Overview of Electric Pulse Generators for Cell and Tissue Electroporation. In *Advanced Electroporation Techniques in Biology and Medicine*, *CRC Press*, 17:341-352, 2010.
Kolb JF. Generation of Ultrashort Pulse. In *Advanced Electroporation Techniques in Biology and Medicine*, *CRC Press*, 17:341-352, 2010.
Smith PW. Transient Electronics: Pulsed Circuit Technology. *Wiley*, 2002.

NOTES & RESULTS

NOTES & RESULTS

E-LEARNING

Electroporation of cells and tissues - interactive e-learning course E1

Selma Čorović and Samo Mahnič-Kalamiza
University of Ljubljana, Faculty of electrical engineering

Duration of the experiment: app. 90 min
Max. number of participants: 18
Location: Computer room (P9-B0)
Level: Basic

PREREQUISITES

No specific knowledge is required for this laboratory practice.

The aim of this laboratory practice is to provide the participants with basic knowledge on local electric field distribution in cells and tissues exposed to high voltage electric pulses (i.e. electroporation pulses) by means of interactive e-learning course content. The e-learning content is based on the available knowledge from the scientific literature.

PROTOCOL OF THE E-LEARNING COURSE

The participants will be gathered in a computer-computer classroom providing each participant with a computer. A short test will be given to establish the baseline knowledge before the e-learning course.
Within the first part of the e-learning course we will bring together the educational material on basic mechanisms underlying electroporation process on the levels of cell membrane, cell and tissues as a composite of cells (Figure 1).

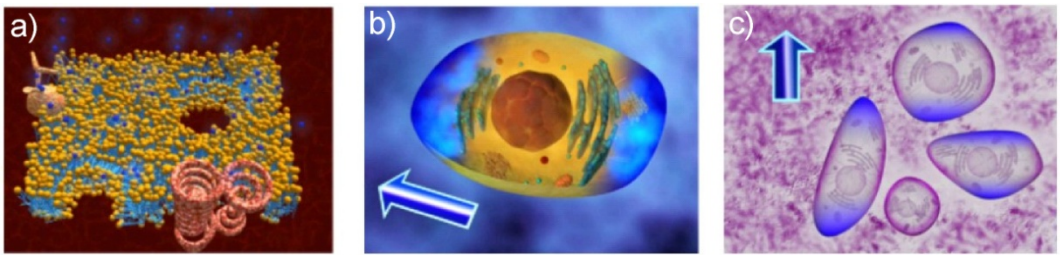

Figure 1: Introduction of small molecules (blue molecules) through a cell membrane (a) into an electroporated cell (b) and into the successfully electroporated cells within an exposed tissue (c) (Čorović et al., 2009).

Within the second part of the course we will provide basic knowledge on important parameters of local electric field needed for efficient cells and tissue electroporation, such as: electrode geometry (needle or plate electrodes as illustrated in Figure 2, electrode position with respect to the target tissue and its surrounding the tissues (Figure 3), the contact surface between the electrode and the tissue, the voltage applied to the electrodes and electroporation threshold values. This part of the e-learning course content will be provided by an interactive module we developed in order to visualize the local electric field distribution in 2D and 3D dimensional tissue models.

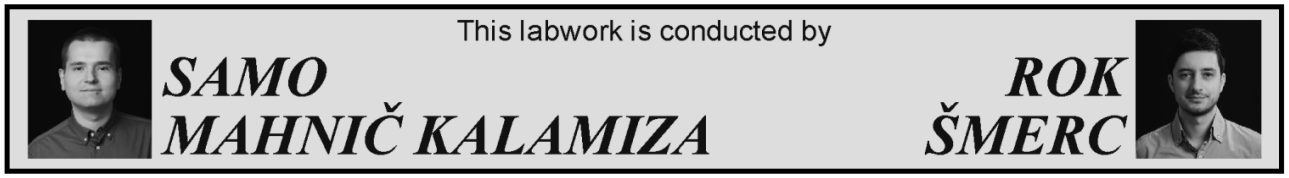

The objective of this module is to provide:
- local electric field visualization in cutaneous (protruding tumors) and subcutaneous tumors (tumors more deeply seeded in the tissue);
- guideline on how to overcome a highly resistive skin tissue in order to permeabilize more conductive underlying tissues and
- visualization and calculation of successfully electroporated volume of the target tissue and its surrounding tissue (i.e. the treated tissue volume exposed to the electric field between reversible and irreversible electroporation threshold value $E_{rev} \leq E < E_{irrev}$) with respect to the selected parameters such as: number and position of electrodes, applied voltage on the electrodes.

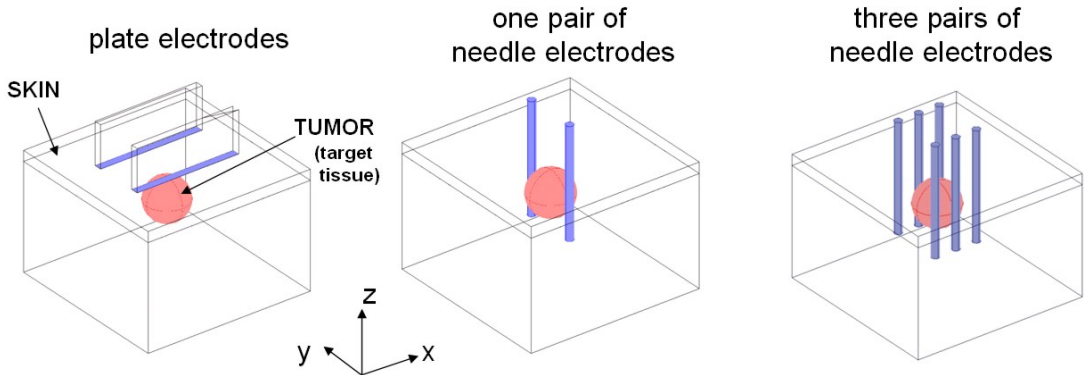

Figure 2: Plate electrodes vs. needle electrodes with respect to the target tissue (e.g. tumor tissue).

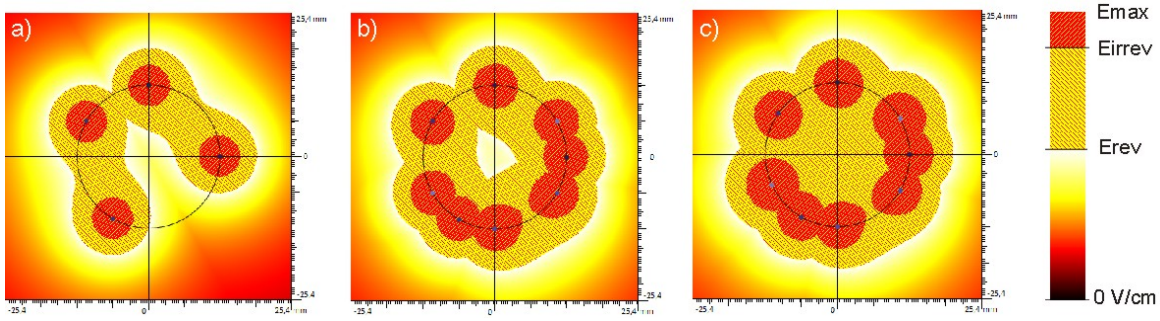

Figure 3: Electric field distribution within the tumor (inside the circle) and within its surrounding tissue (outside the circle) obtained with three different selection of parameters (number and position of electrodes and voltage applied): (a) 4 electrodes, (b) 8 electrodes and (c) 8 electrodes with increased voltage on electrodes so that the entire volume of tumor is exposed to the $E_{rev} \leq E < E_{irrev}$.

After the e-learning course the pedagogical efficiency of presented educational content and the e-learning application usability will be evaluated.

FURTHER READING:

Čorović S, Pavlin M, Miklavčič D. Analytical and numerical quantification and comparison of the local electric field in the tissue for different electrode configurations. *Biomed. Eng. Online* 6: 37, 2007.
Serša G, Miklavcic D: Electrochemotherapy of tumours (Video Article). *J. Visual Exp.* 22: 1038, 2008.
Čorović S, Županič A, Miklavčič D. Numerical modeling and optimization of electric field distribution in subcutaneous tumor treated with electrochemotherapy using needle electrodes. *IEEE T. Plasma Sci.* 36: 1665-1672, 2008.
Čorović S, Bešter J, Miklavčič D. An e-learning application on electrochemotherapy. *Biomed. Eng. Online* 8: 26, 2009.
Čorović S, Županič A, Kranjc S, Al Sakere B, Leroy-Willig A, Mir LM, Miklavčič D. The influence of skeletal muscle anisotropy on

electroporation: in vivo study and numerical modeling. *Med. Biol. Eng. Comput.* 48: 637-648, 2010.
Edhemovic I, Gadzijev EM, Brecelj E, Miklavcic D, Kos B, Zupanic A, Mali B, Jarm T, Pavliha D, Marcan M, Gasljevic G, Gorjup V, Music M, Pecnik Vavpotic T, Cemazar M, Snoj M, Sersa G. Electrochemotherapy: A new technological approach in treatment of metastases in the liver. *Technol Cancer Res Treat* 10:475-485, 2011.
Bergues Pupo AE, Reyes JB, Bergues Cabrales LE, Bergues Cabrales JM. Analitical and numerical quantification of the potential and electric field in the tumor tissue for different conic sections. *Biomed. Eng. Online* 10:85, 2011.
Neal RE II, Garcia PA, Robertson JL, Davalos RV. Experimental characterization and numerical modeling of tissue electrical conductivity during pulsed electric fields for irreversible electroporation treatment planning. *IEEE T. Biomed. Eng.* 59(4):1077-1085, 2012.
Čorović S, Mir LM, Miklavčič D. In vivo muscle electroporation threshold determination: realistic numerical models and in vivo experiments. *Journal of Membrane Biology* 245: 509-520, 2012.
Essone Mezeme M, Pucihar G, Pavlin M, Brosseau C, Miklavčič D. A numerical analysis of multicellular environment for modeling tissue electroporation. *Appl. Phys. Lett.* 100: 143701, 2012.
Mahnič-Kalamiza S, Kotnik T, Miklavčič D. Educational application for visualization and analysis of electric field strength in multiple electrode electroporation. BMC Med. Educ. 12: 102, 2012.
Čorović S, Lacković I, Šuštarič P, Šuštar T, Rodič T, Miklavčič D. Modeling of electric field distribution in tissues during electroporation. Biomed. Eng. Online 12: 16, 2013.

NOTES & RESULTS

NOTES & RESULTS

Faculty members

Damijan Miklavčič
University of Ljubljana, Faculty of Electrical Engineering,
Tržaška 25, SI-1000 Ljubljana, Slovenia
E-mail: damijan.miklavcic@fe.uni-lj.si

Lluis M. Mir
Université Paris-Saclay, CNRS, Institut Gustave Roussy, Metabolic and systemic aspects of oncogenesis (METSY),
114 rue Edouard Vaillant, F-94805 Villejuif Cédex, France
E-mail: Luis.MIR@gustaveroussy.fr

Marie-Pierre Rols
Institute of Pharmacology and Structural Biology, CNRS - University of Toulouse III,
IPBS UMR 5089, 205, route de Narbonne, 31077 Toulouse, France
E-mail: marie-pierre.rols@ipbs.fr

Gregor Serša
Institute of Oncology,
Zaloška 2, SI-1000 Ljubljana, Slovenia
E-mail: gsersa@onko-i.si

Mounir Tarek
Theoretical Physics and Chemistry Laboratory, Université de Lorraine,
CNRS, LPCT, F-54000 Nancy
E-mail: mounir.tarek@univ-lorraine.fr

P. Thomas Vernier
Frank Reidy Research Center for Bioelectrics, Old Dominion University,
4211 Monarch Way, Norfolk, VA 23508, USA
E-mail: pvernier@odu.edu

Julie Gehl
University of Copenhagen, Department of Clinical Medicine,
Blegdamsvej 3, 2200 København N Denmark
E-mail: julie.gehl@sund.ku.dk